9950-633

Final Technical Report

STEAM RANKINE SOLAR RECEIVER PHASE II

80-17527

November 23, 1981

Prepared for

California Institute of Technology
Jet Propulsion Laboratory
Pasadena, California

AIRESEARCH MANUFACTURING COMPANY

Final Technical Report

STEAM RANKINE SOLAR RECEIVER PHASE II

80-17527

November 23, 1981

Prepared by
L.E. De Anda/M. Faust

Approved by

M.V. Greeven
Program Manager

W.J. O'Reilly
Engineering Chief, Heat Transfer
and Cryogenic Systems

Prepared for

California Institute of Technology
Jet Propulsion Laboratory
Pasadena, California

AIRESEARCH MANUFACTURING COMPANY

FOREWORD

This final report is submitted by the AiResearch Manufacturing Company, a division of The Garrett Corporation, in fulfillment of Phase II of Contract No. NAS7-100/955157 with the Jet Propulsion Laboratory of the California Institute of Technology. The report is a discussion of the design and development of a Steam Rankine Solar Receiver (SRSR).

ABSTRACT

The goal of the Phase II project was to design and develop a Steam Rankine Solar Receiver (SRSR) based on the tubular concept recommended in Phase I of the program. The SRSR is an insulated, cylindrical coiled tube boiler which is mounted at the focal plane of a fully tracking parabolic solar reflector. The concentrated solar energy received at the focal plane is then transformed to thermal energy through steam generation. The steam would then be used in a small Rankine cycle heat engine to drive a generator for the production of electrical energy.

The SRSR was designed to have a dual mode capability, performing as a once through boiler with and without reheat. This was achieved by means of two coils which constitute the boiler. The boiler core size of the SRSR is 17.0-inches in diameter and 21.5-inches long. The tube size is 7/16-inch I.D. x 0.070-inch wall for the Primary, and 3/4-inch I.D. x 0.125-inch wall for the Reheat section. The materials used were Corrosion Resistant Steel (CRES) Type 321 and type 347 stainless steel. The core is insulated with 6-inches of Cerablanket insulation wrapped around the outer wall. The aperture end and the reflector back plate at the closed end section are made of silicon carbide. The SRSR accepts 85 kwth and has a design life of 10,000 hrs when producing steam at 1400°F and 2550 psig.

An additional application for the system was investigated. This consisted of Process Heat involving two techniques utilizing the SRSR to produce steam: (a) Pressurized Water Receiver (PWR); and (b) Recirculation Boiler Receiver (RBR).

The study of the SRSR included symmetrical and asymmetrical solar power input into the reciever. The symmetrical cases involved the baseline incident flux and the axially shifted incident fluxes. The asymmetrical cases correspond to the solar fluxes that are caused by reduced solar energy input from one half of the concentrator, or by receiver offset of ± 1 inch from the concentrator optical axis.

CONTENTS

ILLUSTRATIONS

ILLUSTRATIONS (Continued)

TABLES

1. INTRODUCTION

This report records work done by AiResearch during Phase II of the Steam Rankine Solar Receiver (SRSR) development program. The Phase I study, (also performed by AiResearch for the Jet Propulsion Laboratory, under Contract NAS7-100/955157), created and analyzed various concepts for a solar receiver for a steam Rankine cycle. It was designed to operate in conjunction with a point focus concentrator, making steam for the generation of electricity. Figure 1-1 shows the parabolic concentrator of solar energy, while Table 1-1 summarizes its general characteristics. The steam Rankine cycle schematic is presented in Figure 1-2. The Phase I study resulted in the recommendation of a specific design. It consisted of a cylindrical coiled tube heat exchanger, set inside a cylindrical outer containment shell. The front end of the containment shell had an aperture of approximately 10-inches in diameter. The concentrated insolation, approximately 85 kwth (kw, thermal), entered through the aperture, and impinged on the interior wall of the cavity formed by the coiled tube heat exchanger. After radiation interchange had occurred, the absorbed heat flux was transferred to the water flowing through the tube. The Phase I SRSR featured: a) an Inconel 625 heat exchanger with primary and reheat sections; b) a removable ceramic aperature structure; c) a flat closed end of RA-330; d) kaowool insulation; e) an outer containment shell of mild steel; and f) a six-point thin strap support mechanism for the coil. Phase I also studied thermal storage devices and advised the use of lithium chloride as an energy storage medium. The results of Phase I were presented in AiResearch Report No. 79-15663.

Subsequently, work on Phase II commenced. The design was completed according to a revised problem statement submitted by JPL. AiResearch fabricated two complete SRSRs, two extra coils, and other spare parts, designed and purchased test equipment, and performed acceptance tests on the first two cores. This report documents work performed by AiResearch on the Steam Rankine Solar Receiver during Phase II of JPL Contract NAS7-100/955157.

1.1 SUMMARY

At the beginning of Phase II, AiResearch received a revised Phase I problem statement. See Table 1-2. The SRSR was to have a dual mode capability, performing in the all-primary mode and in the primary-reheat mode, i.e., as a once through boiler with and without reheat. Also, an analysis of process heat applications was requested, along with a study of the effect of heat flux irregularities inside the cavity due to unknown concentrator characteristics. The thermal energy storage device was excluded from further study.

The design of the Steam Rankine Solar Receiver was altered by these new requirements. See Figure 1-3. The basic concept remained the same, but several new features were incorporated into the Phase II design. The tubing wall sizes

Figure 1-1. Parabolic Solar Concentrator

TABLE 1-1

SOLAR CONCENTRATOR CHARACTERISTICS

Type: two axis, tracking, faceted parabolic dish

Size: 11-meter aperture

Reflectivity: 0.86 to 0.94 (maximum)

Peak thermal energy at focus: 85 kwt

Tracking error: 0.1 deg

Tracking system: evaluation/azimuth

Slew rates: elevation 400 deg/hr approximate
azimuth 150 deg/hr approximate

Focal length: 0.6 diameter

Slope error: 1 to 2 milliradians (0.1 deg nominal)

were changed. A movable backplate was included in order to equalize steam outlet temperatures from the primary and reheat sections for the primary-reheat mode (in case of flux irregularities inside the cavity). Expansion coils were added at either end of the primary and reheat sections to allow for thermal growth. A hinged joint replaced a solid braze joint between the primary and reheat section to relieve thermally induced bending moment stresses. An 8 point rigid support system which allows for radial and axial thermal growth replaces the 6 point thin strap support mechanism for the heat exchanger. The completed hardware incorporated these features.

The SRSR receives 85 kwth from the concentrator through the aperture, and converts 80 kw of this energy to the working fluid, water. Table 1-3 summarizes the thermal performance of the receiver. The receiver efficiency is estimated at 94% and the pressure drop through the unit is less than 10%.

Creep deformation was dominant over life cycle fatigue as the limiting factor in establishing the expected life of the unit. The design life of the unit was based on 1% creep of the core. The Phase II design, using an Inconel 625 core, has an expected life of 10,000 hours and 1500 cycles. AiResearch fabricated two spare coils of Inconel 625. The first two units used Corrosion Resistant Steel (CRES) type 321 cores for initial testing of the SRSR concept. The CRES 321 have a limited life but should be adequate for shakedown testing of the concentrator-receiver system. Operation of the CRES 321 core at maximum temperatures and pressures could result in rupture within a few hundred hours and less than 100 cycles.

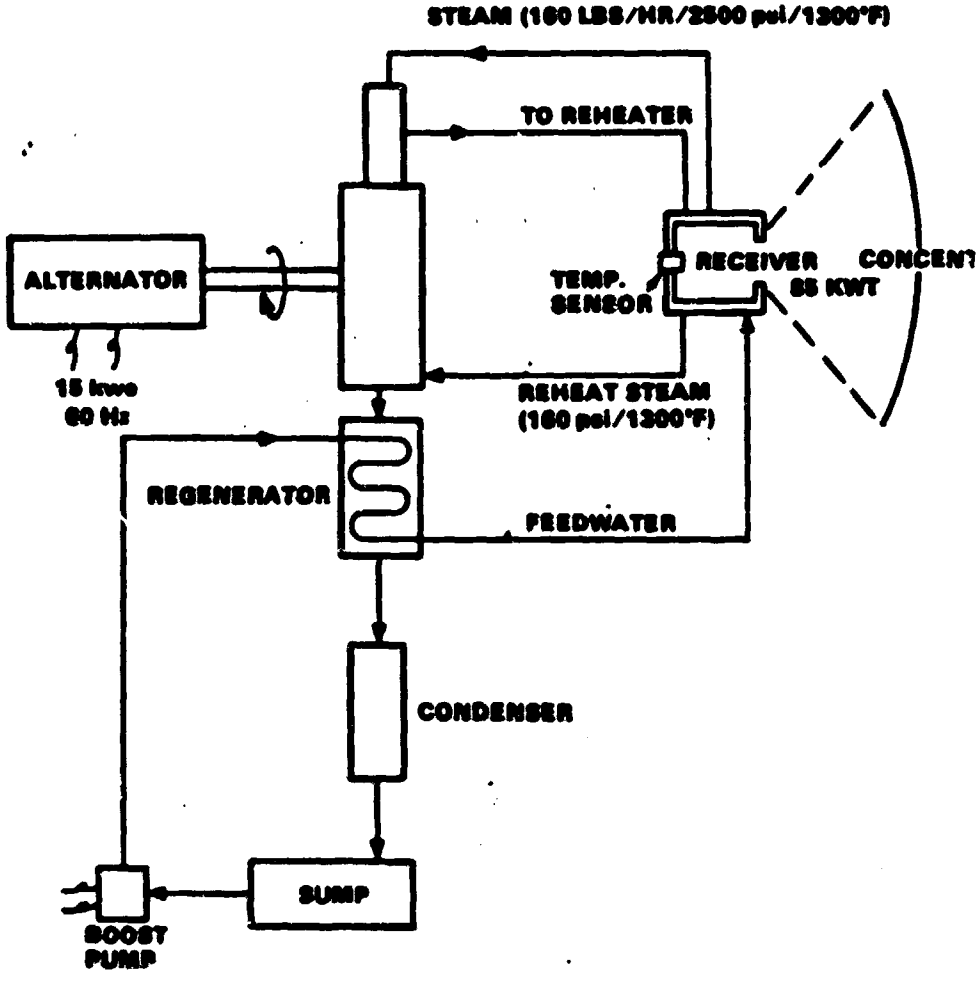

Figure 1-2. Steam Rankine Cycle Schematic

TABLE 1-2

SRSR PHASE II PROBLEM STATEMENT

Solar Power Input

- Average sunny Spring day
- 85 kwth peak
- Receiver must accept input irregularities

  -Symmetrical, axially shifted incident flux profile due to mirror slope errors

  -Asymmetric incident flux profile due to receiver offset of ±1 in. or reduced input (10 percent less total power) from one-half of mirror

Applications

- Process Heat
- Steam/electric with dual mode operating capability
- Size receiver for steam/electric system

Peak Thermal Operating Conditions

- Primary Section

		Process Heat	Steam/Electric
Feedwater Inlet	Temp, F	Up to 300	200 - 300
	Press, psi	Calc.	Calc.
Steam Outlet	Temp, F	Up to 1300	1300
	Press, psi	Up to 2500	2500

- Reheat Section

Steam Inlet	Temp, F	Up to 1300	650
	Press, psi	Up to 2500	175
Steam Outlet	Temp, F	Up to 1300	1300
	Press, psi	Calc.	Calc.

Allowable pressure drop, $\Delta P/P_{sys} = 10\%$

Ceramic Aperture

- Design for convenient change for experimental purpose.

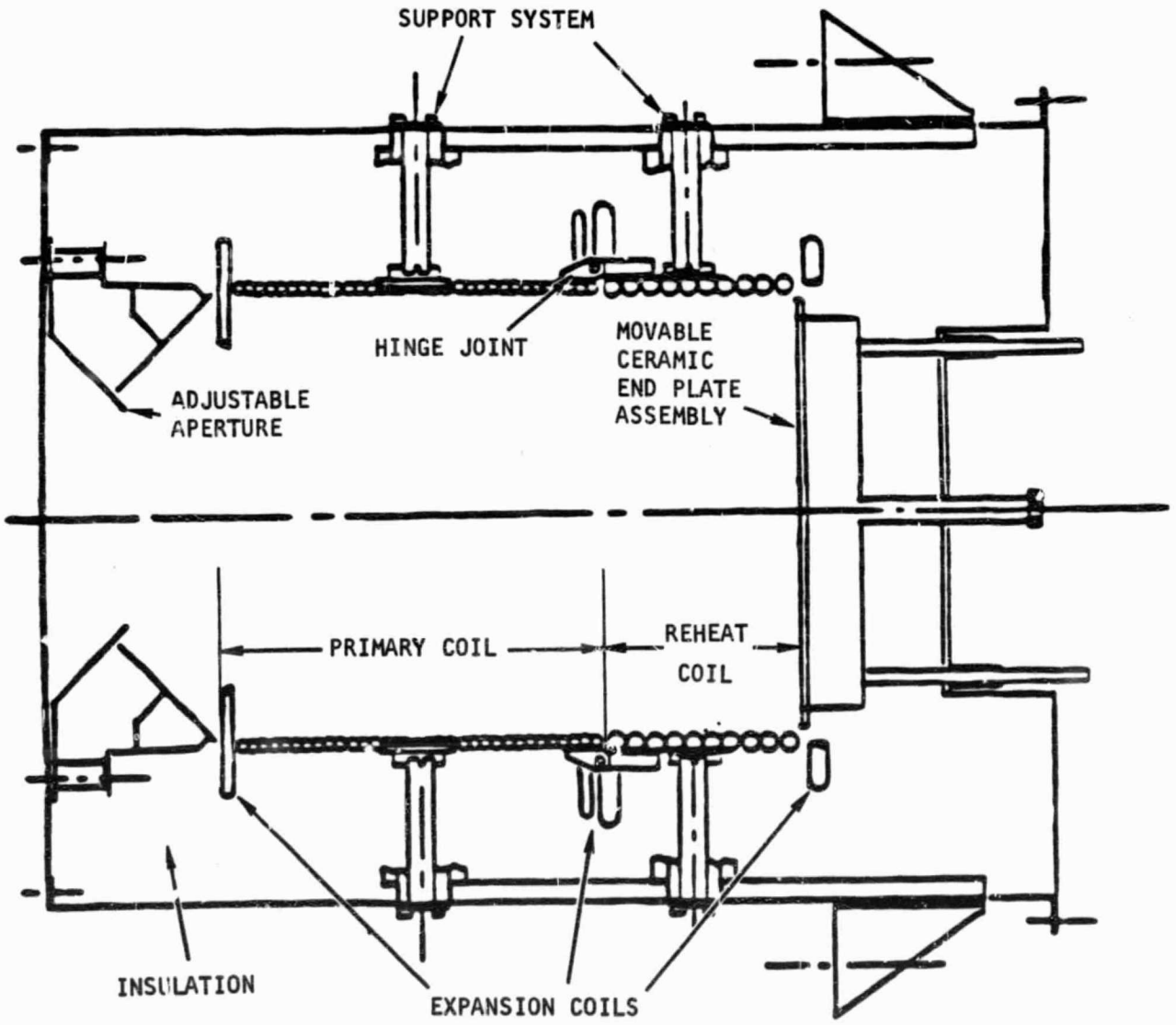

Figure 1-3. Steam Rankine Solar Receiver (SRSR)

TABLE 1-3

SRSR THERMAL PERFORMANCE SUMMARY

- SOLAR INPUT _____ 85 KWTH

- APERTURE (9 IN. DIA) RADIATION LOSS _ 1.3
- INSULATION LOSS _____ 1.2
- ASSUMED APERTURE ASSEMBLY _____ 2.5
  CONVECTION AND RADIATION LOSS
- THERMAL POWER TO FLUID _____ 80
- RECEIVER EFFICIENCY _____ 94%

- FLOW RATE _____ 157 LB/HR
- PRESSURE DROP
  - PRIMARY _____ 2%
  - REHEAT _____ 10%

- PRIMARY MODE ONLY
  - FLOW RATE _____ 196 LB/HR
  - PRESSURE DROP _____ 3%

Acceptance tests were performed on the two CRES 321 cores prior to delivery. They passed proof pressure, leakage, and pressure drop tests.

2. STEAM RANKINE SOLAR RECEIVER (SRSR) DESCRIPTION

The cutaway drawing of the SRSR is shown in Figure 2-1. The main components of the SRSR are a CRES 321 cylindrical tube-coil heat exchanger assembly, an ajustable aperture assembly, and a rear plate assembly.

The tube-core heat exchanger assembly consists of 34 turns of 7/16-inch O.D. by 0.070-inch wall primary section tubing and 10 turns of 3/4-inch O.D. by 0.125-inch wall reheat section tubing. An additional turn of tubing at the ends of each section allows for thermal contraction and expansion of the assembly. Straight runs of tubing are used to route the water or steam to and from the coil. The inner surface of the coil is oxide-coated to produce a surface emissivity of about 0.8. The primary and reheat coils are independent brazements which are mechanically attached to each other. The two coil sections may be connected either in series (for operation in primary mode only) or, parallel to each other (for operation in the primary plus reheat mode). In the latter case, the primary and reheat outlets are adjacent to each other. The core assembly is 17-inches in diameter and 21.5-inches in length.

The aperture assembly consists of: a) a Silicon Carbide (SiC) ceramic plate, 0.28-inch thick; b) an RA-330 stainless steel aperture support skirt; c) an Inconel 625 aperture mount plate; and d) a Type 347 stainless steel aperture support ring assembly. The assembly can be adjusted to incorporate two different ceramic plates whith 8-inch and 10-inch diameter openings. The aperture plate also serves to reflect the re-radiated energy back into the receiver cavity.

The rear plate is also adjustable as it can be moved axially up to 3-inches. Originally it was a 0.28-inch thick SiC plate, but as a result of test experience, it was changed to a 0.375-inch thick chromium nickel steel (RA-330). Furthermore, the rear plate assembly consists of an Inconel 625 support structure and a mild steel rear outer shell.

The cylindrical core is insulated with 6-inches of Cerablanket insulation wrapped around the core's outer wall. It lies within a 0.188-inch thick, carbon steel (1020) case.

The outer case has a maximum diameter of 30.9-inches and an overall length of 38-inches.

The approximate weight of the ABSR was determined to be 476 lbs.

Detailed design drawings of the entire unit are provided in Appendix A at the end of this report.

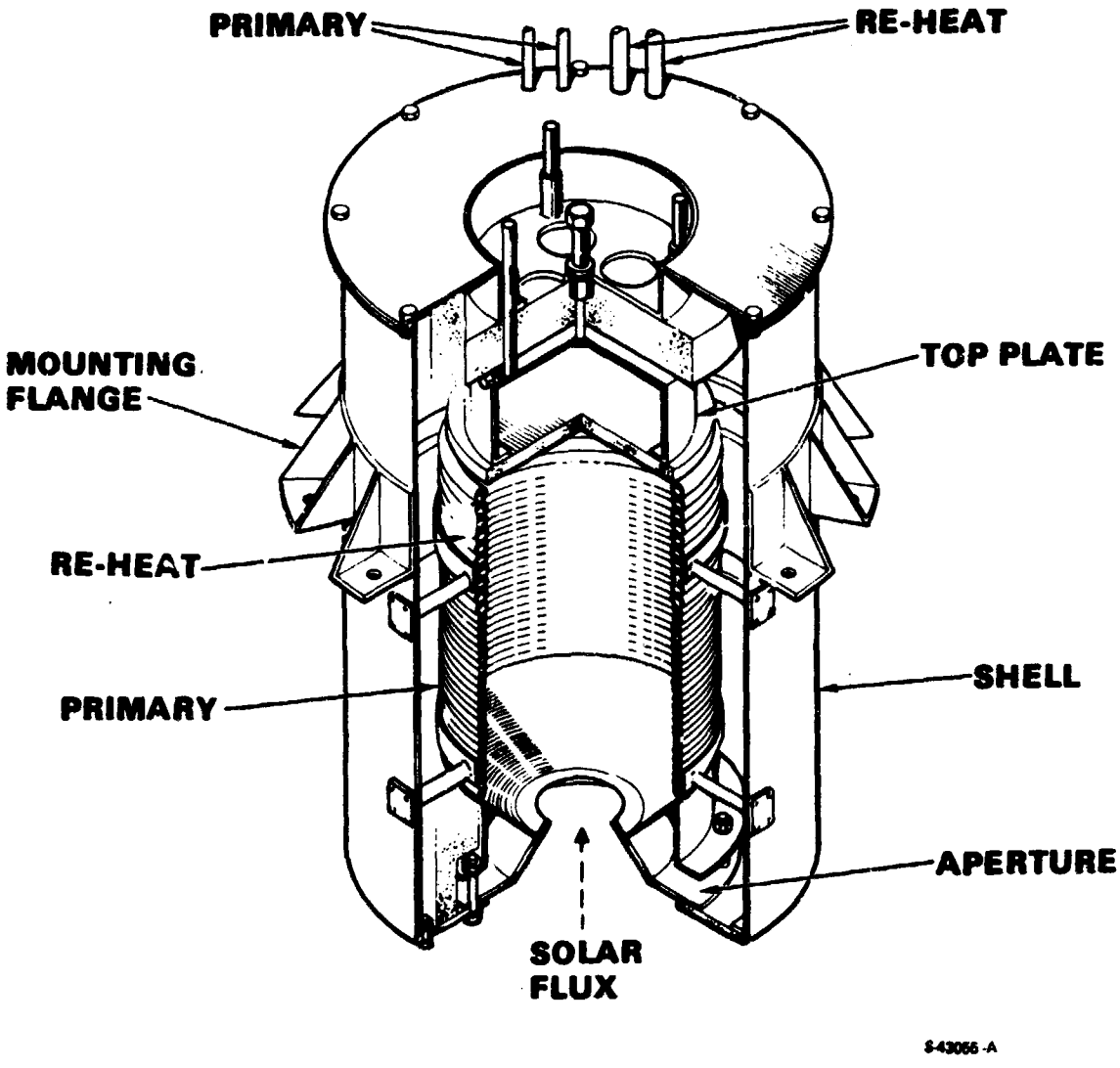

Figure 2-1. Steam Rankine Solar Receiver (SRSR) Cutaway

3. SRSR ANALYSIS

Analysis of the Steam Rankine Solar Receiver (SRSR) included both a thermal analysis of the SRSR to ensure the adequacy of its thermal performance characteristics, and a structural analysis to ensure that the desired lifetime of the receiver is reached.

3.1 THERMAL ANALYSIS

The revised work statement issued by JPL led to study in several areas during Phase II of the SRSR program. Optical modeling of the concentrator-receiver system was performed to determine the thermal inputs to the receiver cavity for concentrators with different characteristics. The final design enables the receiver to accept substantial flux irregularities. Required options included the ability to operate in either the primary-reheat or all-primary configuration while in the steam electric mode. See Figure 3-1. Process heat applications requiring lower pressures and temperatures than the steam-electric configurations were to be analyzed. The receiver was to be sized for the steam-electric function.

The design points specified in Table 1-2 for the steam-electric mode led to the thermodynamic process paths shown in Figure 3-2. The flowrates were determined by the energy balance calculation. The path consists of 28 percent liquid heating, 20 percent boiling, 32 percent superheating, and 20 percent reheating.

The calculated thermal and pressure-drop performance of the receiver under design conditions is summarized in Table 1-3. 94 percent of the 85 kwth solar thermal input is absorbed by the working fluid (water). This produces primary steam at 2500 psia and 1300°F or, both primary steam at the same conditions and reheat steam at 175 psia and 1300°F. As a result of the Phase I parametric study and the Phase II reevaluation, a receiver was chosen for detailed analysis. The detail analysis of the selected receiver included heat flux sensitivity analysis, process heat applications, changes required for 1/2 total power input, and adequacy of heat transfer area margins.

3.1.1 Optical Modeling

The total design power directed toward the receiver by the concentrator was defined as 85 kwth. An estimated distribution of the normal heat flux on planes parallel to the focal plane was provided by JPL from two different concentrators. The concentrators had slope errors of 1- and 2-milliradians (mrad). An additional vertical distribution was provided for the 2-mrad concentrator.

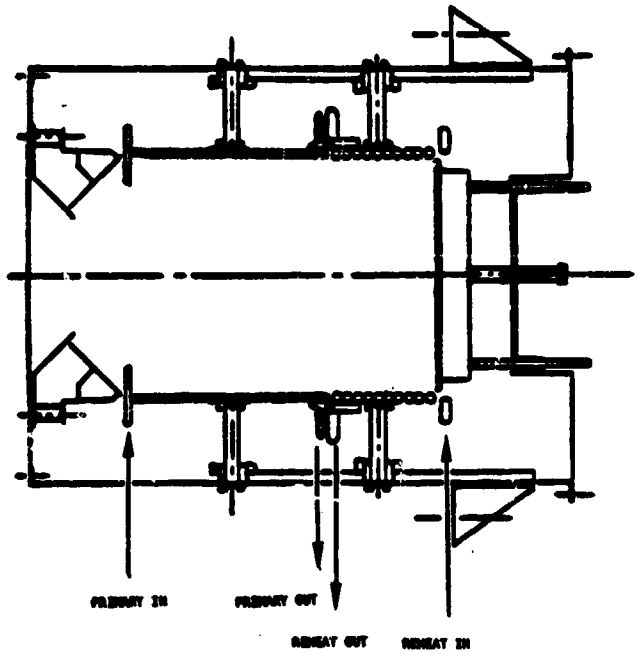

PRIMARY-REHEAT MODE

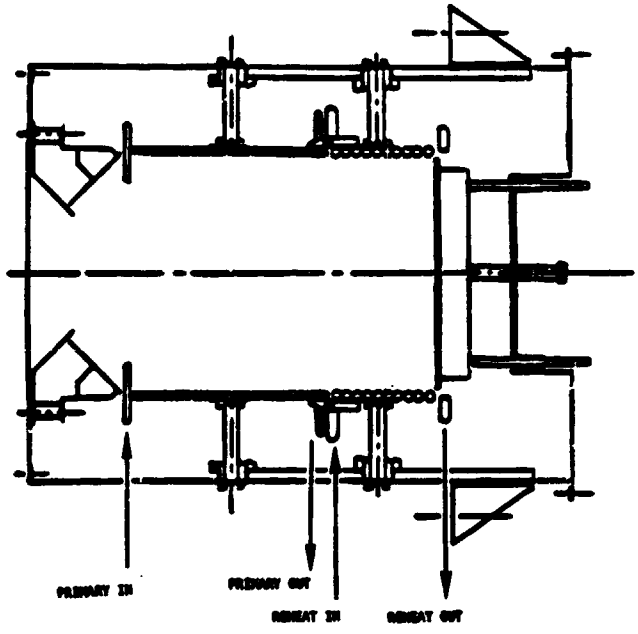

ALL-PRIMARY MODE

Figure 3-1. Steam/Electric Modes. Primary-Reheat and All-Primary Modes

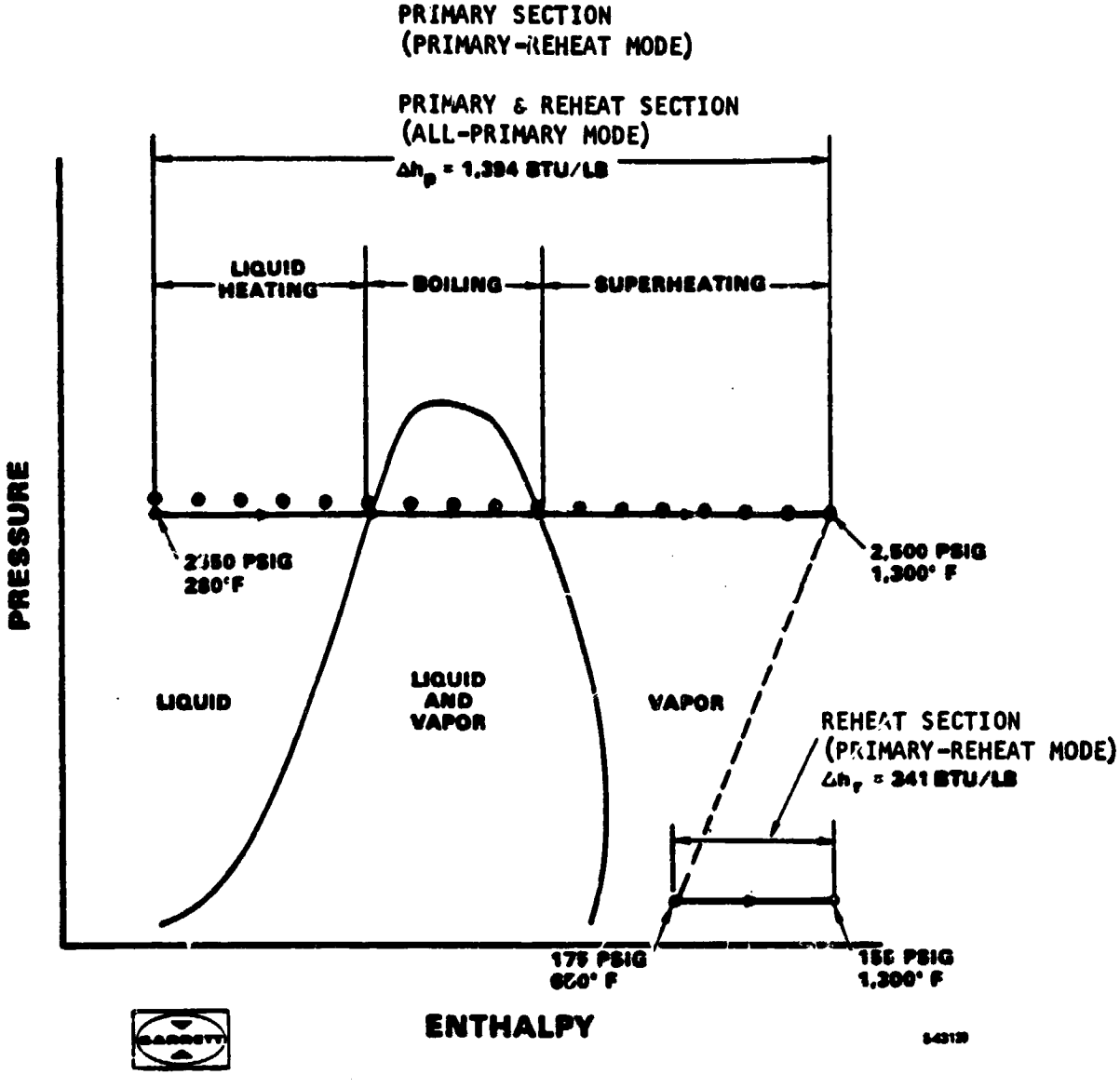

Figure 3-2. Thermodynamic Process Paths

In order to accurately evaluate the performance of a receiver design of Phase II, not only the total incident flux must be known, but also its distribution over the interior surfaces of the cavity. This flux distribution depends on a number of factors, including: (a) the characterization of the optical source; (b) the overall geometry of the concentrator (surface shape and speed, i.e., the smaller the angular size of the source, the slower the optical system). AiResearch had the availability of a mathematical solar simulator program developed by Dr. George Schrenk and supplied through Scientific Time Sharing Corporation (STSC). This program properly treats the sun as a source of finite angular dimensions and uses an efficient cone-optics method of evaluating the incident concentrated-flux, rather than using a ray-trace technique (which is used in analyzing image producing optical systems). The effects of concentrator slope errors and of radiation due to atmospheric scattering are taken into account by specifying an effective sun half-angle (α_{eff}) which is larger than the actual half-angle (α).

A simple but effective model was used to determine the receiver heat inputs for the parametric study of Phase I of the program. The results from this model were seen to be essentially indistinguishable from those obtained via the STSC program.

Figure 3-3 illustrates the optical differences between a very distant point source (resulting in parallel incident rays) and a source of finite angular dimensions. The paraboloidal concentrator shown has an f/D ratio of 0.6. On the right hand side of the figure, the paths of the incident and reflected rays from a finite source are shown being reflected from selected points on the reflecting surface. Similarly, the left hand side shows the results for flux incident from a distant point source. The drawing is to scale and the paths of the reflected rays were determined by an exact ray trace program. Two observations can be made:

(1) For a distant point source on the optical axis, a parboloid of revolution focuses all the incident rays through the prime focus. Thus, the aperture flux distribution is a poor approximation to the actual flux distribution from an extended source.

(2) For regions away from the focal plane, the character of the flux field produced by the distant point source is not substantially different from that for an extended source.

By adopting the distant point source approximation (simple model), the flux in the cavity can now be represented by a simple vector field. The flux vector, $\vec{F}$, is fully described once its magnitude F and polar angle θ are specified (there being azimuthal symmetry). At a location (r, z) in the cavity, F and θ are given by

$$F(r,z) = \frac{\rho \, SRH \cos\left[\arctan\left(R/2f\right)\right]}{\cos\left[\arctan\left(r/z\right) - \arctan\left(R/2f\right)\right] r\sqrt{r^2 + z^2}} \qquad (3\text{-}1)$$

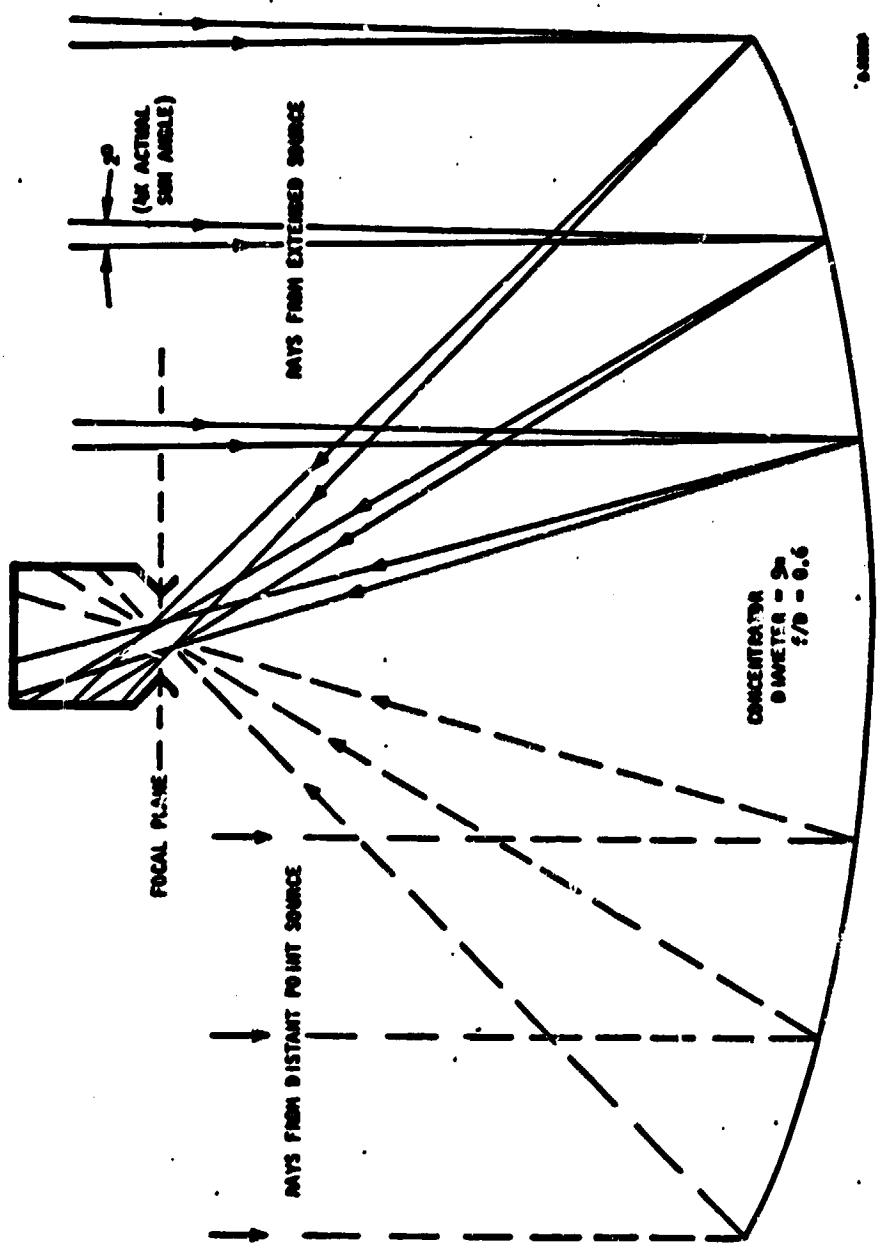

Figure 3-3. Concentrator and Receiver Optics

where

$$H = \sqrt{R^2 + (f - R^2/4f)^2} \tag{3-2}$$

and

$$R = [2f/(r/z)]\left(\sqrt{1 + r^2/z^2} - 1\right), \; r/z > 0, \tag{3-3}$$
$$= 0, \; r/z = 0, \tag{3-4}$$

and

$$\theta\,(r/z) = \arctan\,(r/z). \tag{3-5}$$

The geometric quantities r, z, r, H, and f are defined in Figure 3-4. The physical quantities ρ and S are the concentrator reflectivity and the direct normal incident solar radiation, respectively. F will have the same units as S (e.g., kW/m^2) if all the geometric quantities use the same linear unit (e.g., meters).

The effect of the concentrator diameter, D, is applied through the additional constraint

$$F = 0 \text{ if } \theta > \theta_{max} \tag{3-6}$$

where

$$\theta_{max} = \arctan \frac{D/2}{f-s} \tag{3-7}$$

and

$$s = \frac{1}{4f}\,(D/2)^2 \tag{3-8}$$

Also, shadowing by the receiver itself results in the constraint

$$F = 0 \text{ if } \theta < \theta_{min} \tag{3-9}$$

where

$$\theta_{min} = \arctan \frac{D_R/2}{f-d} \tag{3-10}$$

and

$$d = \frac{1}{4f}\,(D_R/2)^2 \tag{3-11}$$

Finally, the incident energy per unit area of cavity wall, q, is

$$q = (r,z) = \vec{F}\,(r,z) \cdot \vec{n}\,(r,z) \tag{3-12}$$

where $\vec{n}$ is the outward directed unit vector normal to the cavity wall at the point of interest.

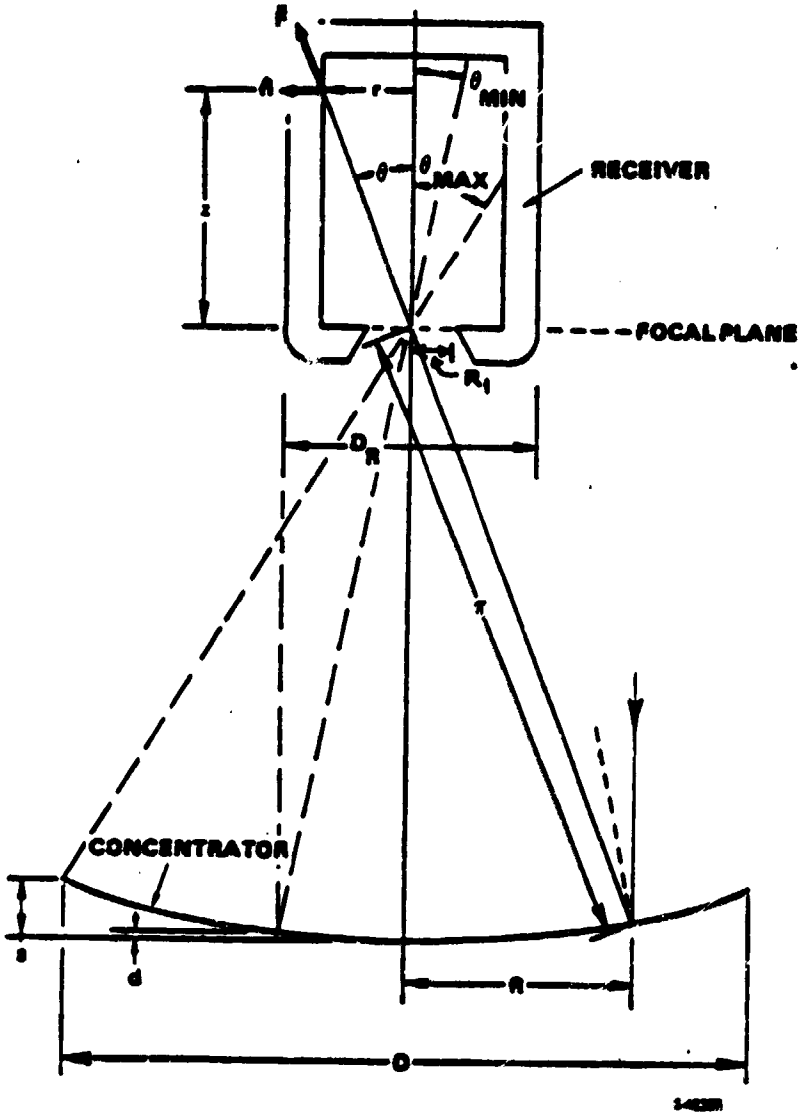

Figure 3-4. Optical Flux Parameters

A comparison of q determined by both the STSC program and this simple approximation is shown in the upper portion of Figure 3-5. The results shown are for the typical cavity represented in the insert at the lower portion of the figure. The simple model's sharp cutoff occurs at $\theta = \theta_{max}$. The fact that the peak value of the simple model curve is quite a bit higher than the STSC curve is really of little concern. What is of importance here is not the instantaneous value of q (z, r), but the integral of this quantity over the finite area of a wall element (the cavity is divided into six finite elements). The lower portion of Figure 3-5 shows two superimposed histograms. They give the total energy incident upon each element, using both the STSC program (solid line) and the distant point source model (dashed line). The difference between the two is seen to be rather small, with a maximum difference of 12.0 percent. Because of radiation effects, the absorbed power curve is more smeared out than the incident power curve. This serves to further reduce the importance of choosing the more exact flux model. The final and most important result is that the wall temperature distribution and peak temperature value are not significantly influenced by using the simpler flux model.

The effect of the concentrator imperfections is to apply a smoothing function to the distribution that would otherwise result from reflection from a perfect mirror. Thus, the simple model histograph can be improved by applying a smoothing technique which employs two empirically determined parameters, N and S_1. N is the number of times the smoothing is applied to the histogram. S_1 measures the amount of smoothing per pass. The optical input for the thermal analysis of the receiver under development was obtained using the distant point source model and the smoothing function.

Figure 3-6. compares the vertical flux distribution given in Exhibit II of the JPL work statement with a histogram obtained in the described manner. The excellent agreement far from the aperture is as expected; nearer the aperture, the Exhibit II curve seems to be deficient in integrated power.

Knowledge of the flux distribution across the focal plane is necessary in order to establish the receiver aperture size. Figure 3-7 is a collection of aperture flux plots presented as concentration ratio vs the radius R_1. The plots on the right side of the figure are a continuation of the plots on the left side on a greatly expanded scale. The rectangular "simple optics" plot ignores all optical aberrations that accompany non-paraxial rays and fast optical systems. It does, however, provide a convenient datum against which all others can be compared. The Schrenk" plot was generated by the STSC program. The 1.7 factor was chosen to give reasonable agreement with the "1.75 mrad" curve which was supplied by JPL for the Phase I proposal effort. The curves labeled "1 mrad" and "2mrad" are from the Exhibit II supplied in Phase II; interpolation between these two gives the "1.75 interpolated" curve for the specified nominal value of 1.75 mrad. The new curves clearly are in disagreement with the older 1.75 mrad curve and, especially for the 1 mrad case, exhibit unusual behavior for small R_1. Based on these considerations, a conservative value of R_1 = 5-inches was chosen for the baseline aperture size for the analysis, but the actual receiver was provided with aperture size adjusting features.

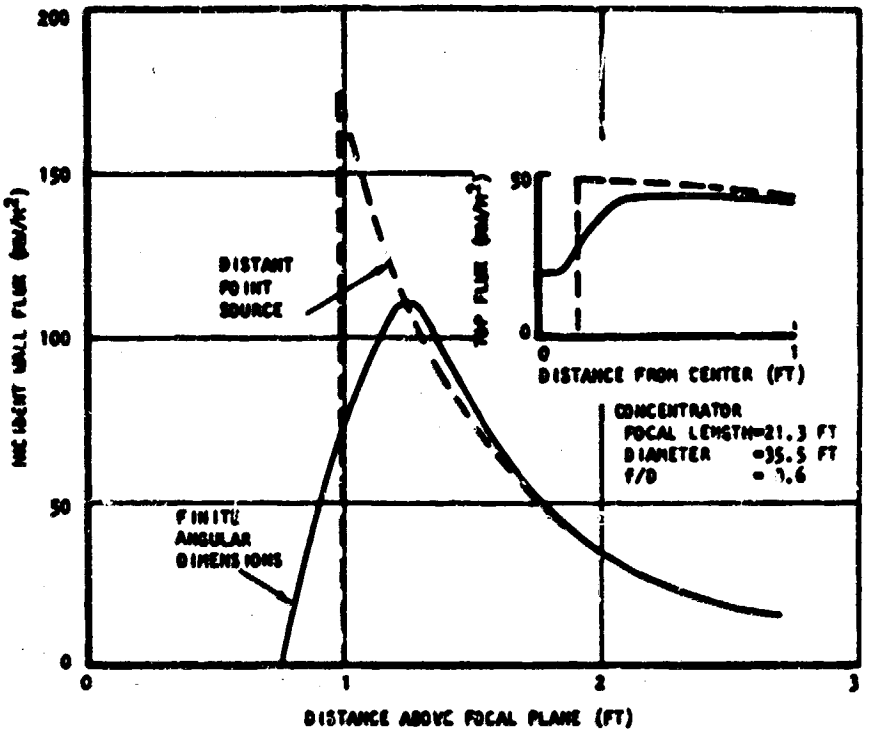

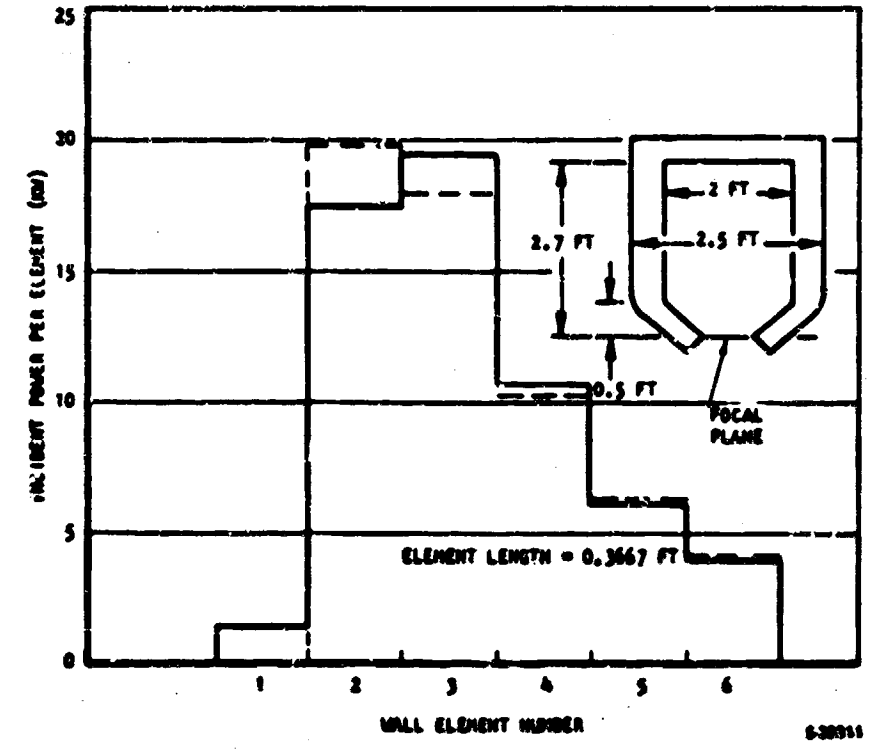

Figure 3-5. Comparison of Parallel Ray and Cone Optics Models

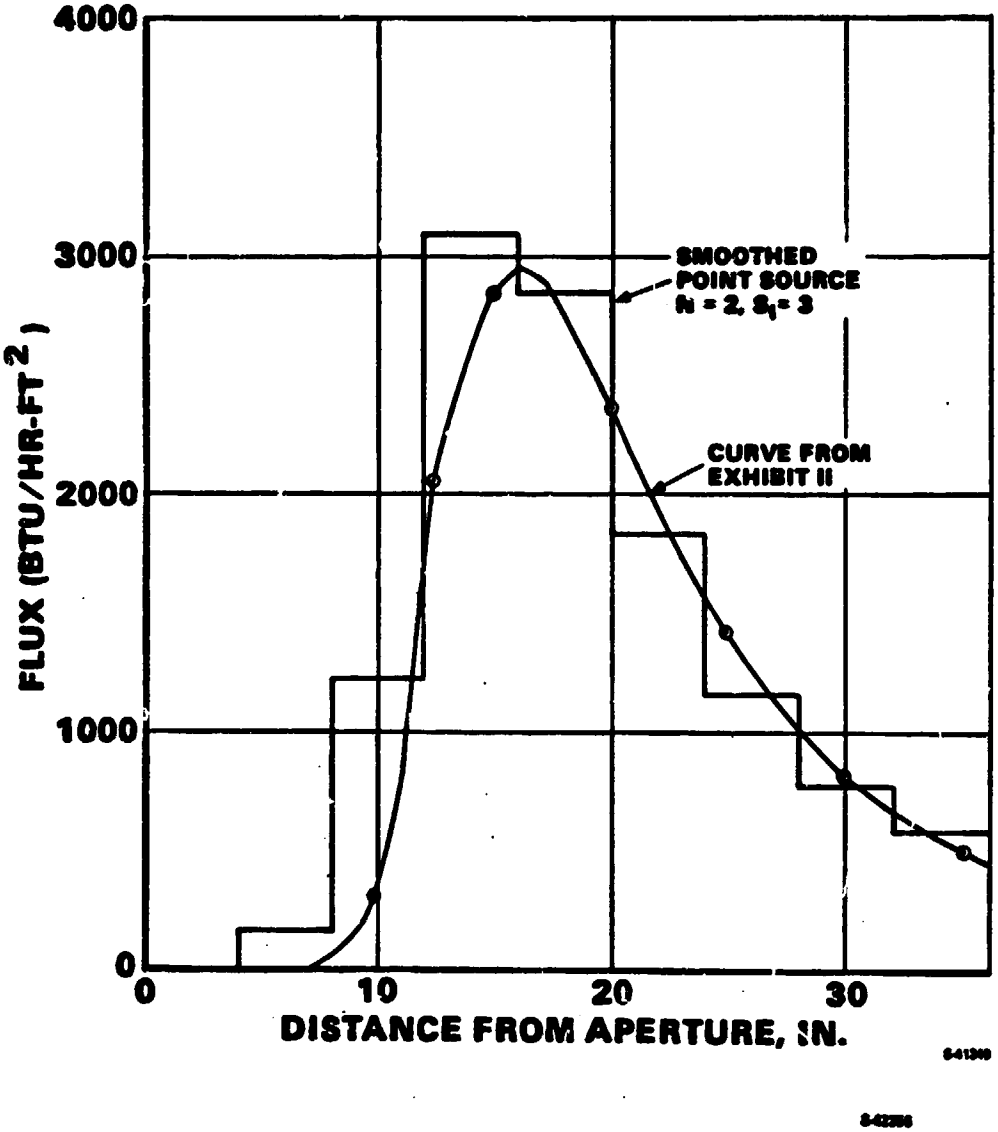

Figure 3-6. Comparison of AiResearch and JPL Flux Plots for a 12-in. Radius Cylinder

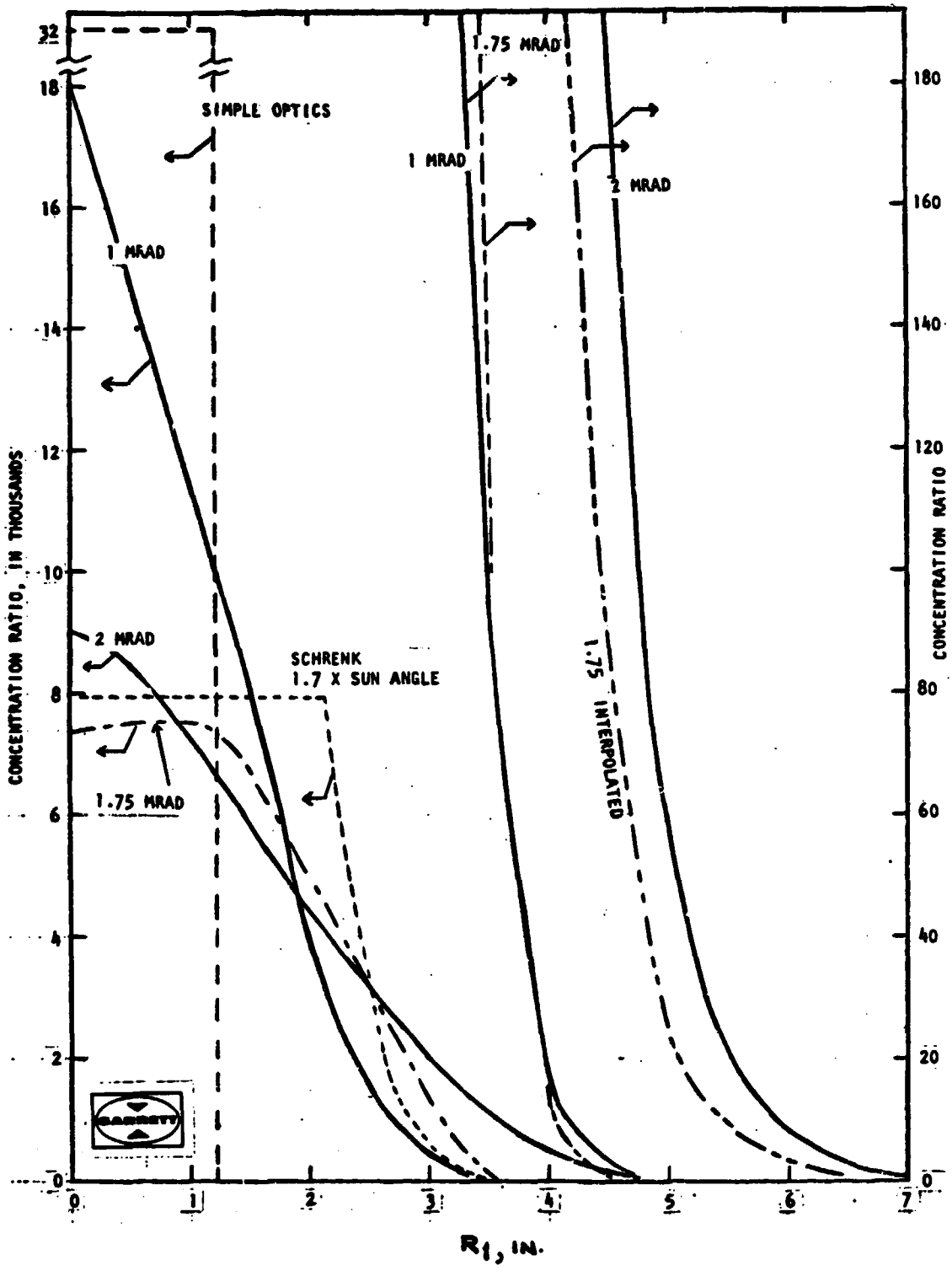

Figure 3-7. Aperture Flux Plots

3.1.2 Final Design

The SRSR was designed with several objectives in mind: The maximum cavity efficiency was desired. The metal temperatures had to be kept under certain limits for acceptable receiver life. The pressure drop was intended to be below a certain value so that system performance would not be significantly affected. The weight of the unit was kept to a minimum to keep the receiver support system simple. The basic parametric analysis of the receiver involving these variables was performed during Phase I.

Phase II specifications required changes in the receiver; these alterations were guided with the aid of the parametric study. As a result, a solar receiver was defined which had the characteristics shown in Table 3-1.

Conduction, convection, and radiation losses were calculated. Conduction losses through the insulation were calculated to total approximately 1.2 KWth. External convection and radiation losses to the air environment were estimated at 2.5 KWth. Radiation losses from a 9-inch diameter aperture were approximately 1.3 KWth. These figures were based on an 85 KWth input from a concentrator with a receiver efficiency of 94%.

The pressure drop calculated for the primary-reheat mode and primary mode only were in the range of 2- to -10 percent per coil. These numbers satisfied the conditions required in the problem statement for Phase II.

A finite element method of analysis was used to estimate the receiver performance. AiResearch developed a computer program that uses the SRSR model shown in Figure 3-8.

Incident solar flux on the inner surfaces of the receiver was computed by assuming parallel rays from the sun (point source) as being reflected from a perfect parabolic concentrator. The resulting flux profile was smoothed out (Section 3.1.1 Optical Modeling) and represented in a histogram input to the computer program for computation of the radiation interchange, fluid heat transfer, and pressure drop.

The computer program handles liquid heating, boiling, and vapor superheating heat transfer modes on the cylindrical core with uncooled front and back ends. Radiation interchange computations were based on the assumption of flat surfaces, an equal solar absorptance and infrared emittance of 0.80, and diffuse radiation (both reflected solar and emitted infrared). Also, the heated surface of the tubes was assumed to be one-third (120 deg) of the total tube outside area.

Heat transfer to the fluid inside the tube in the subcooled liquid and the superheated vapor regions was computed from Colburn modulus versus Reynolds number data for flow in round trubes. A tube-length-to-diameter ratio of L/D = 25 was used to account for the effects of tube coil curvature. In the boiling region, the John Chen correlation was used for a steam quality of up to 70 percent. Vapor heat transfer coefficients were used thereafter.

TABLE 3-1

RECEIVER SELECTED FOR DETAILED ANALYSIS

As a result of Phase I Parametric Study and Phase II Reevaluation

- Cavity Size

  D_{cyl} = 17 in.

  L_{cyl} = 21.5 in.

  L_o = 2.5 to 4

  D_a = 7 to 12 in.

- Insulation Thickness

  Open end and cylinder (tc), 4 in.
  Closed end (te), 6 in.

- Tube Size

Primary	7/16 in. OD x .070 in. wall
Reheat	3/4 in. OD x .125 in. wall

- Location of Reheat Outlet

  Adjacent to primary outlet

- Materials

  Tubes, Inconel 625
  Insulation, cerablanket 8 lb/ft^3
  Aperture plate, 0.28 in. SIC ceramic
  Reflector plate, 0.28 in. SIC ceramic

- Surface Emissivity, .80

- Outside Environment

  70°F and 30 mph wind

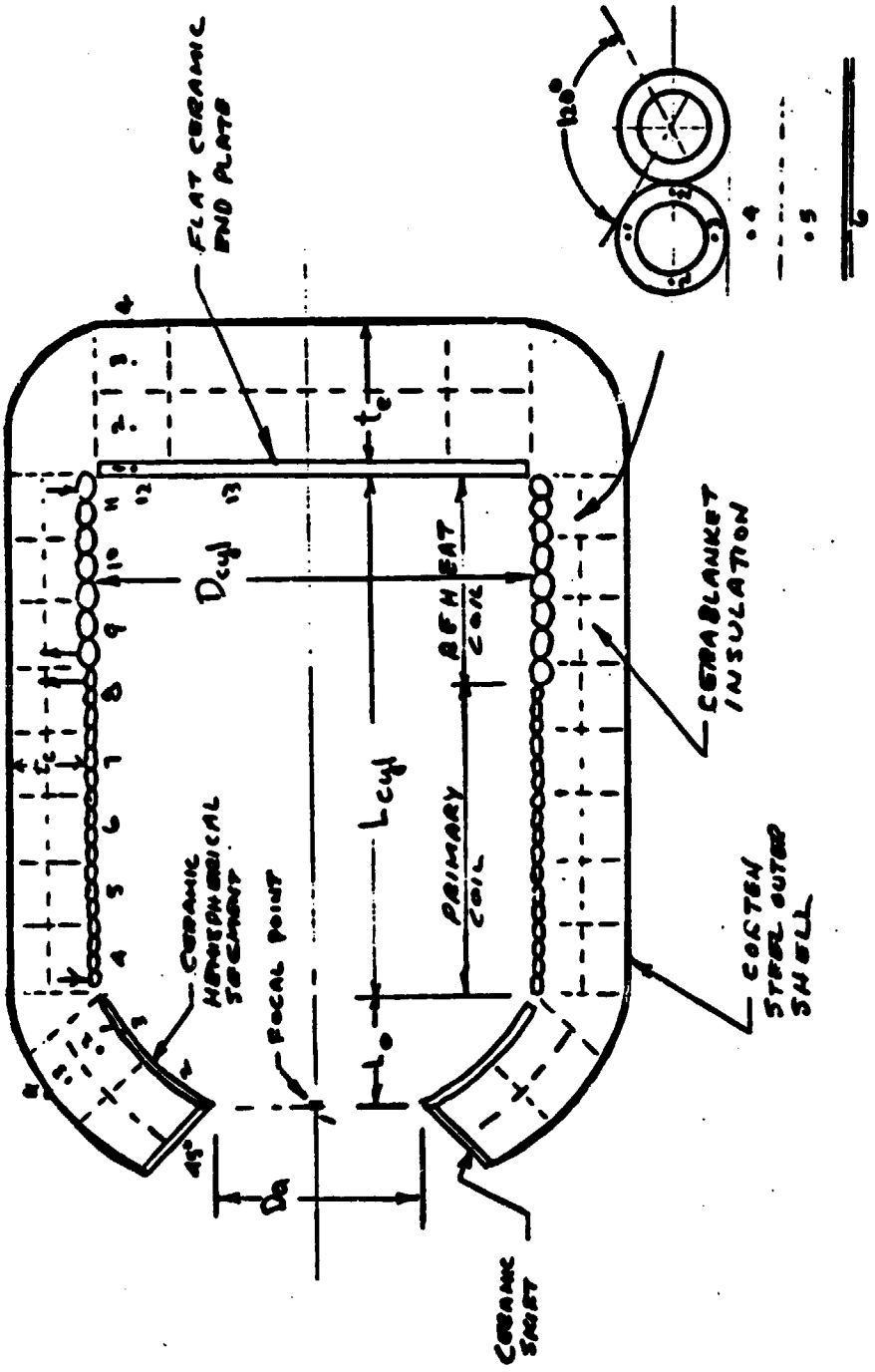

Figure 3-8. Computer Model for Thermal Analysis

Pressure drop in the liquid and vapor regions was computed from Fanning friction factor versus Reynolds number data for round tubes having an L/D = 25. Pressure drop in the boiling region resulting from momentum change and friction losses was computed with the Lockhart and Martinelli correlation for two-phase flow pressure drop. Stable and homogeneous flow was assumed.

The program is capable of handling several modes of operation as described in Table 3-2.

3.1.3 Heat Flux Sensitivity Analysis

The smoothed incident flux profile described in Section 3.1.2 (Final Design) of this report constitutes the baseline flux. It was used for the sensitivity analysis of various possible incident flux profiles caused by concentrator irregularities.

This analysis examined the effect of both symmetric (flux profiles which vary in the axial direction only) and asymmetric incident solar fluxes on the receiver. The symmetric incident fluxes include the baseline flux and axially shifted flux profiles with reduced peak flux patterns. The asymmetric flux patterns, in one case, offset the receiver ± 1 inch, and in another case, reduced the input (10% less total power) from one-half of the concentrator.

A sensitivity analysis based on two assumed symmetrical incident flux profiles was performed; it considered the cylindrical section of the receiver only, with no ends involved.

The first or baseline flux profile, (Figure 3-9) approximates the input from a collector having a slope error of approximately 2-mrad. This results in a receiver design in which the primary and reheat outlets are located about 14.6-inches from the front end of the cylindrical section. The cavity wall temperature profile resulting from this baseline flux is shown in Figure 3-10. Tube wall nodal temperatures along the cavity wall are summarized in Table 3-3 for the baseline flux, primary-reheat configuration. The second flux profile is a greatly exaggerated maldistributed incident heat flux profile--the peak flux was reduced by 25 percent and shifted about 8-inches further toward the closed end. This distribution results in a location of the two outlets at about 16.9-inches from the front end, (2.3-inches closer to the closed end than in the first coil). This situation seemed to indicate that axial variation in incident solar flux can be accommodated by using a separate design for each type of solar flux input or by installing a movable coil that can be adjusted either forward or aft to a position that results in equal steam outlet temperatures from the primary and reheat coils.

A revised analysis based on a third heat flux profile was also made. This profile was similar to the first profile mentioned above except that the incident peak flux was lowered by about 20 percent; the location of the peak was shifted axially about 3-inches further towards the closed end; and the incident flux on the rear portion of the cylindrical section was increased by about 50 percent. Figure 3-11. In this case, the two steam outlets must be located about 15.6-inches from the front end of the cylinder to obtain equal outlet steam temperatures. If the two steam outlets are not relocated, but are

TABLE 3-2

COMPUTER PROGRAM MODEL

Options

- Primary only
- Dual Mode

  -Primary plus reheat

    Reheat inlet at closed end
    Reheat exit at closed end

  -Equal or unequal tube sizes

  -Primary and reheat coils in series

Heat Input

- Smoothed point source from collector
- Arbitrary symmetrical heat rate input for each surface node

Heat Transfer and Pressure Drop

- Tubes heated on one side (1/3 of surface)
- Radiation interchange based on grey body radiosity network
- Axial heat conduction neglected
- Single phase heat transfer

  -Basic flow friction and heat transfer

- Boiling

  -Chen correlation with completely wetted wall to 70% quality

  -Lockhart/Martinelli two phase flow ΔP

ORIGINAL PAGE IS
OF POOR QUALITY

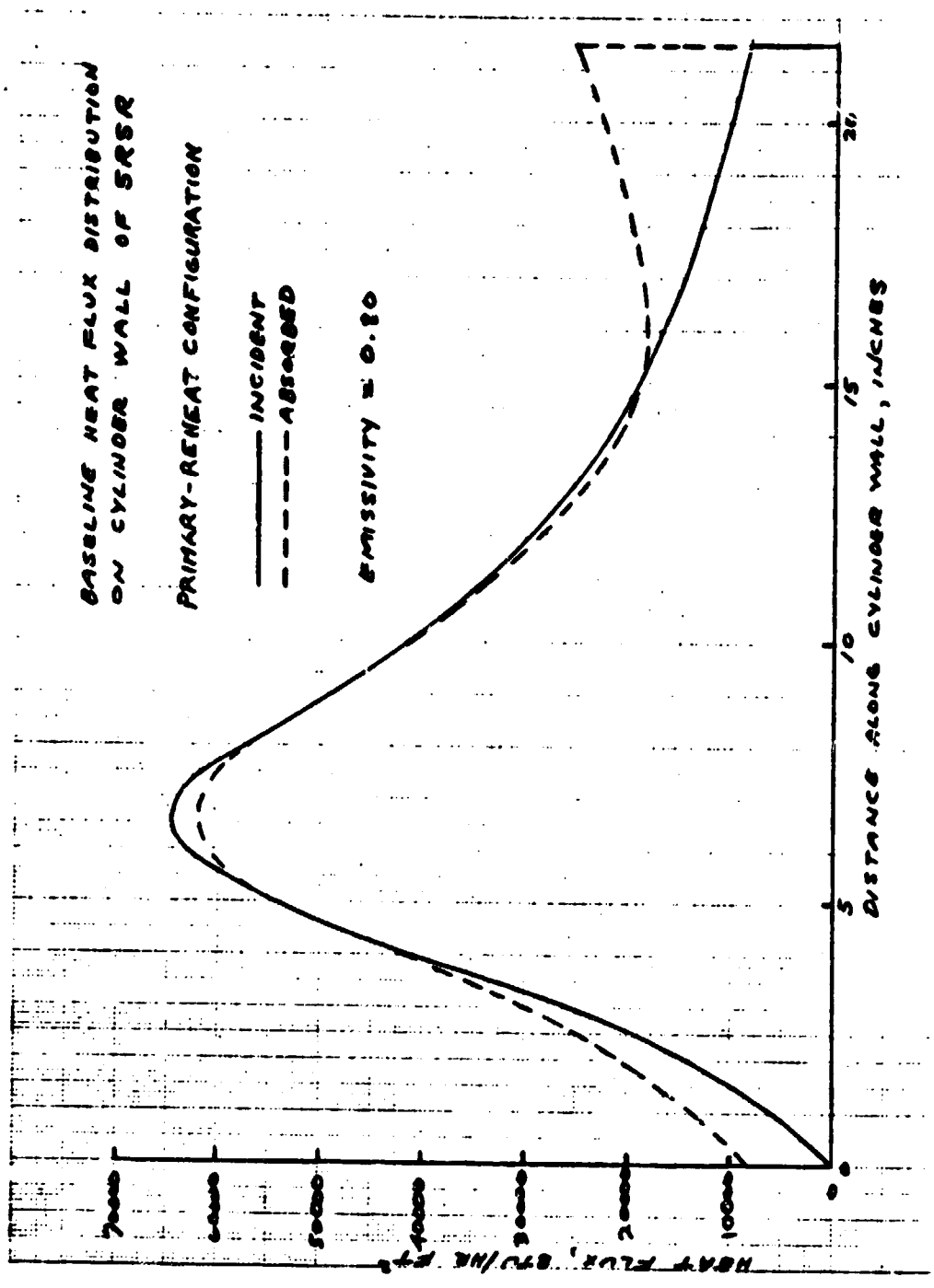

Figure 3-9. Baseline Heat Flux Distribution, Primary-Reheat Mode

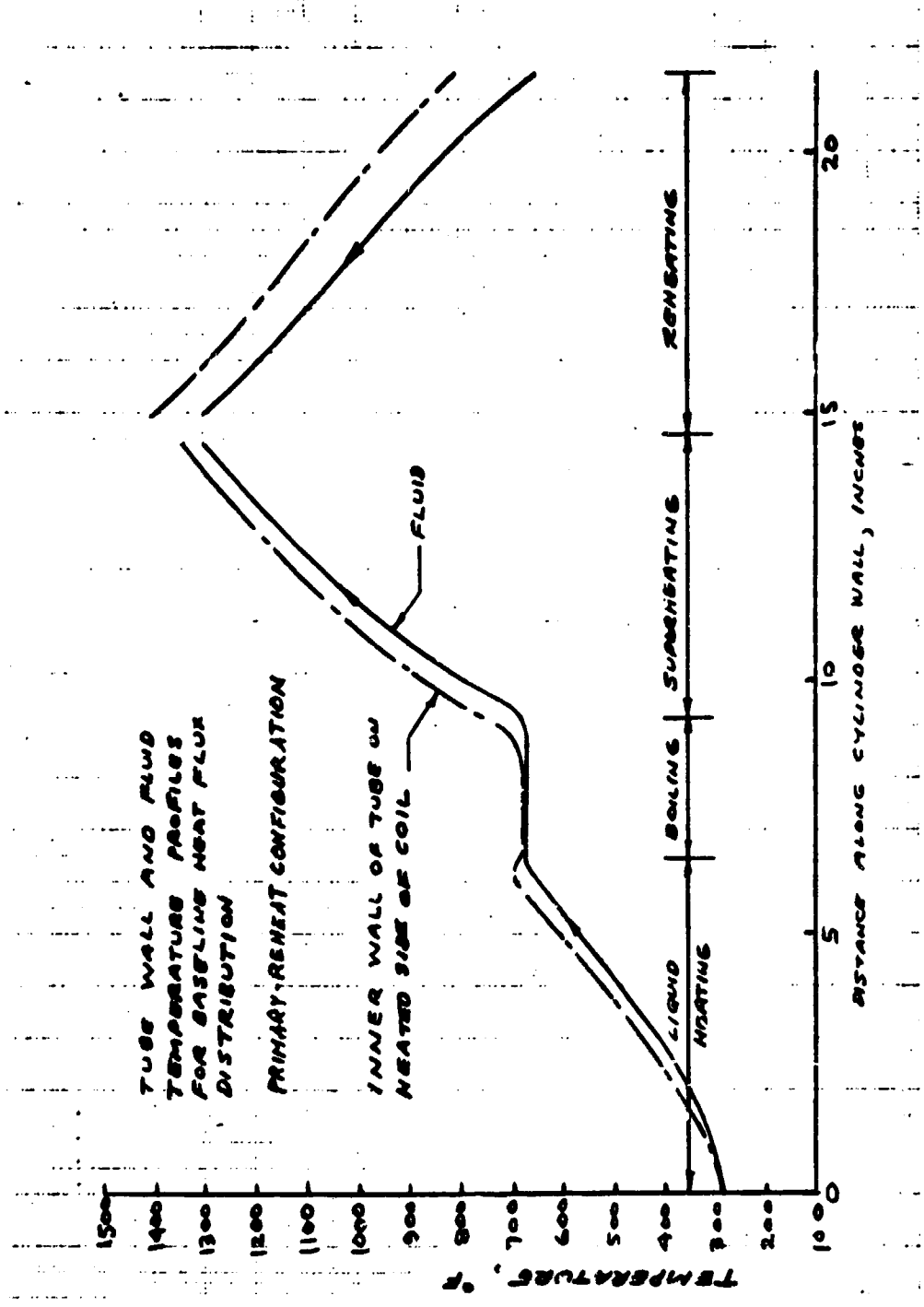

Figure 3-10. Temperature Profiles for Baseline Heat Flux

TABLE 3-3

SUMMARY OF AXIAL AND CIRCUMFERENTIAL TUBE WALL TEMPERATURES FOR THE BASELINE ABSORBED HEAT FLUX DISTRIBUTION CASE

Axial Distance From Primary Inlet in.	Fluid Temp °F	Wall Temps at Indicated Nodes, °F				
		1	2	3	4	5
0.2	280	295	-	-	-	282
1.3	318	340	336	332	327	321
3.9	481	538	528	517	504	492
6.7	670	704	689	673	671	670
9.6	740	854	843	831	827	823
12.1	1080	1181	1174	1167	1153	1138
14.4	1300	1353	1346	1339	1325	1310
14.9	1300	1420	1411	1401	1384	1364
17.2	1066	1188	1180	1171	1153	1133
20.3	785	941	931	920	898	874
21.1	650	850	-	-	-	775

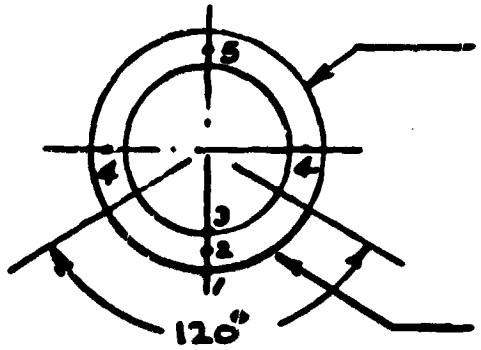

Unheated and Insulated Rear Half of Tube Wall

Heat Portion of Tube Wall

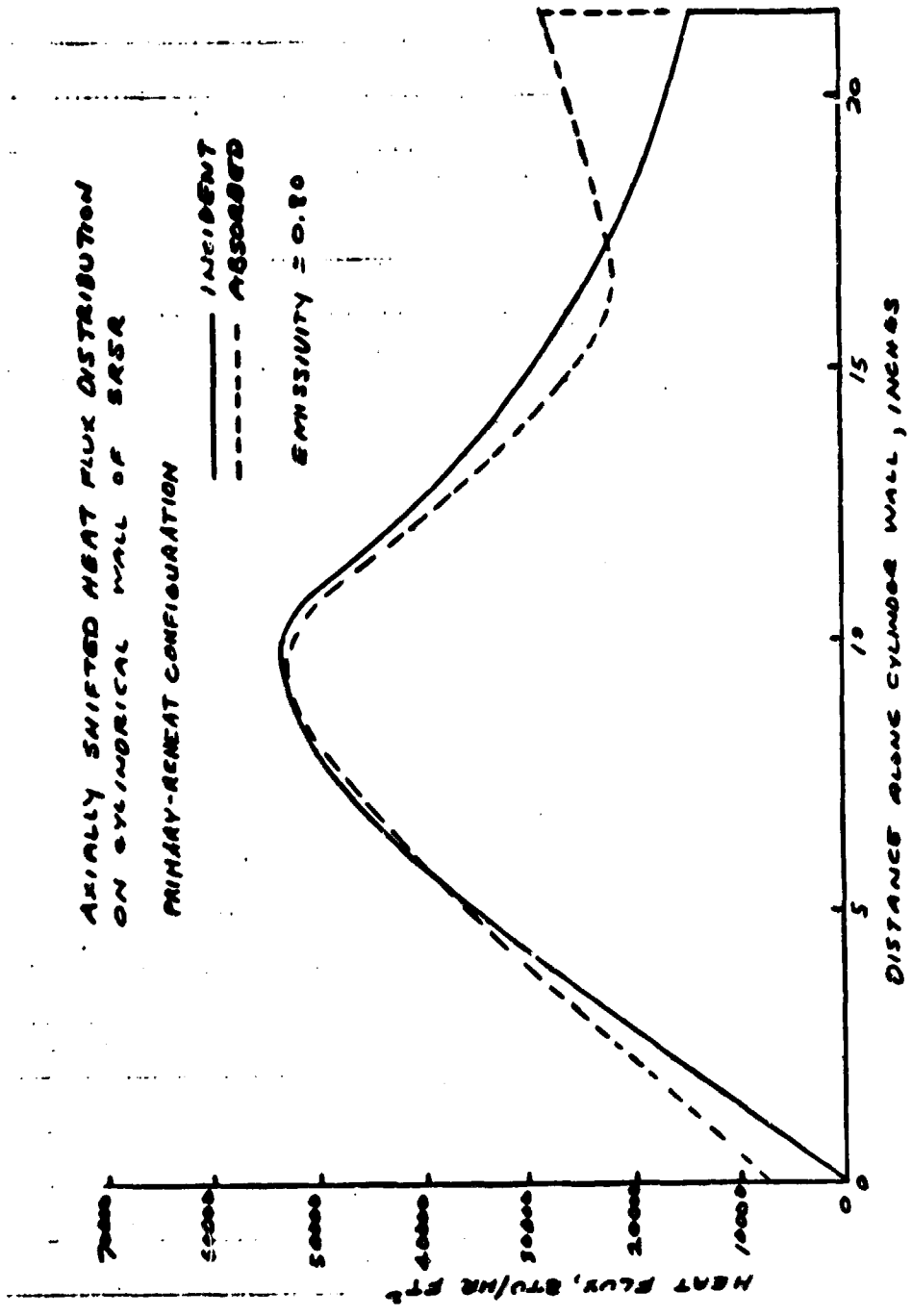

Figure 3-11. Axially Shifted Heat Flux Distribution

left the same as for the baseline flux case (14.6-inches from the front of the cylinder), a temperature mismatch of about 210°F will exist between the reheat and primary steam outlets. Also, the reheat maximum wall temperature will be increased from 1440° to 1570°F. Figure 3-12.

The solution to any temperature mismatch resulting from axially shifting the incident heat flux is to install a movable back plate at the closed end of the cavity. The large mismatch described above can be eliminated by moving the back wall forward by only about 1.5-inches. Figure 3-13. The final design will incorporate a movable back plate so that a portion of the reheat coil can be covered or uncovered by the amount needed to equalize the steam outlet temperatures. Figure 3-14. Thus, any axial shift in incident heat flux distribution can be accepted.

The effects of asymmetric heat flux caused by a ±1 inch offset of the receiver from the optical axis are acceptable. The resulting absorbed heat profiles are plotted in Figure 3-15, and wall temperatures in Table 3-4.

The cavity was divided into 12 axial nodes of equal length and 12 circumferential equal nodes. The No.1 circumferential node is the closest to the focal point. The absorbed heat flux is very pronounced at axial node No. 3 (boiling regime) and it is here that the peak flux takes place. The heat distribution for any axial node behaves symmetrically with respect to the circumferential node No. 1. In the superheating region, the heat is more uniformly distributed among the circumferential nodes. For example, axial node No. 9 shows an absorbed heat variation of from 1150 Btu/hr to 1550 Btu/hr. For this same axial location, the baseline flux shows a constant heat input of about 1375 Btu/hr (Figure 3-9). By comparing these two cases, a circumferential variation between +12.7% and -16.3% is determined; thus, approximately the same total heat input applies to both symmetrical and 1-inch offset asymmetrical cases.

The flux distribution curves for nodes 4 through 12 in Figure 3-15 also show a depression along the circumferential node No. 1. This is caused by the apparent shifting effect that the heat distribution on the two halves of the receiver undergoes with respect to each other (the closest and furthest halves to the focal point). This is due to the offsetting of the cavity.

The second asymmetric flux input analyzed had a heat input reduction originating from half of the concentrator, with full power input originating from the other half of the concentrator. The total power input to the receiver was decreased by 10%. In this case, the working fluid flow must be reduced in order to maintain the required outlet temperature. It is also evident that the maximum tube wall temperature occurs on the side of the cavity that receives the normal (non-reduced) heat flux. This case has less effect on the receiver than the 1-inch offset condition, which was acceptable. This analysis is summarized in Table 3-5. Canting of the receiver at an angle of ±0.25° from the optical axis is also acceptable. Any combination of the above mentioned axially shifted and asymmetric incident heat flux profiles can be accepted, provided the back plate is positioned to equalize the primary and reheat steam outlet temperatures.

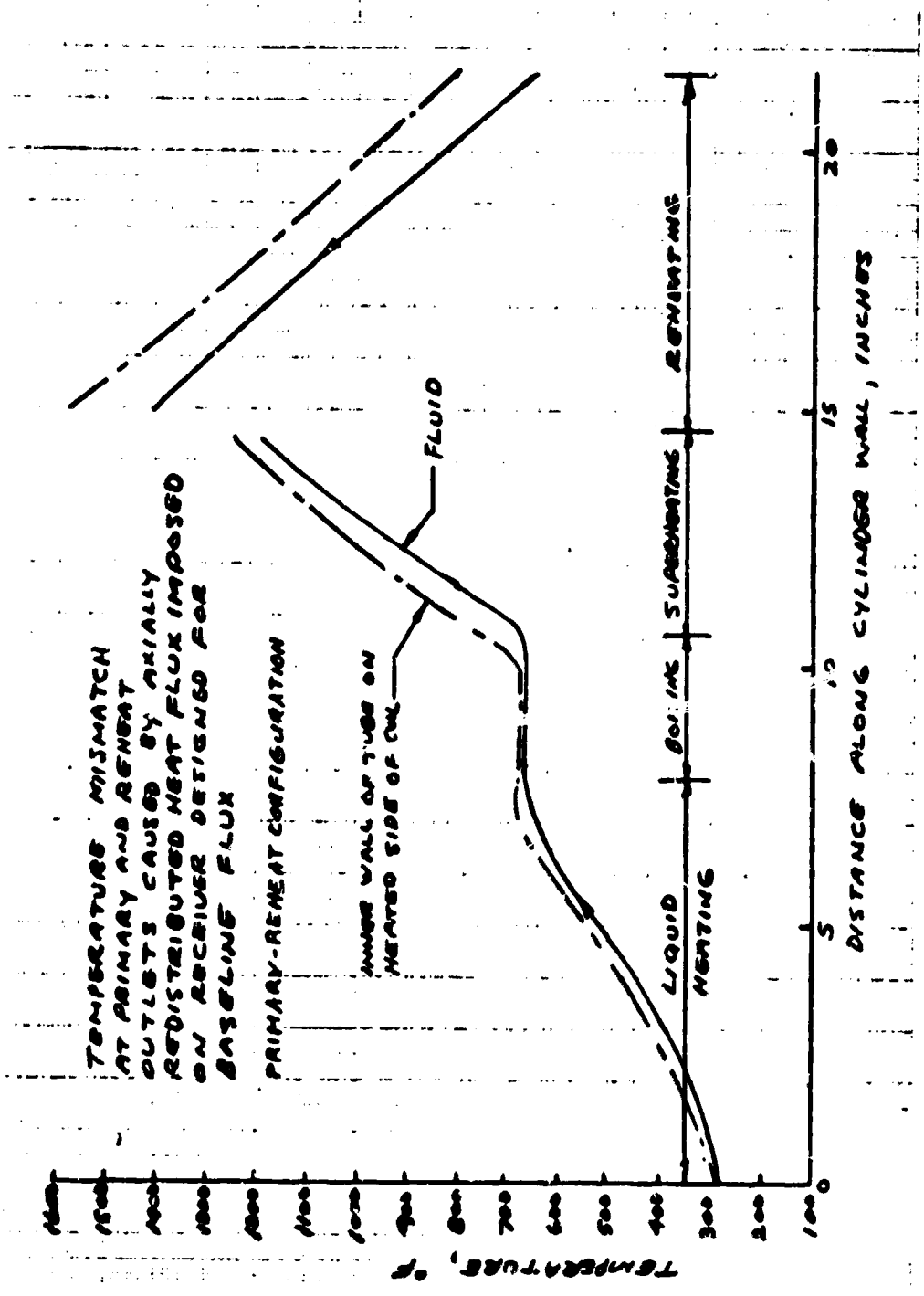

Figure 3-12. Temperature Profile Mismatch

ORIGINAL PAGE IS
OF POOR QUALITY

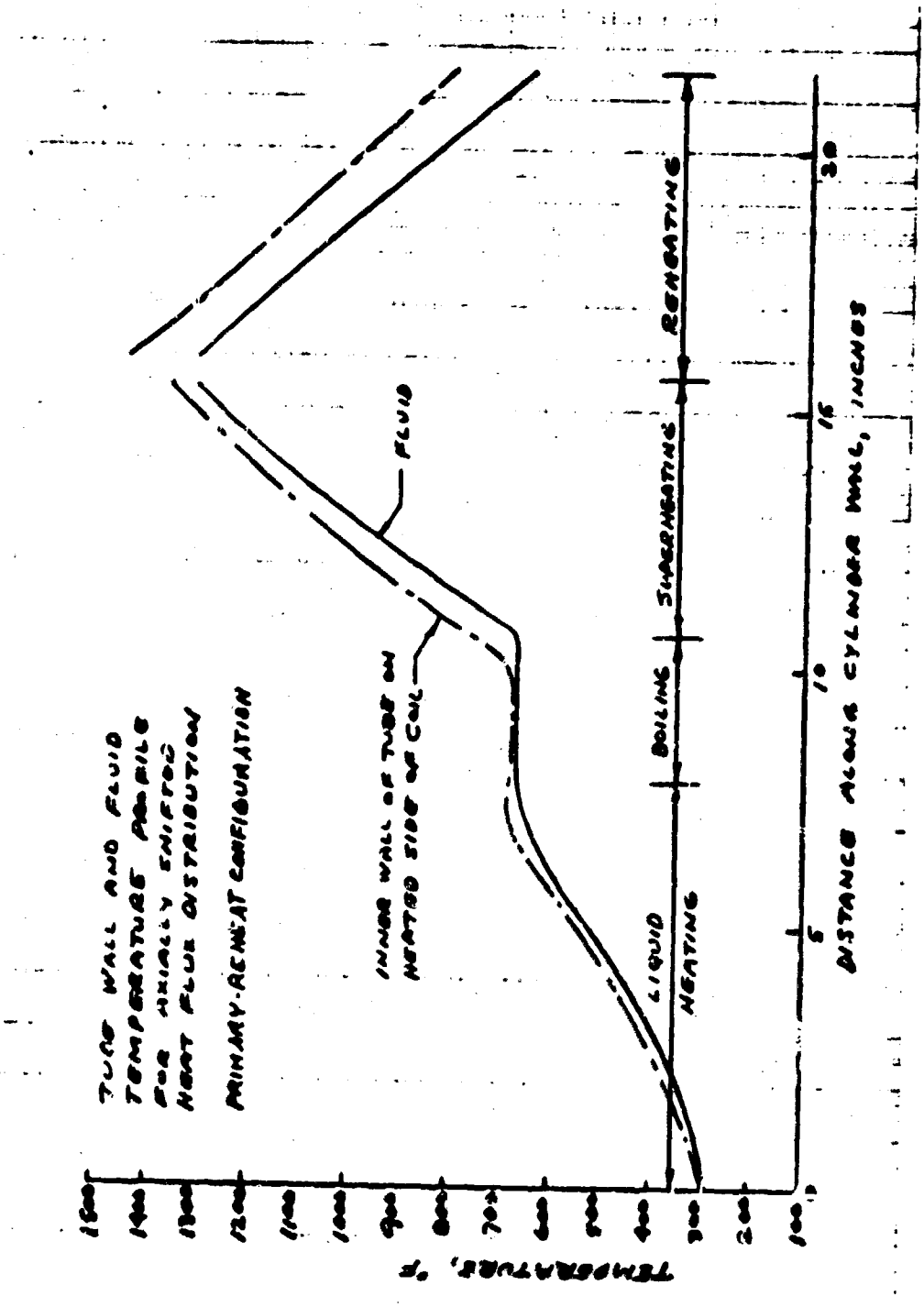

Figure 3-13. Temperature Profile Correction

SOLUTION TO TEMPERATURE
MISMATCH AT PRIMARY AND REHEAT OUTLETS

Cause: Axially Shifted Incident Heat Flux

Solution: Movable Back Plate

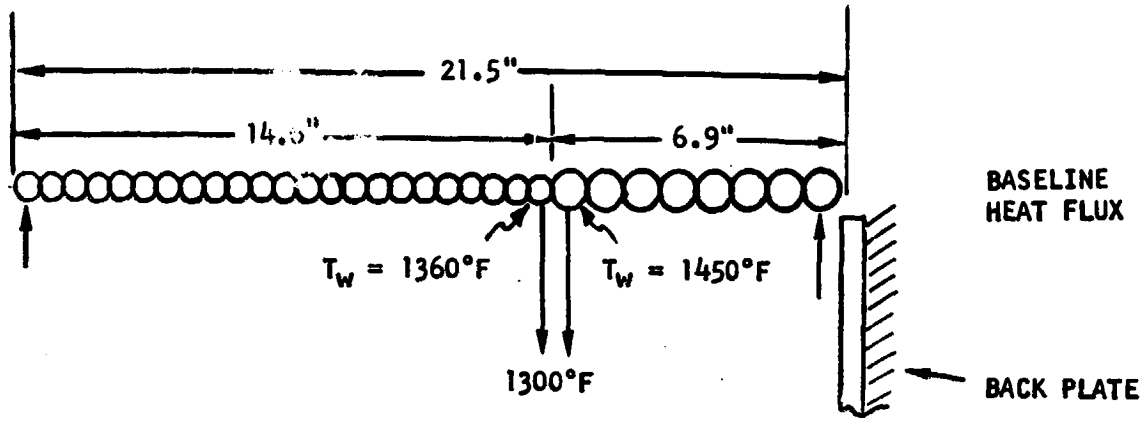

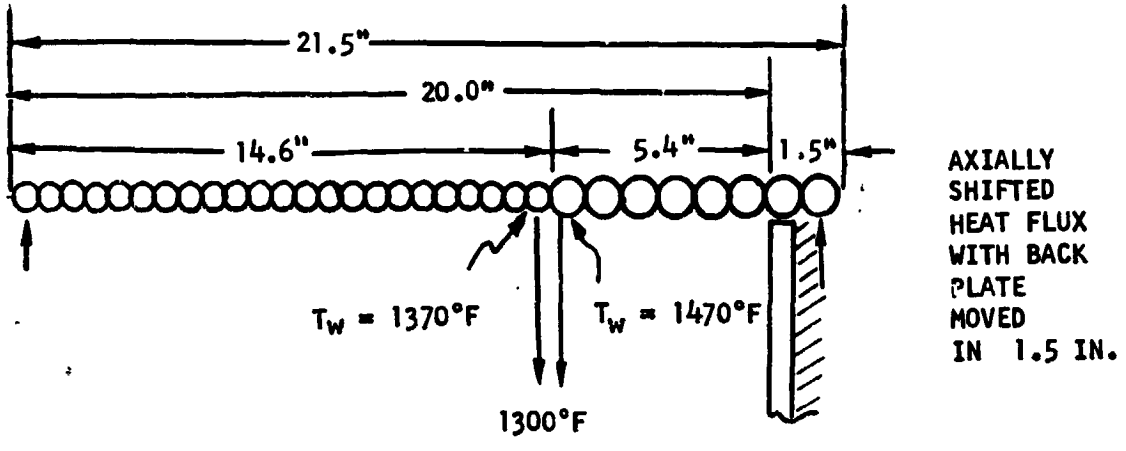

SLIGHTLY HIGHER TUBE WALL TEMPS

SAME ΔP

Figure 3-14. Movable Reflector Plate

ORIGINAL PAGE IS
OF POOR QUALITY

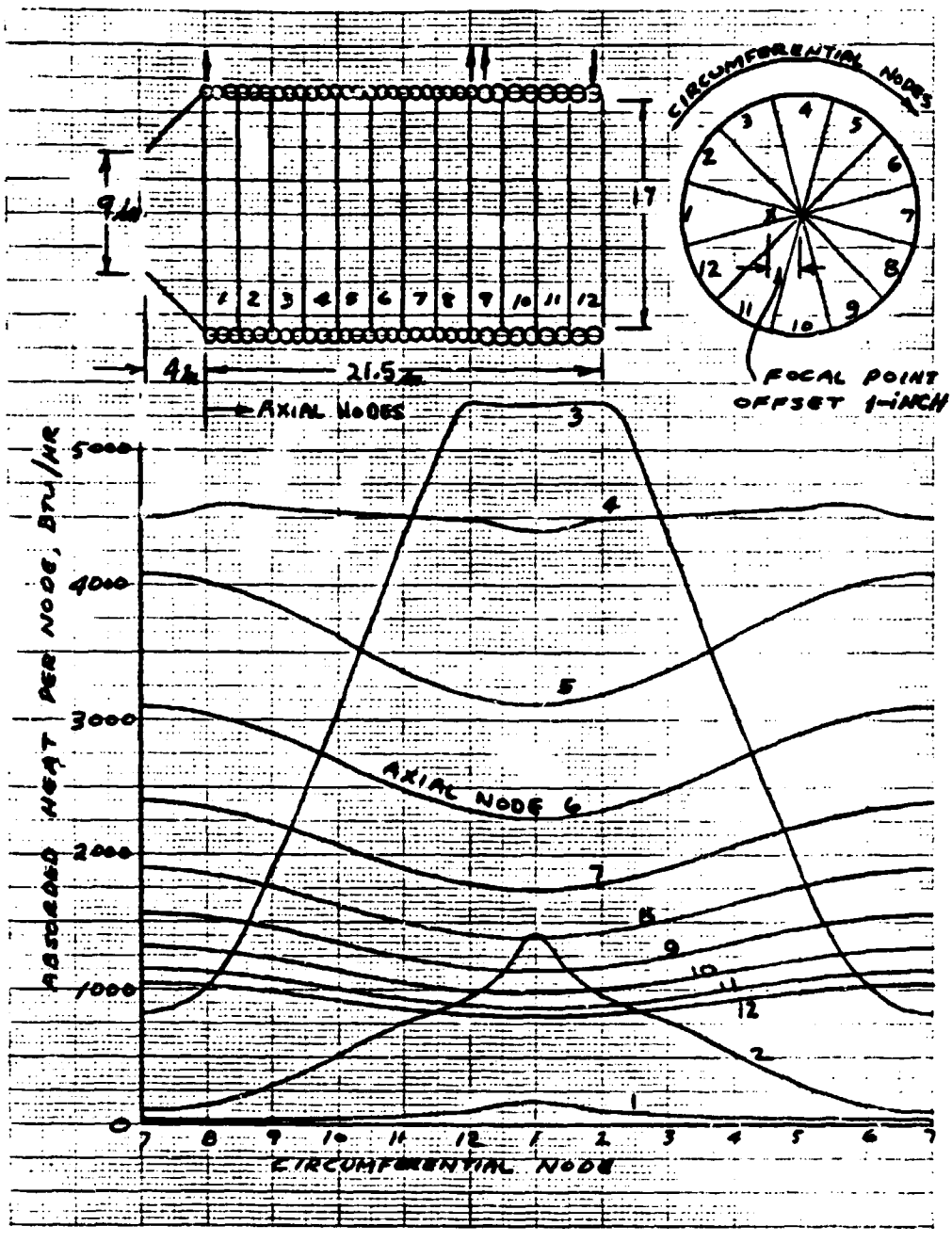

Figure 3-15. Asymmetrically Shifted Heat Flux Distribution Due to One-Inch Cavity Offset at Baseline Incident Heat Flux Condition

TABLE 3-4

ASYMMETRIC HEAT FLUX INPUT DISTRIBUTION EFFECTS

- Incident flux determined by smoothing of point source flux from perfect parabolic concentrator
- Concentrator characteristics

  Diameter = 37.2 ft
  Focal length/diameter = 0.60
  Reflectivity = 0.86
  Solar flux = 310.5 Btu/hr
  Total power reflected = 85 kwth

- Receiver offset ±1 in. from optical axis

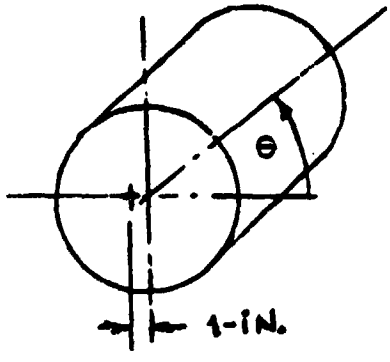

Coil

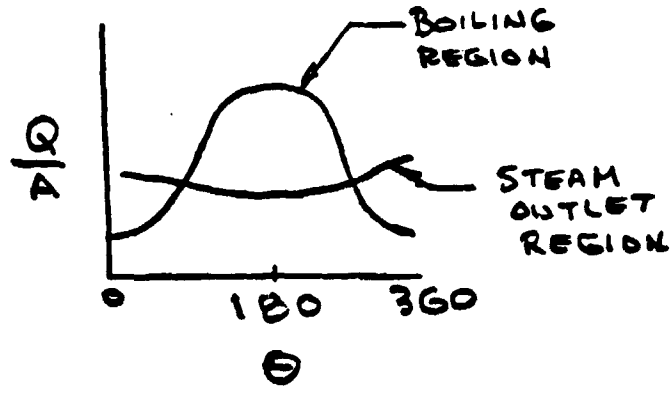

Flux Patterns

CIRCUMFERENTIAL TEMPERATURE VARIATIONS (°F)

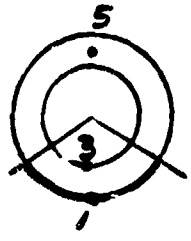

Region		Boiling	Primary Outlet	Reheat Outlet
Angular Position, θ		0 180	0 180	0 180
Portion of Tube	1. Heated surface	670 - 740	1345 - 1360	1400 - 1440
	3. Fluid side	670 - 675	1330 - 1345	1385 - 1415
	5. Back wall	670 - 670	1305 - 1315	1360 - 1385

TABLE 3-5

REDUCED INPUT FROM ONE-HALF OF CONCENTRATOR

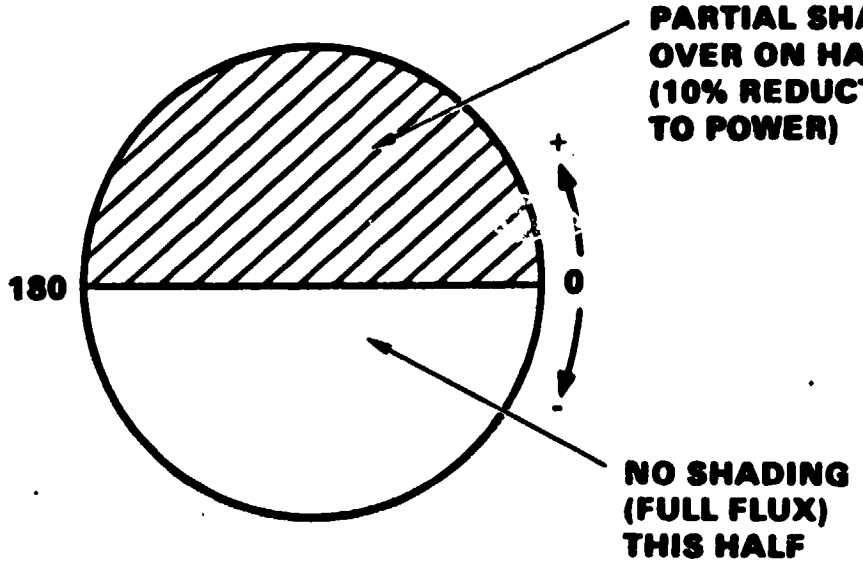

CONCENTRATOR

- EFFECTS ON RECEIVER
  - 10% REDUCTION IN FLOW TO MAINTAIN SAME STEAM OUT TEMP
  - MAX WALL TO FLUID ΔT DECREASED BY 2 °F (0 TO 180 DEG)
  - MAX WALL TO FLUID ΔT INCREASED BY 9 °F (0 TO -180 DEG)
  - LESS THAN OFFSET RECEIVER

S-43134

For the all-primary configuration in the steam-electric application, the receiver is less sensitive to heat flux irregularities. Since the primary section outlet steam is returned directly to the adjacent reheater tube and exits the reheater from the closed end, there is no temperature mismatch between the primary and reheater sections. The baseline flux profile is shown in Figure 3-16, and the resultant temperatures in Figure 3-17.

3.1.4 Process Heat Applications

AiResearch was asked to examine ways in which the Steam Rankine Solar Receiver (SRSR) could be used to produce process heat for various industrial uses. The conditions supplied by JPL were inlet water at 70°F, and outlet steam at 50,100 and 150 psia with 50 and 100°F superheat at each pressure.

Two techniques utilizing the SRSR to produce process steam were studied. One technique, called Pressurized Water Receiver (PWR), uses the existing receiver to heat water at 2500 psia to 668°F. The flow-rate is increased from 157 lb/hr (the steam/electric application flow-rate) to 640 lb/hr to prevent fouling in the receiver. The hot, pressurized water is pumped through a steam generator, which boils and super heats treated tap water to produce 227 lb/hr of process steam at the conditions described. The cooled pressurized water from the steam generator is pumped back to the receiver in a closed loop. The relationship of the receiver in the pressurized water receiver system is shown in Figure 3-18. The thermodynamic process path for the PWR is shown in Figure 3-19. The steam generator used in the PWR system is detailed in Figures 3-20 and 3-21.

The other technique, called a Recirculation Boiler Receiver (RBR), uses the same receiver except for a new coil. Treated tap water is pumped into the receiver, boiled to 15 percent quality, and piped to a vapor/liquid separator. The vapor is separated and piped back to the receiver super heat section to produce process steam. The water from the separator is pumped back to the receiver, where it is mixed with make up tap water before undergoing the boiling process. The new coil consists of 1/2-inch O.D. x .049 wall tubing having a mean diameter of about 19-inches and an overall length of 24-inches. The operating pressure is about 250 psia, which can be throttled down at the exit to produce the desired process steam conditions. Figure 3-22. The coil material is 304 stainless steel. Both of these techniques require the use of a liquid/vapor separator.

3.1.5 One-Half Power Foreshortened Coil

The capacity of the receiver can be reduced by up to 50 percent (42.5 Kwth) by removing and replacing the tubular coil with a new foreshortened coil and by adding insulation in the closed end. The mean diameter of the coil would remain the same (17-3/4 inches). Also, the movable back plate mechanism would have to be repositioned to accommodate the foreshortened coil.

The overall length of the new coil is one-half that of the full power coil, and the tubing size must be reduced to maintain the same fluid mass velocities. Consequently, the primary coil tube size must be reduced from 7/16 O.D. x 0.070 wall to 5/16 O.D. x 0.048 wall, and the reheat coil tube size must be reduced

ORIGINAL PAGE IS
OF POOR QUALITY

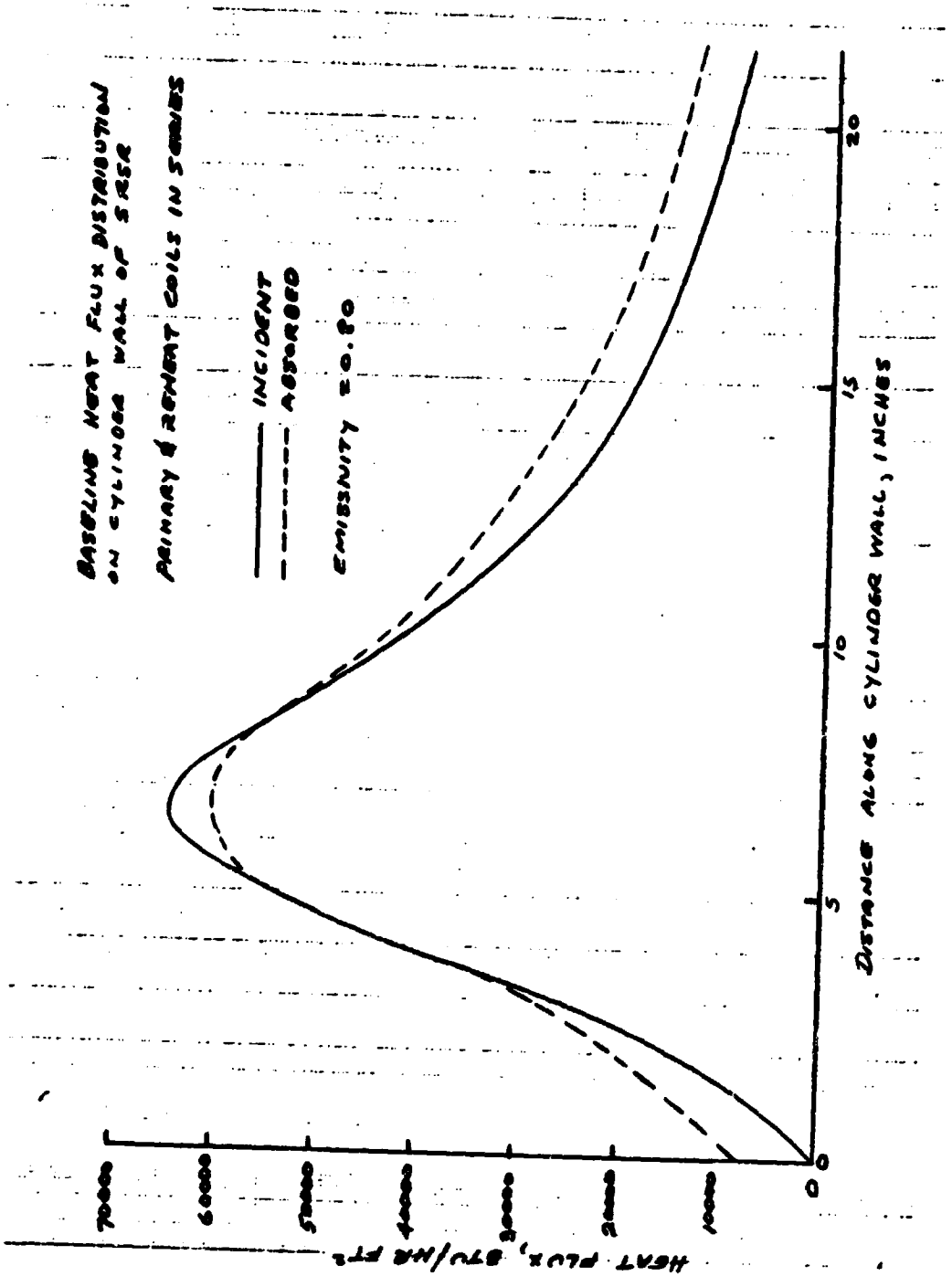

Figure 3-16. Baseline Heat Flux Distribution, All-Primary Mode

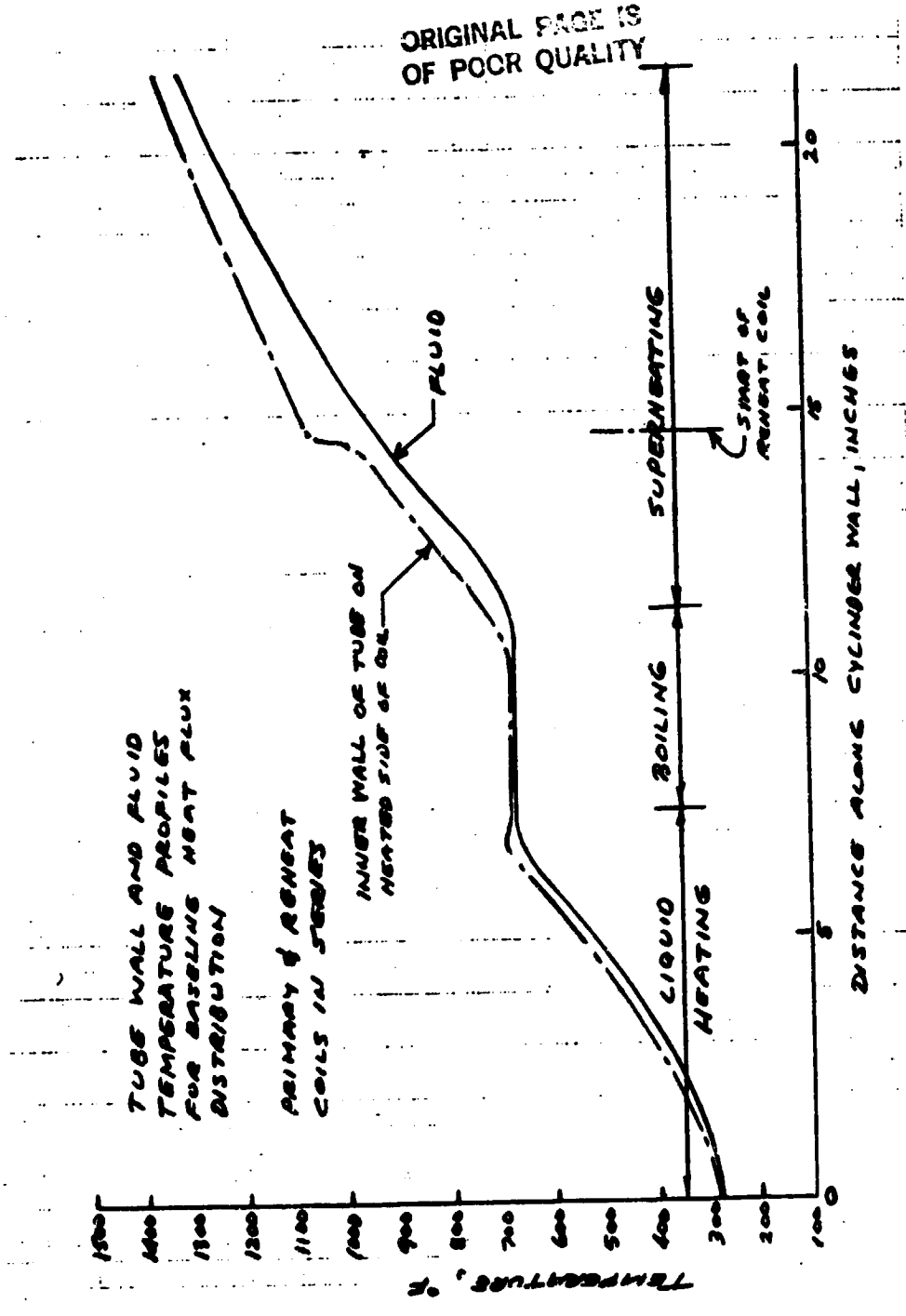

Figure 3-17. Temperature Profiles for Baseline Heat Flux, All-Primary Mode

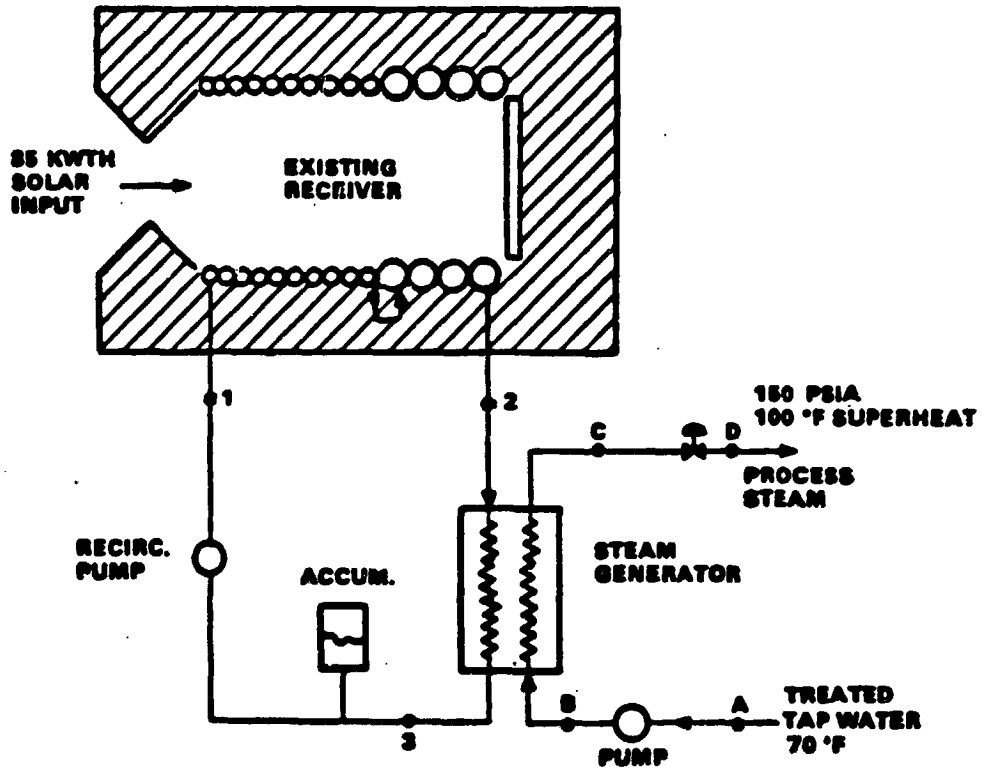

Figure 3-18. Pressurized Water Receiver (PWR) Schematic, For Process Steam

PWR FLOW = 640 LB/HR
STEAM FLOW = 227 LB/HR

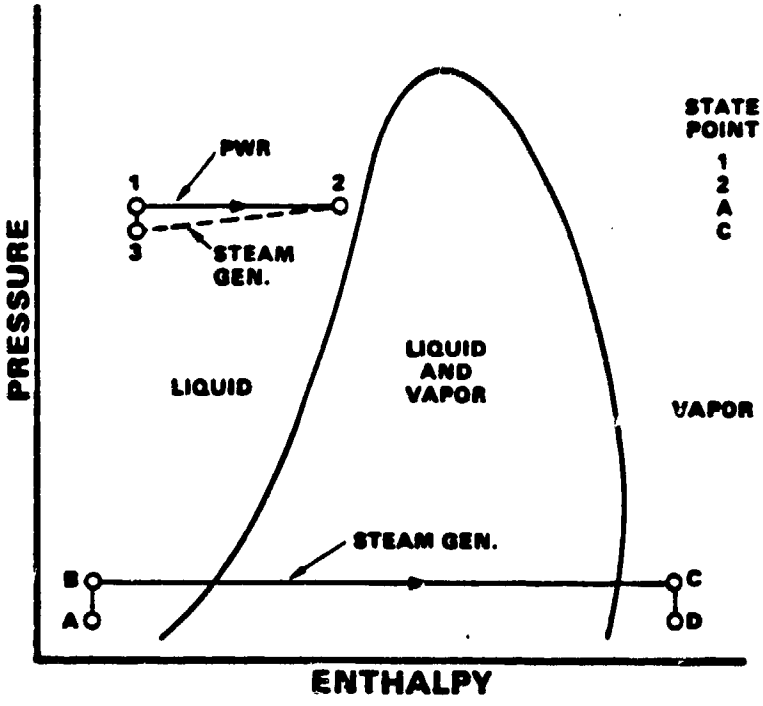

STATE POINT	PRESS PSIA	TEMP °F
1	2,510	305
2	2,500	668
A	14.7	70
C	150	480

Figure 3-19. PWR Thermodynamic Process Path

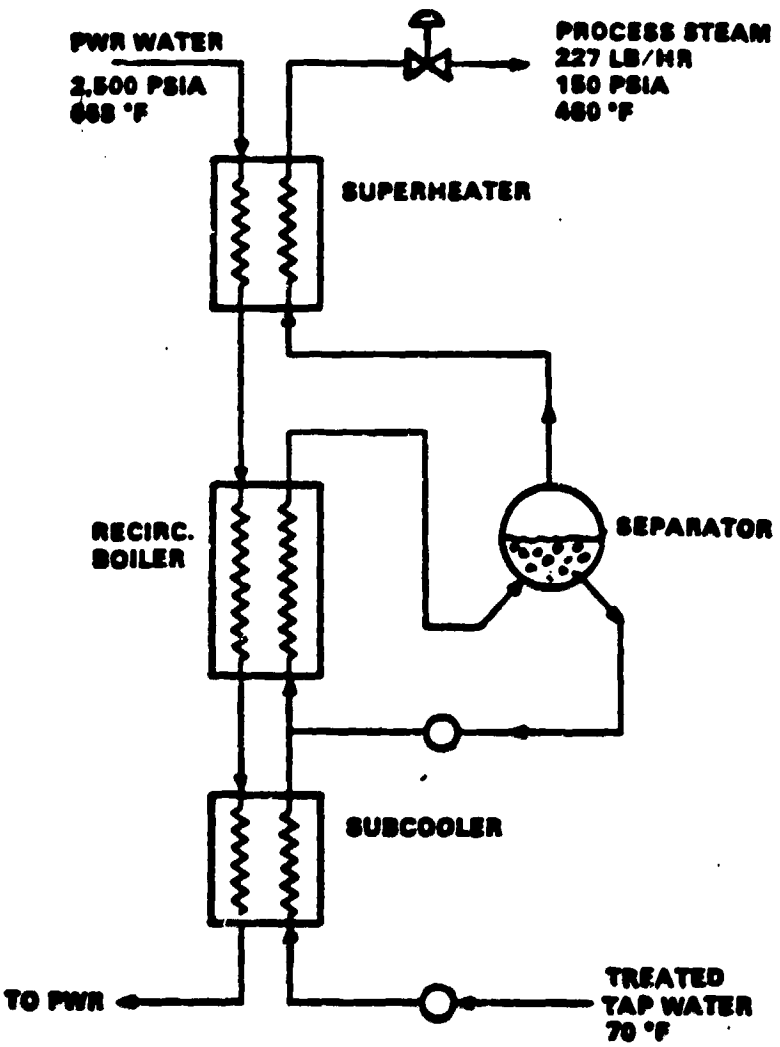

Figure 3-20. High Pressure Water Steam Generator Used with PWR

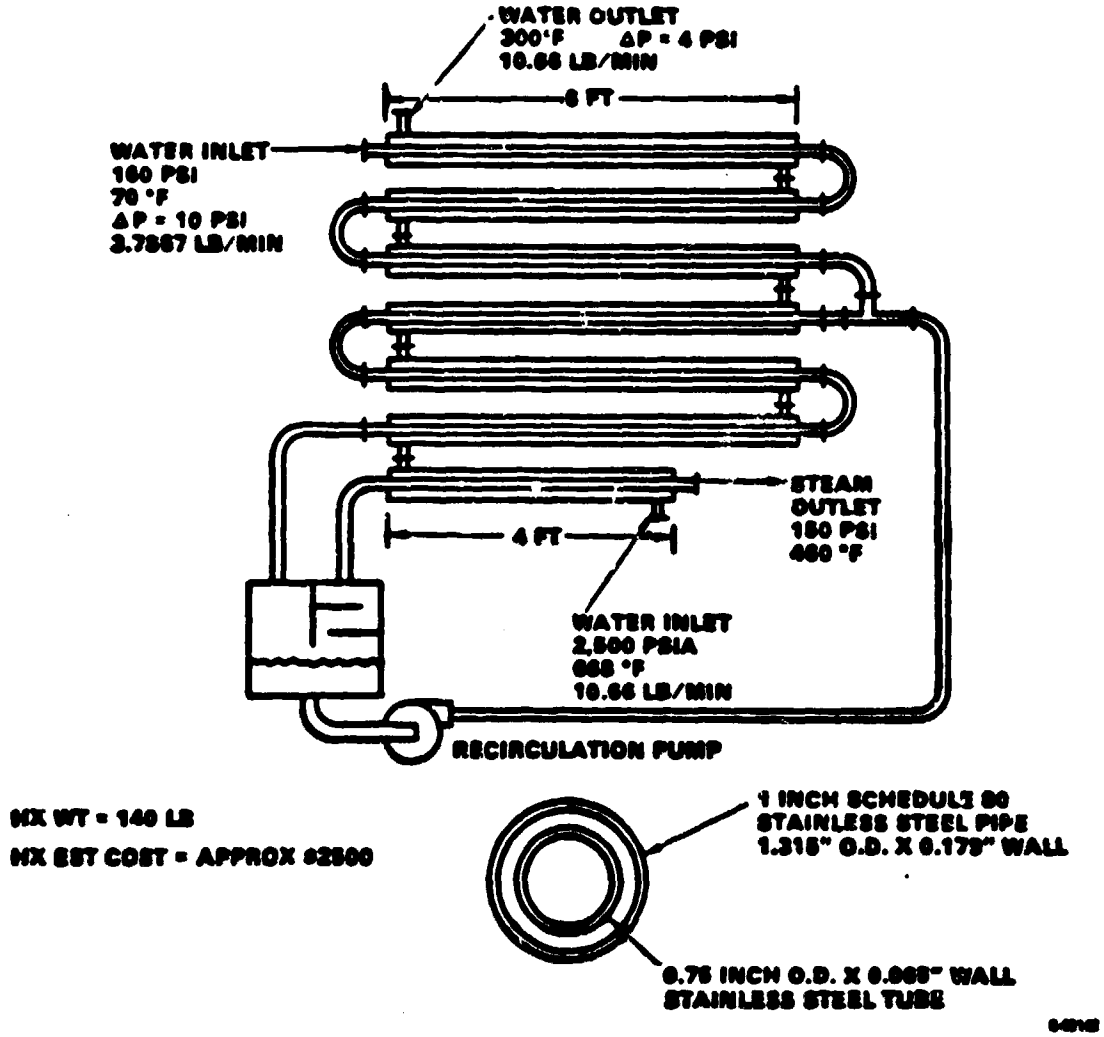

Figure 3-21. High Pressure Steam Generator Hardware

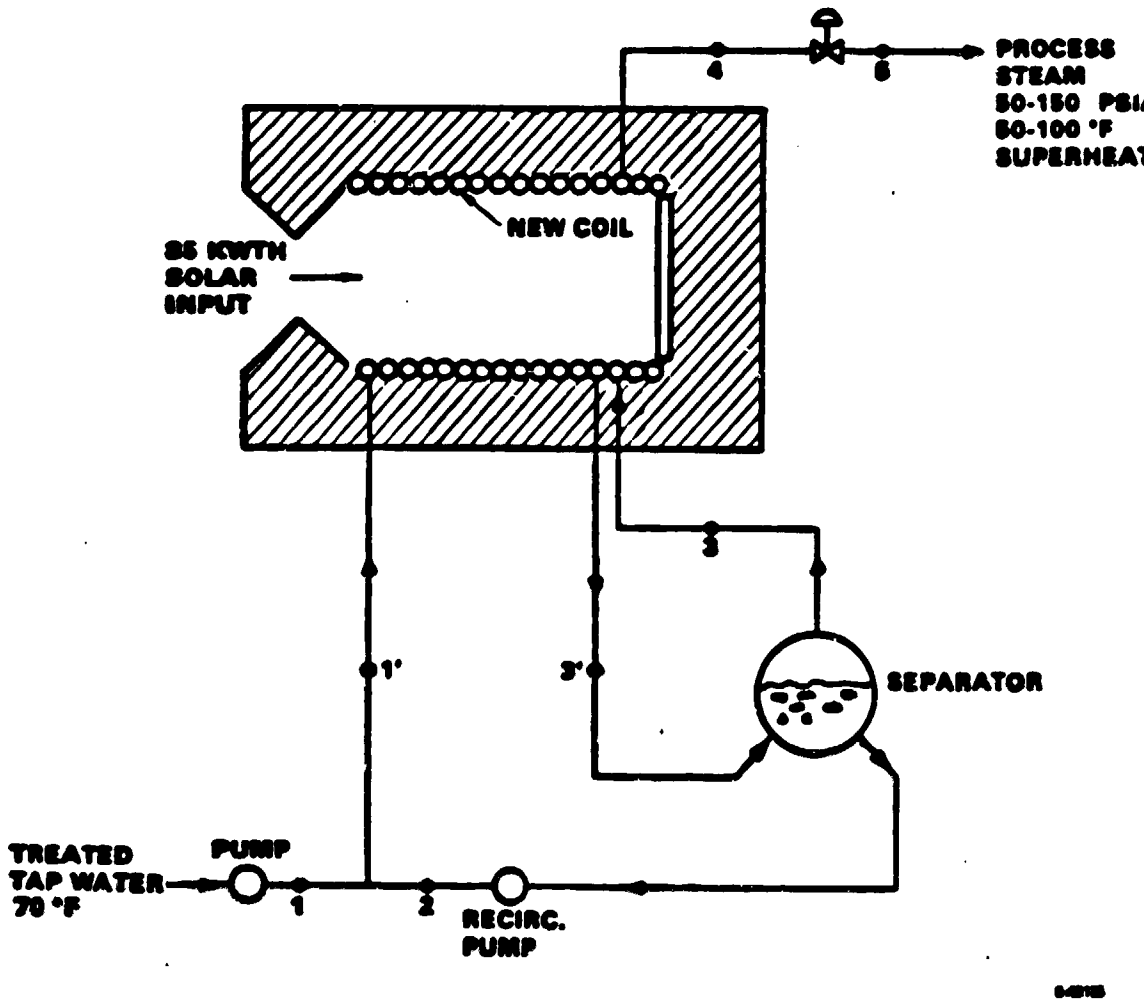

Figure 3-22. Recirculation Boiler Receiver Schematic, for Process Steam

from 3/4 O.D. x 0.120 wall to 9/16 O.D. x 0.090 wall. The foreshortened coil design can accept variations in the incident heat flux, provided the movable end plate is relocated.

Although the capacity of the receiver can be reduced by using a fore-shortened coil, a better solution to reduced power input is to use the full length coil without any changes. The full length coil actually does operate at one-half power for short periods (one in the morning and the other in the afternoon) as a consequence of the normal diurnal solar input.

3.1.6 Adequacy of Heat Transfer Area Margins

A review of the heat transfer in the single phase and especially the boiling regions of the coil was made for the baseline heat flux input. An analysis of the boiling region was made by assuming the heated half of the tube was dry and the boiling liquid wetted only the insulated (back side) half. The tube wall temperatures were higher than normal, but acceptable. Higher stress results, but these were structurally acceptable too. It was concluded that the area was adequate.

In the single phase region a maximum wall temperature of 1400°F at the primary steam outlet is the limiting design factor. Figure 3-23 summarizes the analysis performed by AiResearch on the margins.

3.1.7 Pressure Drop Requirements

The allowable pressure drop established by JPL for the SRSR was 10%. The primary coil diameter and wall thickness were increased from Phase I to allow for higher steam pressures and temperatures. The pressure drop remained well under 10%. The reheater I.D. was increased in order to stay within the 10% pressure drop limit when the Phase II work statement indicated a lower reheater inlet pressure in the primary-reheat mode. The reheater also had the requirement of operating in the all-primary mode with significantly higher pressures, and the tube wall thicknesses were increased accordingly.

These changes in the tubing dimensions and the addition of the movable back plate were the major design changes brought about by the thermal analysis performed by AiResearch in Phase II.

3.2 STRUCTURAL ANALYSIS

Structural analysis of the Steam Rankine Solar Receiver (SRSR) was conducted to determine the design stresses and expected operational life. The solar reciever unit was designed to withstand the operational and test pressures and temperatures and the environmental conditions under normal operation (as specified in the design requirements outlined in Exhibit II of the Phase II contract). Normal operational conditions include wind conditions of 30-mph steady-state, with a 20-percent gust factor; temperature and humidity extremes (0° to 125°F and 0 to 100 percent, respectively); blowing dust; and altitude conditions of 0 to 6000 ft. In addition, survival environmental conditions such as 100-mph winds, seismic lateral loads, and snow and ice loads were considered. Codes and standards such as the ASME Boiler and Pressure Vessel Code

• BOILING REGION

Q/A = 62,000 BTU/HR FT²

VAPOR 50% BY VOL
18% BY WT

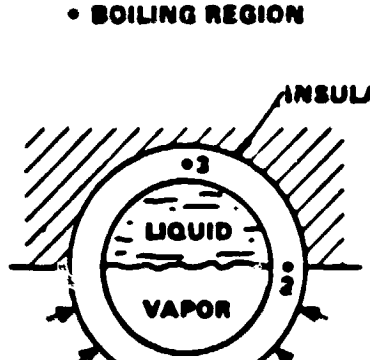

h_ℓ ≈ 2,000 BTU/HR FT² °F

h_v = 650 BTU/HR FT² °F

$T_\ell = T_v$ = 668 °F

T_1 = 756 °F WALL ΔT_1 = 42 °F

T_2 = 702 °F

T_3 = 668 °F

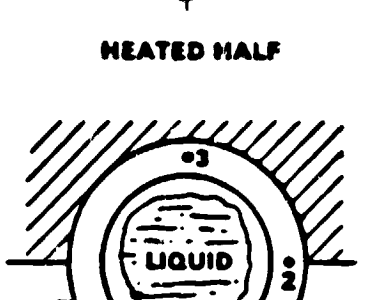

h_v = 400 BTU/HR FT²F

T_1 = 807 °F

T_2 = 748 °F

T_3 = 668 °F

• HIGHER, BUT ACCEPTABLE TUBE WALL TEMPERATURE

• AREA IS ADEQUATE

Figure 3-23. Adequacy of Heat Transfer Area Margins

as well as the Safety Regulations of the California Occupational Safety and Health Administration are also recognized. The major areas of study included:

-the combined pressure and thermal loads in the tubing walls;

-thermal stresses in the cavity walls;

-inertial load in the core mounting structure; and

-the solar receiver housing assembly.

The SRSR was subsequently designed to withstand several factors. These include:

-internal pressure load of 2550 psig;

-thermal loads associated with the 85 KWth peak input;

-realistic combinations of these two load conditions to determine the stresses that would cause cumulative fatigue and creep damage to the unit in operation; and

-inertial loads of 3 g's (nonoperating), resulting in a life of 10,000 hours and 1500 cycles.

Table 3-6 summarizes the analyses performed by AiResearch on various components of the SRSR.

3.2.1 Internal Pressure and Thermal Load Analysis

The core design life of 10,000 hours and 1500 cycles applies to a core of Inconel 625, a nickel-chromium alloy. Creep deformation appears to be more restrictive on the receiver life than cycle fatigue. The design life is based on 1-percent creep deformation of the core while operating at the maximum temperature and pressure of 1400°F and 2550 psig. Design changes would be necessary to increase the expected life of future units to 100,000 hours. Two Inconel 625 cores and two CRES 321 cores were fabricated by AiResearch. The CRES 321 cores have a significantly shorter life than the Inconel 625 cores and are to be used for testing of the SRSR. The expected life of the CRES cores, based on creep rupture data at the maximum operating temperature and pressure, is a few hundred hours. Less than 100 cycles can be expected from the CRES unit at those maximum conditions. Table 3-7 shows strength properties, estimated maximum stresses and time to rupture for the CRES 321 cores.

Computer models were utilized in the analysis of the SRSR. Figure 3-24 depicts the models used to determine tube wall stresses and the cavity wall stresses. The computer model of the coiled tube heat exchanger core assembly shows that the internal pressure will cause an equivalent stress of 8300 psi in the tube wall. At the high temperature region of the coil, where metal temperatures exceed approximately 1250°F, the creep strength of the Inconel 625 tubing limits the life of the solar receiver core. Although localized creep deformations in the prototype core will exceed 1.0 percent at the 10,000

TABLE 3-6

STRUCTURAL EVALUATION AND ANALYSIS

INTERNAL PRESSURE LOAD ANALYSIS:	**PRIMARY TUBE** **REHEAT TUBE**
THERMAL LOAD ANALYSIS:	**CYLINDRICAL SHELL MODEL WITH LONGITUDINAL TEMPERATURE DISTRIBUTION (ANSYS)**
	TUBE CROSS SECTION MODEL WITH CIRCUMFERENTIAL TEMPERATURE DISTRIBUTION (ANSYS)
	LOW CYCLE FATIGUE (AIRESEARCH X0875)
INERTIA LOAD ANALYSIS:	**CORE HINGE CONNECTION**
	CORE SUPPORT STRUCTURE
	HOUSING

TABLE 3-7

CRES 321 PROPERTIES

Yield and Ultimate Strengths of Type 321 Stainless Steel

Metal Temperature, °F			1,000	1,100	1,200	1,300	1,400
Strength, psi	Yield	Typical	21,000	20,400	19,500	18,300	16,500
		Minimum	14,400	16,300	15,600	14,500	13,300
	Ultimate	Typical	57,000	53,000	47,000	38,300	30,000
		Minimum	48,500	44,000	36,500	30,000	23,800

Ref. AiResearch Materials Manual

SRSR ESTIMATED TUBE WALL MAXIMUM STRESS AND TIME TO RUPTURE

Reheat Coil (0.750 in. OD x 0.120 in. wall)
Type 321 Stainless Steel

Pressure, P = 2500 psi
Combined Maximum Wall Stress = 8300 psi*

Wall Temp, °F		1000	1100	1200	1300	1400
Time to Rupture, hr	Typical	6.85×10^8	9.71×10^6	2.30×10^5	8300	430
	3σ Minimum	7.07×10^6	1.34×10^5	4100	187	12

*The maximum wall hoop stress is

$$S = P\left[\frac{(D_o/D_i)^2 + 1}{(D_o/D_i)^2 - 1}\right] = 2.72\ P = 2.72 \times 2500 = 6800\ \text{psi}$$

The combined stress is the result of the fluid pressure and thermal gradients in the tube wall at baseline incident solar flux conditions.

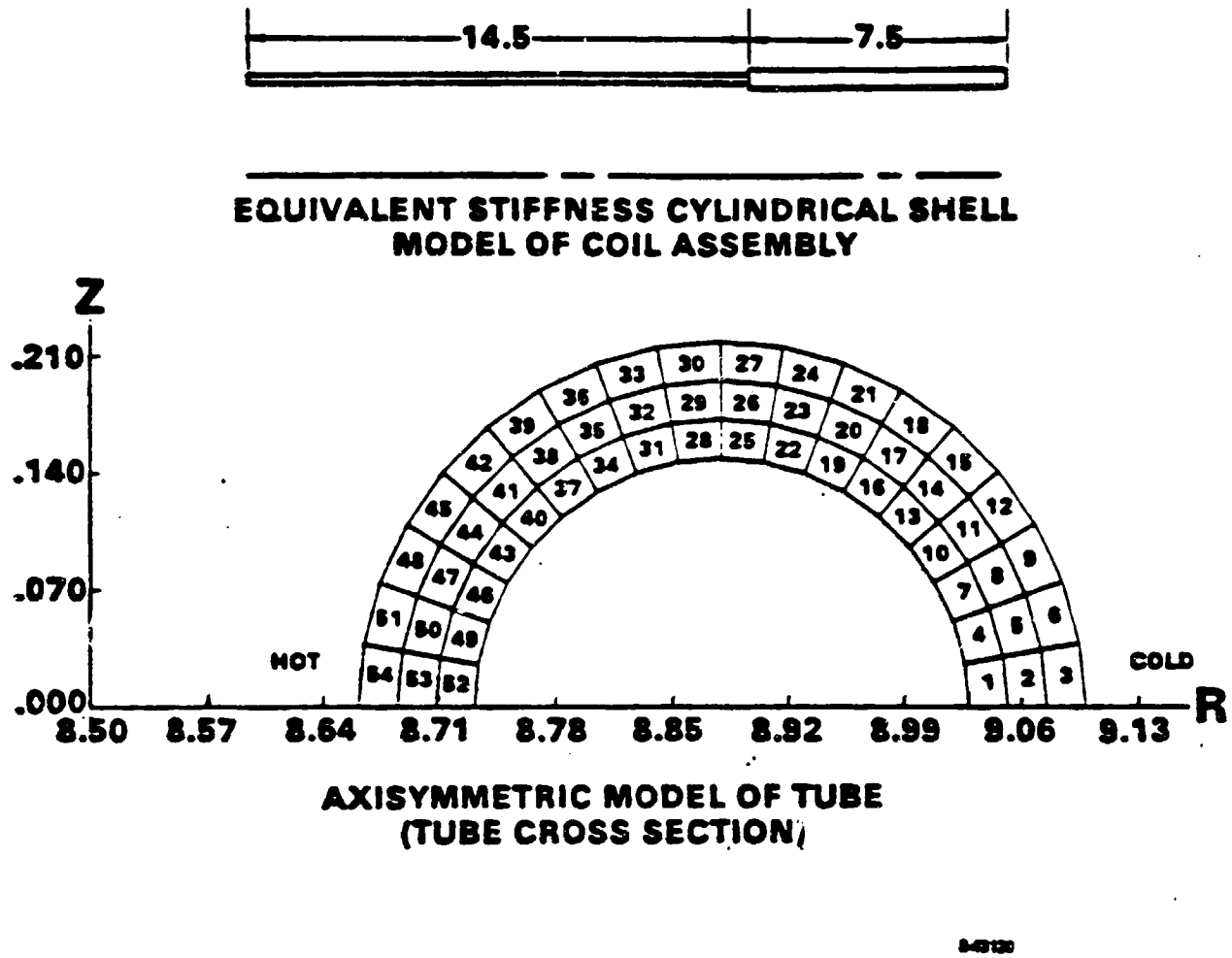

Figure 3-24. ANSYS Computer Models of SRSR Core for Stress Analysis

hour life, the margin on rupture stress is 63 percent. This margin is considered satisfactory for the prototype, but production units with 100,000 hour life will require a design change to increase the tubing strength in the high temperature region of the core.

Thermal stresses in the coil assembly will reach a maximum in the boiling region. Under the most adverse boiling condition with a dry wall in two phase flow, the tube wall maximum stress is 22,300 psi at 700°F. Figure 3-25. Creep is not a factor at this temperature and the stress is less than the 45,000 psi yield strength. Thermal stresses are low in the high temperature region of the coil where tube wall gradients are small, and the pressure stress dominates.

A thermal stress analysis of the coil was made with an ANSYS finite element computer model of an equivalent stiffness cylindrical shell. The results showed that a large bending moment will occur with a rigid connection between the steam generation coil and the reheat coil. Therefore, the two coils are joined with pin connections that will minimize moments by allowing small local rotations. The bending moment reduction is shown in Figure 3-26.

The expansion coils added to the inlet and outlet of both the primary and reheat sections relieve stresses in the core and in the SRSR housing at the entry-exit point of the inlet and outlet tubes, and also allow the end of the tubes to be fixed relative to the housing.

3.2.2 Life Prediction

An effort was made to predict the fatigue life in the areas where the calculated transient stresses obtained with an elastic stress analysis exceed the yield strength of the material. To do so, AiResearch uses the latest, state-of-the-art, elastic-plastic analysis. The Wetzel-Morrow method, employing Neuber hyperbolas, is used to establish the stabilized total cyclic strain range; this strain range is input to the Manson-Coffin equation to predict the cyclic life. Some of the details involved in this method, which were computerized and thoroughly checked out by AiResearch (digital program X0870), are shown in Figure 3-27.

To ascertain the effects of cumulative fatigue and creep damage, the intensity, duration, and frequency of the various imposed loadings are established. The number of cycles to failure and the time to failure at a given stress condition are then calculated. The two effects are then combined for any number of load conditions by using a linear damage function law (such as the Miner-Palmgren rule) where

$$\sum_{i=1}^{n} = \frac{N_{i\ \text{actual}}}{N_{i\ \text{predicted}}} + \frac{T_{i\ \text{actual}}}{T_{i\ \text{predicted, creep}}} \leq 1.0$$

3.2.3 Inertial Load Analysis

Analysis of the solar receiver housing assembly, including the core mounting structure, was analyzed for a 3 g shock load condition. Hat section rings

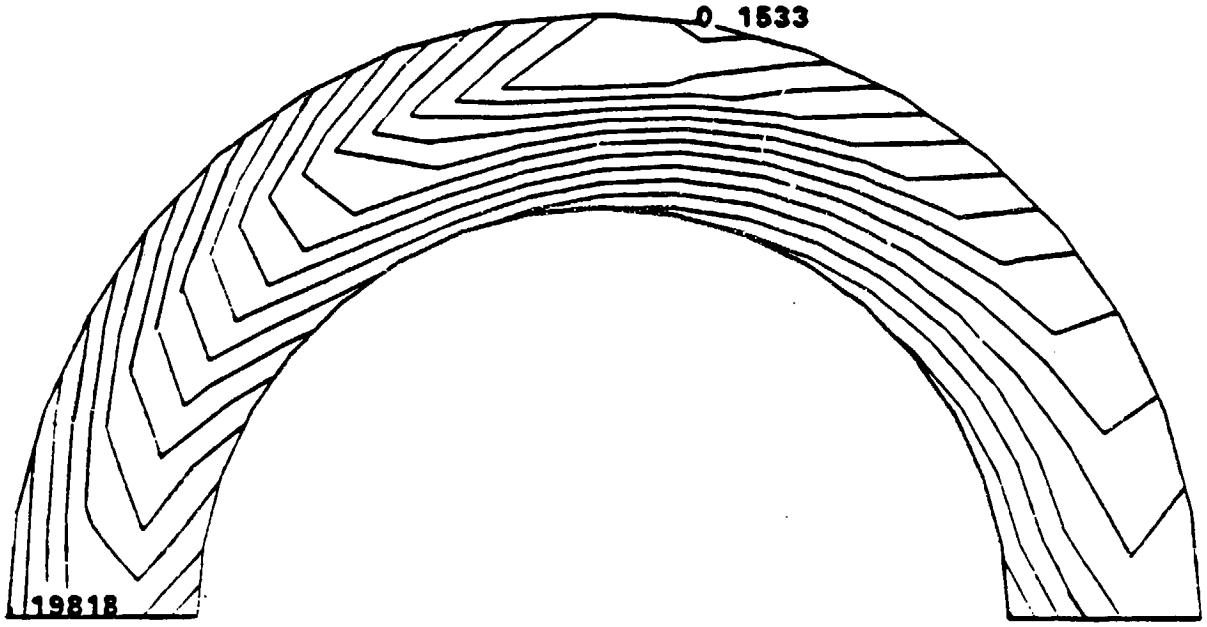

- COMBINED TEMPERATURE AND PRESSURE EQUIVALENT STRESS AT BOILING SECTION. CONTOUR LINE INCREMENT = 1000 PSI

LIFE CYCLE STRESSES

AT 700 °F

MAX _ _ _ _ _ _ 22,340 PSI
MIN _ _ _ _ _ _ _ _ _ _ 0 PSI

AT 1400 °F

MAX _ _ _ _ _ _ _ 8,290 PSI
MIN _ _ _ _ _ _ _ _ _ _ 0 PSI

S-43119

Figure 3-25. Combined Temperature and Pressure Stresses

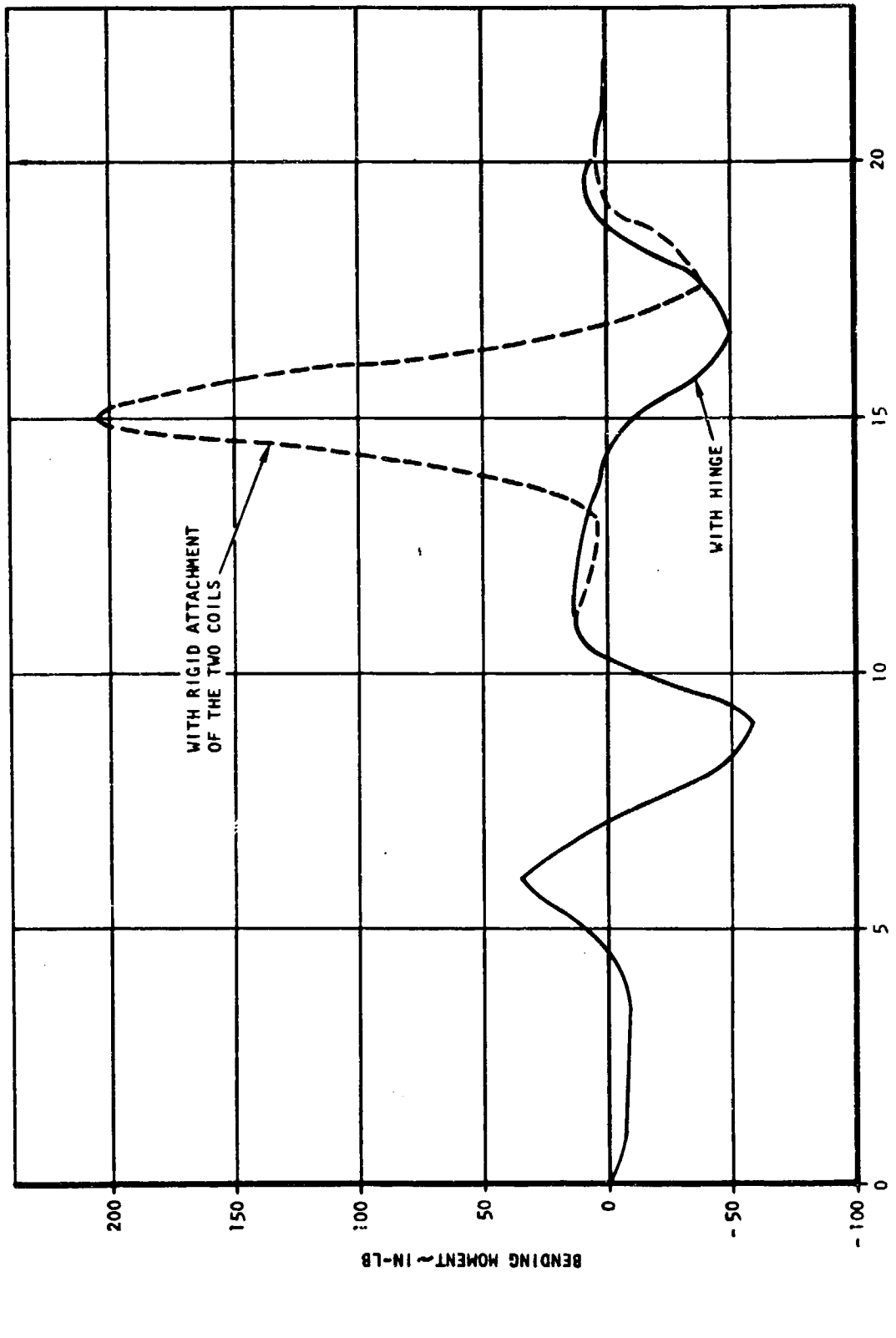

Figure 3-26. Coil Bending Moment

PREDICTION OF UNIT LIFE FROM LEVELS OF APPARENT ELASTIC STRESS REACHED DURING TRANSIENT LOADINGS (AIRESEARCH COMPUTER PROGRAM X0870)

- METZEL-MORROW ELASTIC-PLASTIC ANALYSIS USING NEUBER HYPERBOLAS TO OBTAIN STABILIZED CYCLIC STRAIN RANGE.
- NUMBER OF CYCLES TO CRACK INITIATION OBTAINED USING MANSON-HIRSCHBERG EQUATION OR MODIFIED MANSON-COFFIN EQUATION.

$$\epsilon_{TOT} = 3.5 \frac{\sigma_f'}{E N_f^{0.12}} + \frac{(\epsilon_f')^{0.6}}{N_f^{0.6}}$$

WHERE σ_{f_1}' = TRUE ULT. FAILURE STRESS

ϵ_{f_1}' = FAILURE STRAIN

} FROM PULL TEST

n = STRAIN HARDENING EXPONENT

- ACCUMULATIVE FATIGUE DAMAGE. (MINER-PALMGREN RULE)

$$\sum_{i=1}^{n} = \frac{N_i \text{ ACTUAL}}{N_i \text{ PREDICTED, FATIGUE}} \leq 1.0$$

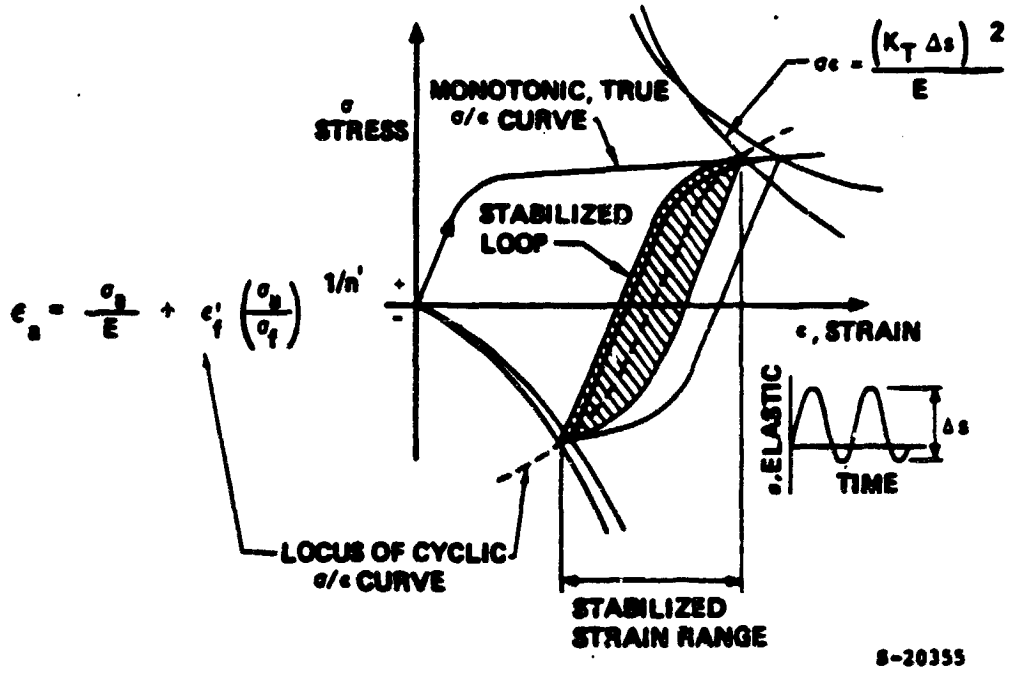

Figure 3-27. Low-Cycle Fatigue Analysis

and longitudinal stiffeners were added to the outer cylindrical shell to resist potential buckling at load concentrations. Figure 3-28 shows margins of safety for the major load points of the assembly. The margins of safety are high and indicate that the receiver will have a good tolerance for mechanical loads.

Significant features were incorporated into the SRSR design as a result of the structural analysis. The Phase I solid braze joint between the primary and reheat sections was replaced with pin connections to minimize bending moments at the junction. Expansion coils were added to the primary and reheat sections for stress relief and to isolate the inlet and outlet tubes' system interface from the thermal growth of the core. The core support system was simplified. Various stiffeners were added in the housing structure to meet the inertial load requirements.

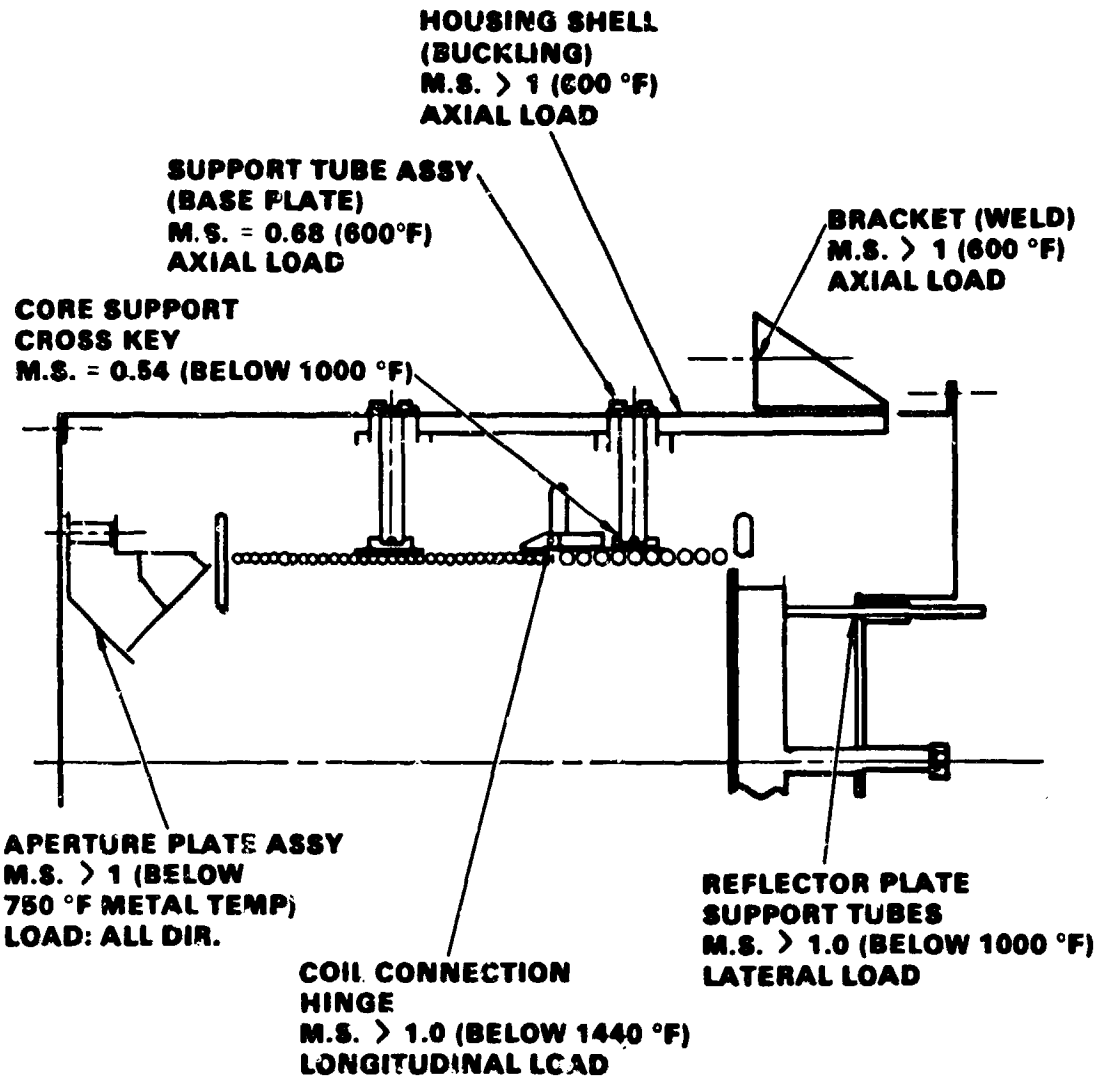

Figure 3-28. SRSR Inertia Load Analysis Results

4. SRSR FABRICATION

Fabrication efforts by AiResearch commenced on the Steam Rankine Solar Receiver (SRSR) once the Phase II final design was completed. Two Inconel 625 cores and two CRES 321 cores were fabricated by AiResearch. The SRSR is composed of several sub-assemblies that bolt onto the outer shell. The brazed core, the aperture assembly, and the reflector plate assembly individually attach to the outer shell in the final assembly. This allows for greater accessibility to the aperture plate and reflector plate components. Since these sub-assemblies do not attach directly to each other in the final assembly, the individual components can grow thermally at different rates without interference.

The core assembly was fabricated from a series of random length tubes which were welded together. The welds were X-rayed and reworked if necessary until they passed the X-ray inspection. The tube was then coiled into the desired cylindrical shape and brazed. The inlet and outlet tubes were welded onto the primary and reheat sections, and the welds were inspected. The two sections were attached to each other with the pin connection. The core was then ready for final assembly into the outer shell.

Final assembly of the SRSR occurs in three stages. (1) The complete heat exchanger assembly is wrapped in insulation, slipped inside of, and attached to, the outer housing. The core mounting structure was designed to allow unrestrained thermal deformation in all directions. The Phase I hook and tee arrangement for receiver coil suspension has been changed. The coil is suspended using eight tubes, four each located at the center of gravity of the primary and secondary coils. The tubes are fixed at one end to the receiver enclosure, extend radially inwards toward the receiver coil, and are slotted at the other end. Longitudinal keys are located on the reciever coil and mate the slots at the support tube end. On the primary coil, this part is a longitudinal strip which allows for radial and longitudinal growth of the receiver. On the reheat coil, intersecting keys in the form of a cross mate with corresponding slots at the ends of the support tubes. This restrains the coil from longitudinal and lateral motion while allowing radial growth. (2) The aperture plate assembly is bolted to the aperture end of the outer shell. (3) The reflector plate assembly is bolted to the other end of the outer shell. The inlet and outlet ducts are guided through holes in the rear outlet shell of the reflector plate assembly for hookup with the rest of the system. Tube retainers anchor the inlet and outlet tubes to the rear cover.

Insulation was filled in all gaps in the receiver as the final assembly progressed.

Connection to the solar concentrator is made by means of a mounting ring with six mount points. Mounting shims are provided to allow for 8-inches of adjustment along the optical line of the concentrator.

Figures 4-1 through 4-5 show the various stages of fabrication, and Figure 4-6 represents the SRSR final assembly.

The materials used in the fabrication of the SRSR, as well as the general dimensions and parts that constitute the unit, are referred to in Section 2 of this report (SRSR description) and in the detailed drawings of Appendix A.

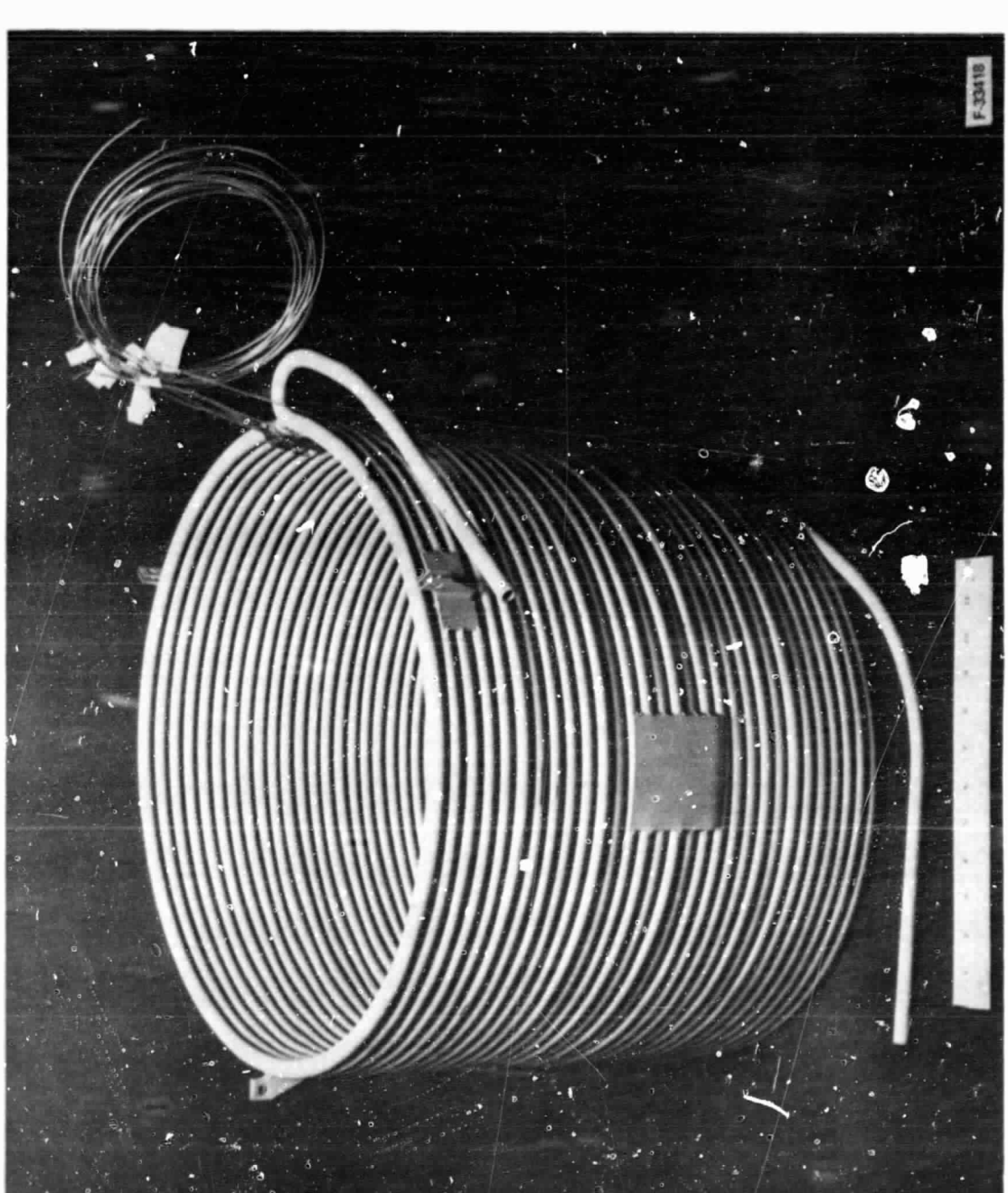

Figure 4-1. Brazed Primary Core

ORIGINAL PAGE
BLACK AND WHITE PHOTOGRAPH

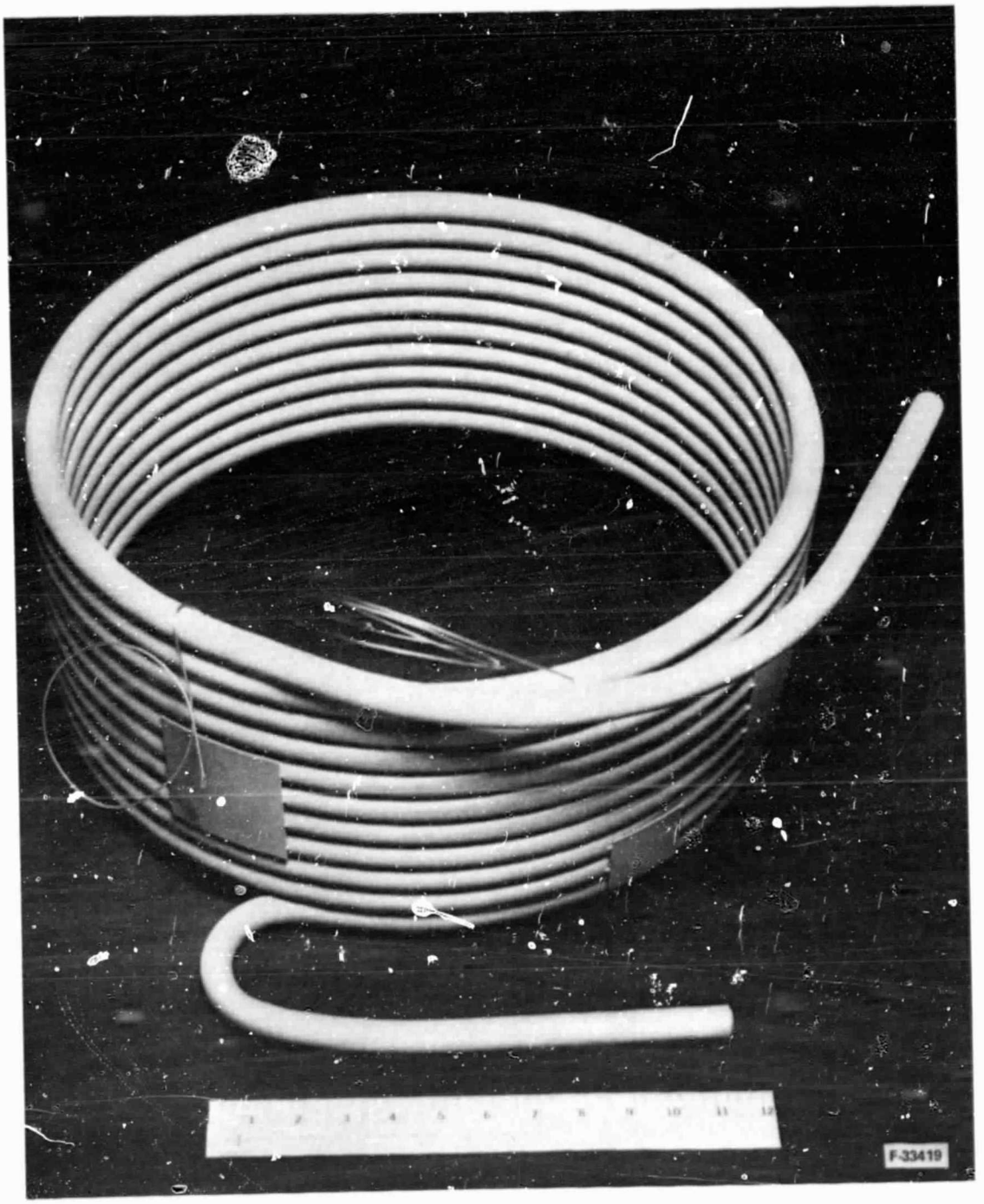

Figure 4-2. Brazed Reheat Core

ORIGINAL PAGE
BLACK AND WHITE PHOTOGRAPH

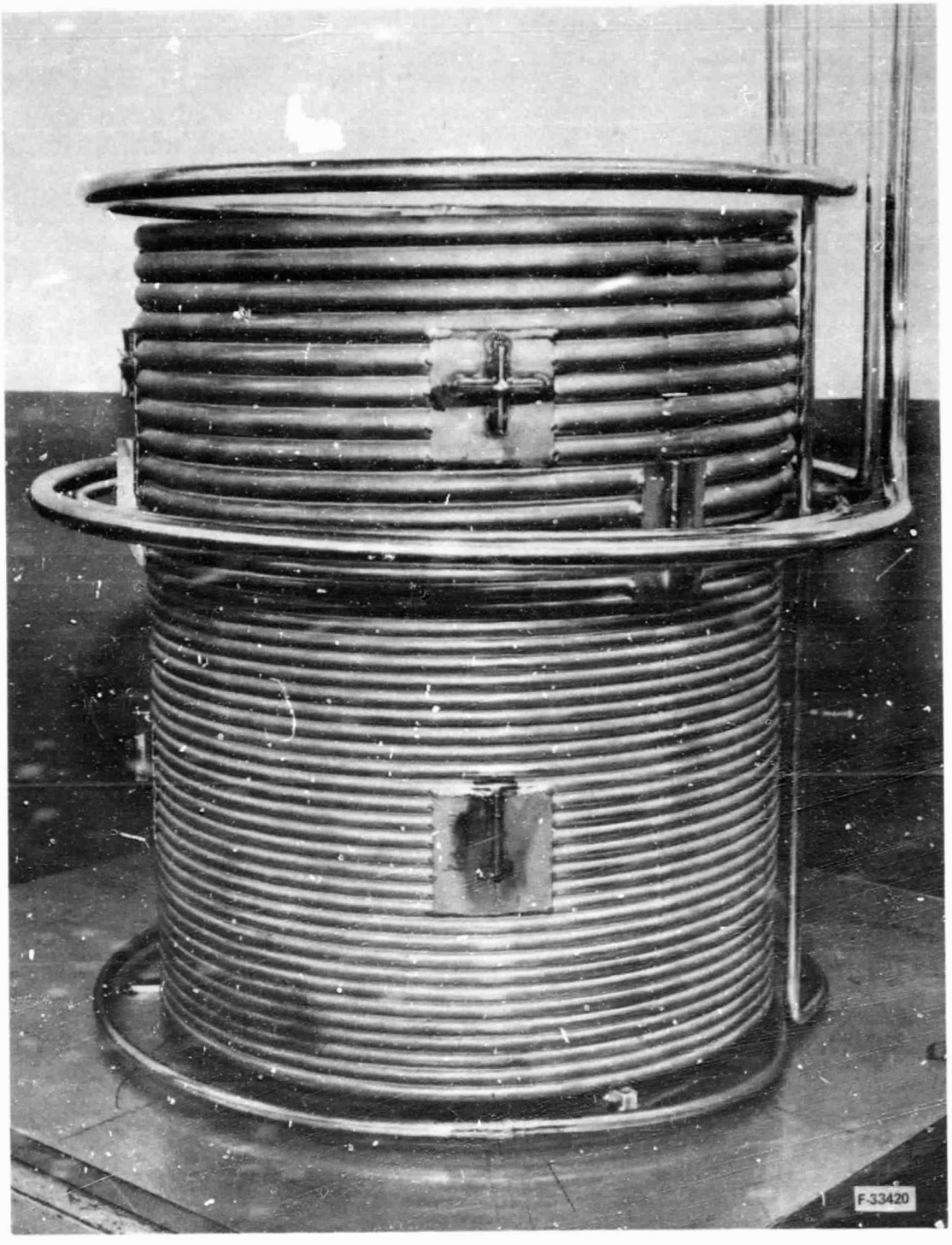

Figure 4-3. Assembled SRSR Core

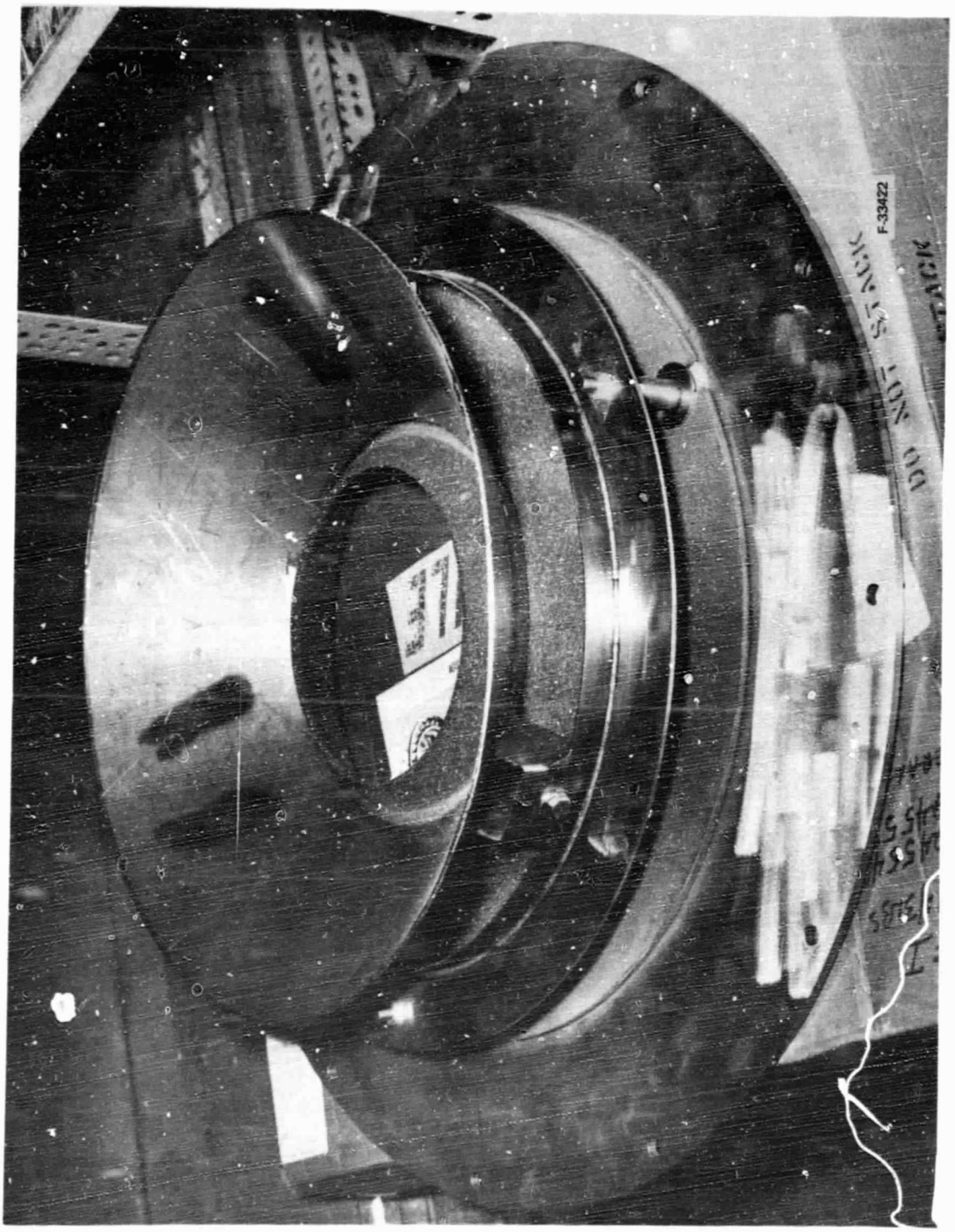

Figure 4-4. Ceramic Aperture Assembly

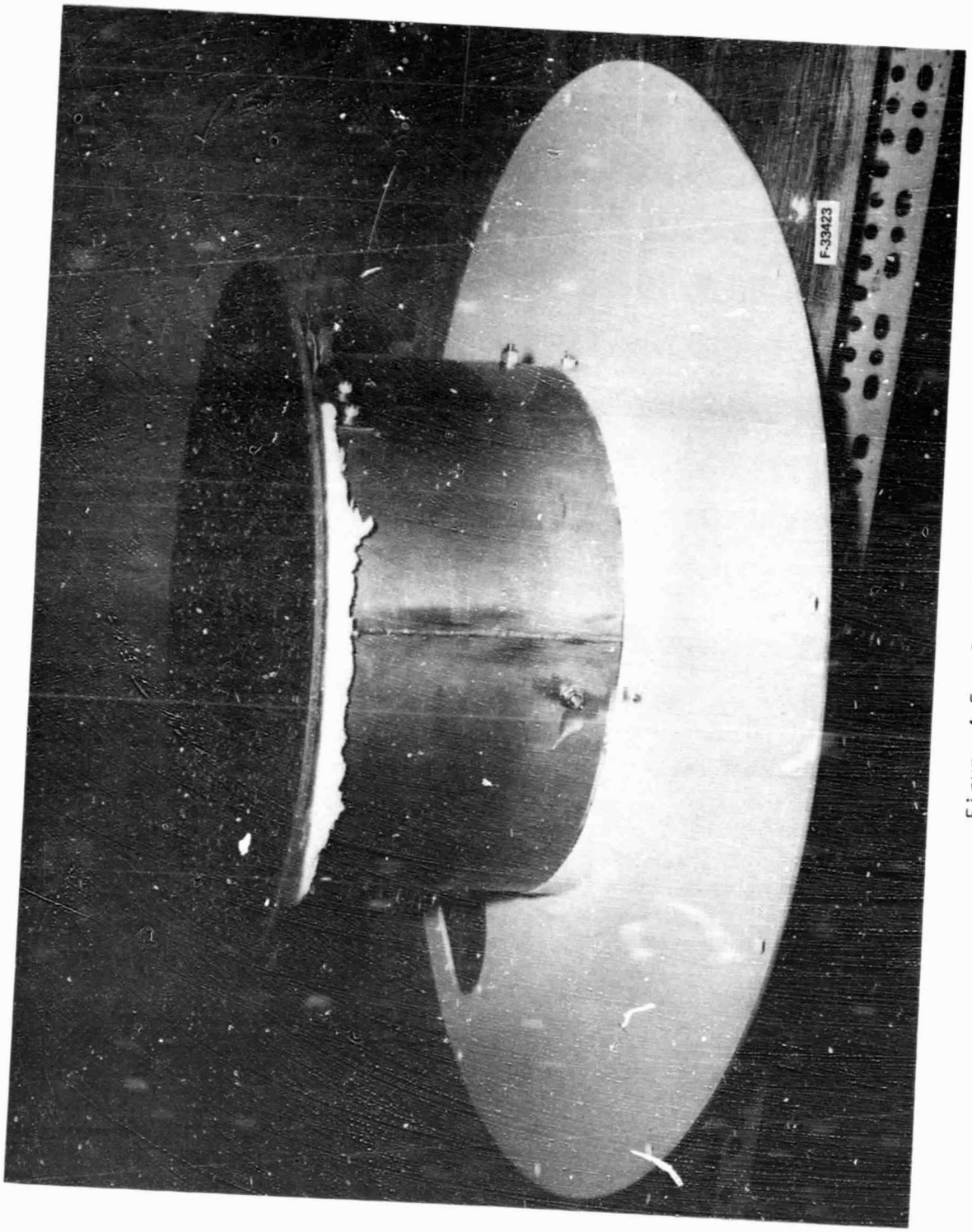

Figure 4-5. Ceramic Reflector Assembly

ORIGINAL PAGE
BLACK AND WHITE PHOTOGRAPH

Figure 4-6. SRSR Final Assembly

5. SRSR TESTING PROCEDURES AND RESULTS

Acceptance tests were performed on the two Solar Receiver CRES 321 core assemblies. They included leakage, proof pressure, and pressure drop tests.

5.1 LEAKAGE TEST

The leakage test consisted of applying a pneumatic pressure of 500 psig to the primary and reheat coil sections. The pressure in the system was held for 5 minutes. The sections were observed for any evidence of leakage. No leakage was observed from any of the tested units. Figure 5-1 shows the test setup.

5.2 PROOF PRESSURE TEST

The proof pressure test procedure included applying hydrostatic pressure of 5400 psig to the primary and reheat sections. The proof pressure value is greater than the operating pressure of 2500 psig in order to compensate for testing at room temperature. During the testing of the cores the hydrostatic pressure was held for 5 minutes. The coil sections were observed under pressure for any deformation or leakage. No evidence of leakage or permanent deformation was noted in any of the tested units. The proof pressure and leakage test determine the structural integrity of the tubes and the welds.

5.3 PRESSURE DROP TEST

This was an isothermal pressure drop test that consisted of passing air through the primary and reheat coil sections of the cores at various flow rates, while measuring the inlet pressure and pressure difference across each coil. The schematic of the test setup is shown in Figure 5-2.

The test results for the two cores tested are reported in Tables 5-1 and 5-2. It was observed that the test results were approximately the same as the predicted values. This holds true for both the primary and reheat coils. See Figures 5-3, 5-4, 5-5 and 5-6.

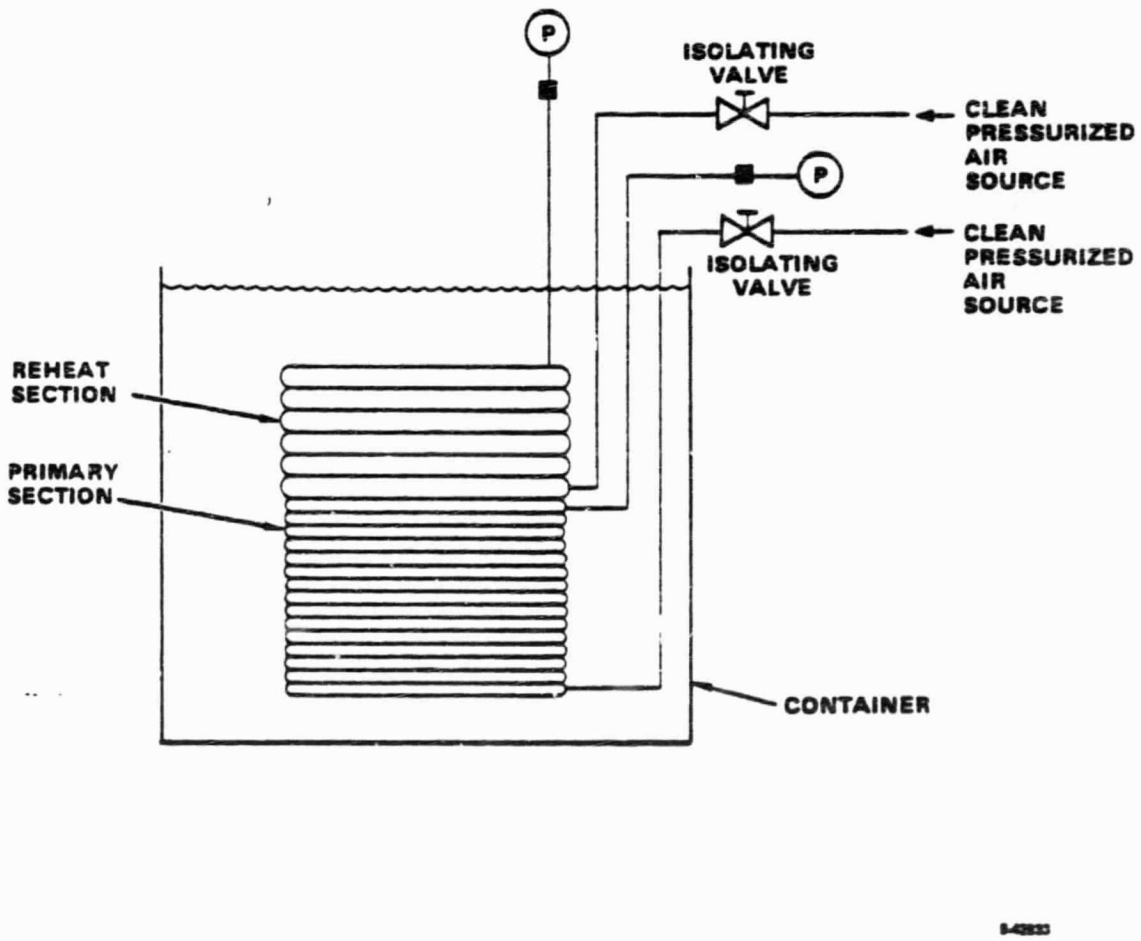

Figure 5-1. SRSR Leakage Test Setup

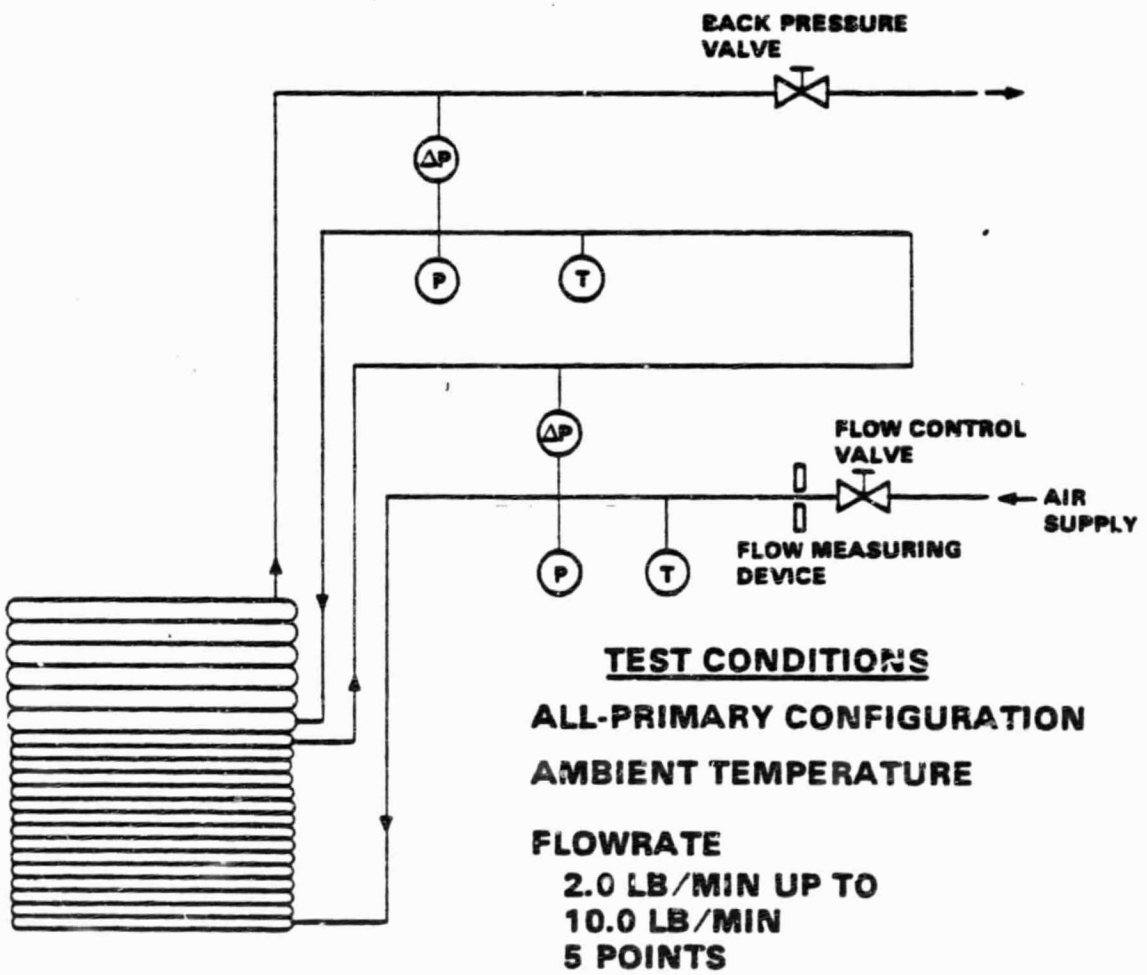

Figure 5-2. SRSR Pressure Drop Test Setup

TABLE 5-1

TEST RESULTS CORE S/N 1

FORM #2580A AiRESEARCH Mfg. Co.

HEAT TRANSFER LAB DATA SHEET

Page 1 of 1

EWO 3400-250563-03-0297 DATE 5/3/80 TEST PURPOSE STEAM RANKINE SOLAR RECEIVER CORE,

P/N 194306-1 BAROM 29.79 "Hg ISOTHERMAL PRESSURE DROP

S/N 1 TEMP 66.0 °F TEST PERS. D. CLIFFORD

	← PRIMARY →				← REHEAT →				ORIFICE DATA							
	INLET PRESS. PSIG	OUTLET PRESS. "Hg	ΔP "Hg	σΔP "Hg	INLET PRESS "Hg GAUGE	ΔP "Hg	σΔP "Hg		ST. P. ORIFICE PSI	ΔP "H_2O	T °F	ORIFICE PIPE INCH.	ORIFICE PLATE INCH.	σΔP "H_2O	FLOW LB/MIN	
NO.	1	2	3	4	5	6	7	8	9	10	11	12	13	14	15	REMARKS
1	73.7	21.1	129.2	145.5	19.0	18.7	24.0		80.0	9.25	66.1	1.5	0.375	58.75	1.067	$\sigma = \frac{P_{ave}}{P_{STD}} = \frac{P_{ave}}{P_{STD}}$
2	53.4	14.0	99.0	28.5	12.4	12.3	14.4		60.0	6.90	66.1	↓	↓	31.55	0.82	
3	36.7	7.7	67.2	48.1	6.8	6.70	7.25		40.0	4.60	66.1			16.84	0.56	
4	19.3	2.9	36.5	55.0	2.5	2.5	2.53		20.0	2.35	66.1			5.32	0.326	$\sigma = 0.034\ (P_{in} + P_{out})$
5	13.6	1.9	25.84	38.9	1.65	1.65	1.64		15.0	1.75	66.1			3.47	0.236	
6	9.2	1.1	17.66	22.6	1.02	1.02	1.00		10.0	1.25	66.1	1.5	0.375	2.05	0.203	$P_{STD} = 14.7$ PSIA
7																
8																$P_{IN}, P_{OUT} \Rightarrow$ PSIA
9																
10																
11																
12																
13																
14																
15																
16																
17																
18																
19																
20																
21																

TABLE 5-2

TEST RESULTS CORE S/N 2

FORM 61339A
AiResearch Mfg. Co.

HEAT TRANSFER LAB DATA SHEET

Page 1 of 1

WO 3400-250563-02-0297 DATE 7/2/80 TEST PURPOSE STEAM RANKINE SOLAR RECEIVER CORE,

P/N 194306-1 BAROM 29.79 "Hg ISOTHERMAL PRESSURE DROP

S/N 2 TEMP 74.0°F TEST PERS. D. CLIFFORD

	← PRIMARY →				← REHEAT →				ORIFICE DATA							
NO.	INLET PRESS. PSIG 1	OUTLET PRESS. "Hg 2	ΔP "Hg 3	σΔP "Hg 4	INLET PRESS "Hg GAUGE 5	ΔP "Hg 6	σΔP "Hg 7	8	ST. P. ORIFICE "Hg A 9	ΔP "H2O 10	T °F 11	ORIFICE PIPE INCH. 12	ORIFICE PLATE INCH. 13	σΔP "H2O 14	FLOW LB/MIN 15	REMARKS
1	65.0	15.10	117.5	367.6	14.65	14.40	17.46		164	9.05	74.0	1.5	0.375	48.2	0.973	$\sigma = \frac{P_{ave}}{P_{STD}} = \frac{P_{ave}}{P_{STD}}$
2	54.0	11.15	98.7	272.8	11.05	10.85	12.52		140	7.90	74.0			39.7	0.813	
3	39.0	7.20	72.4	164.1	6.90	6.75	7.34		110	5.30	74.0			18.9	0.607	
4	25.0	3.90	47.1	89.9	3.65	3.55	3.67		80	3.40	74.0	↓	↓	8.84	0.416	$\sigma = 0.034 (P_{IN} + P_{OUT})$
5	11.0	1.35	21.1	28.3	1.15	1.10	1.09		50	1.55	74.0	1.5	0.375	2.52	0.225	
6																$P_{STD} = 14.7$ PSIA
7																
8																P_{IN}, P_{OUT} = PSIA
9																
10																
11																
12																
13																
14																
15																
16																
17																
18																
19																
20																
21																

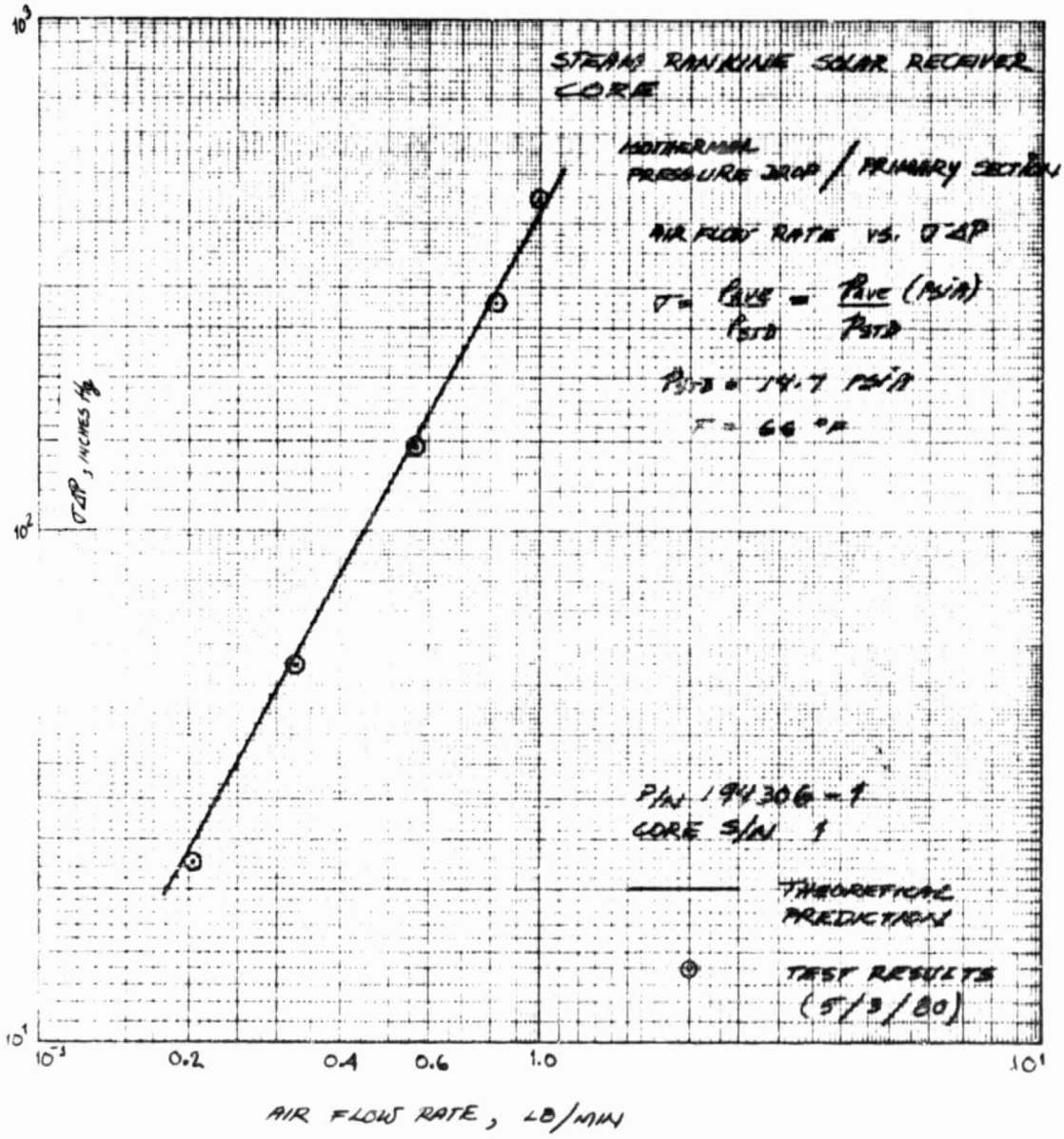

Figure 5-3. Isothermal Pressure Drop/Primary Section, Core S/N 1

ORIGINAL PAGE IS
OF POOR QUALITY

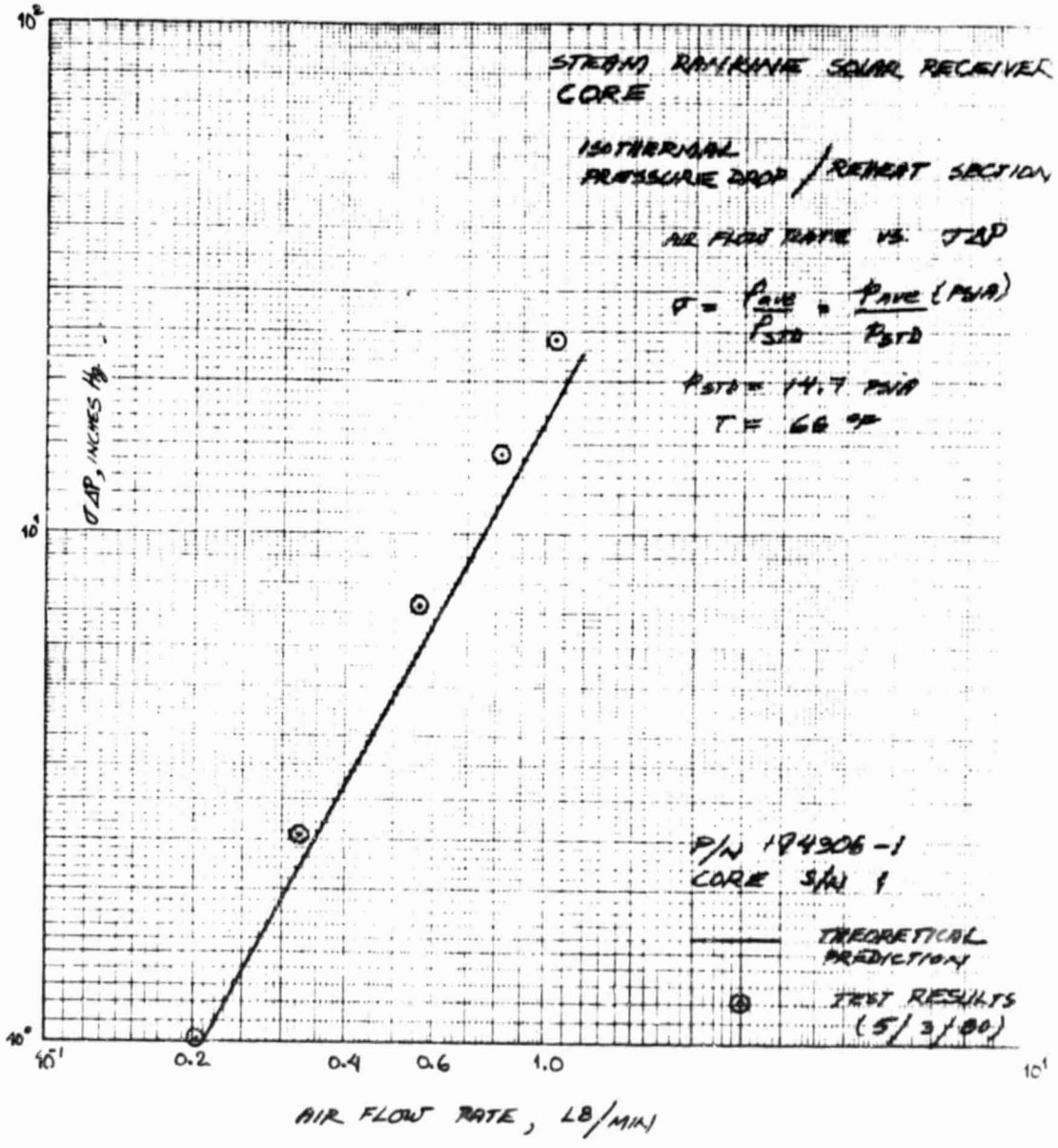

Figure 5-4. Isothermal Pressure Drop/Reheat Section, Core S/N 1

ORIGINAL PAGE IS
OF POOR QUALITY

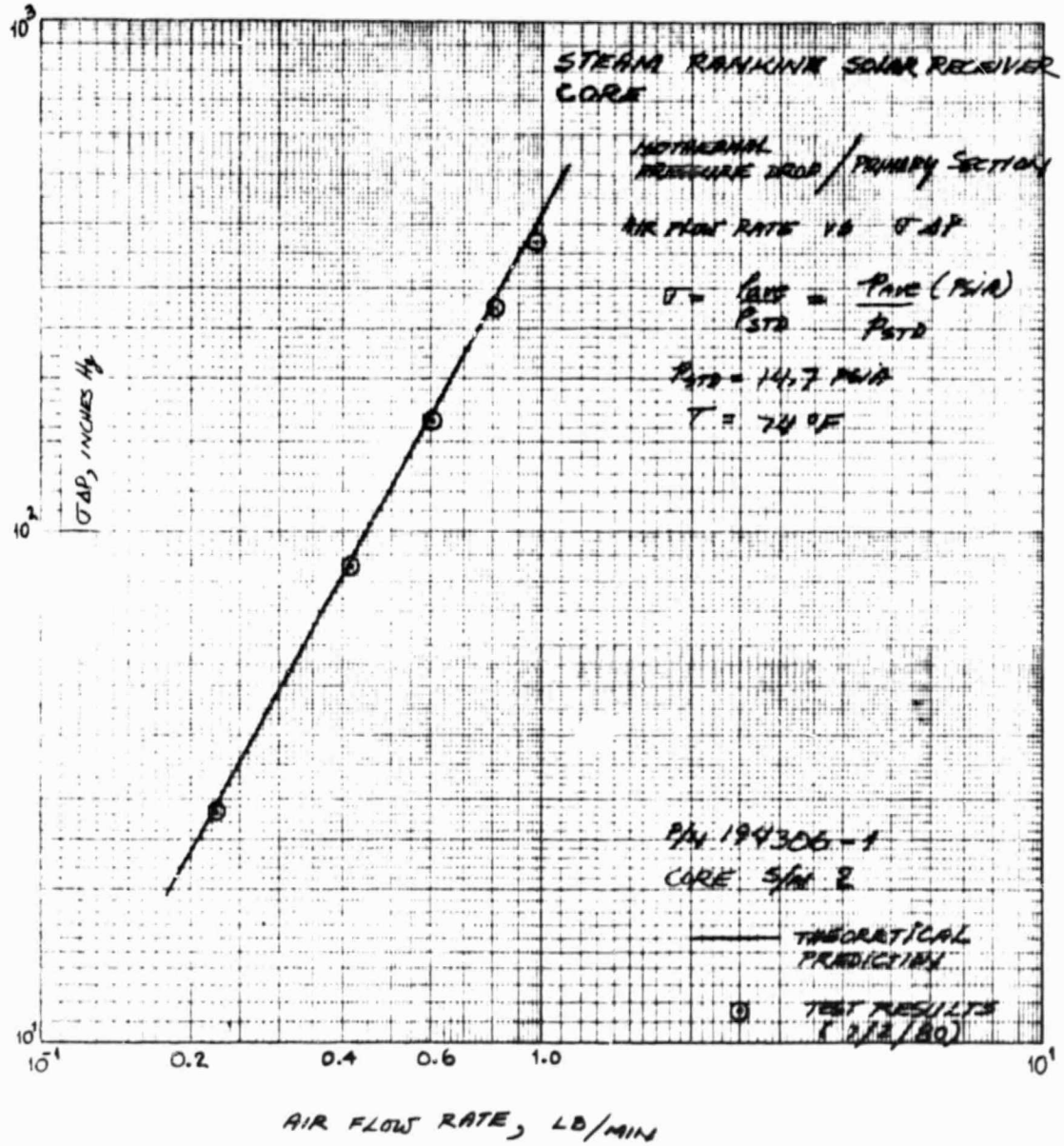

Figure 5-5. Isothermal Pressure Drop/Primary Section, Core S/N 2

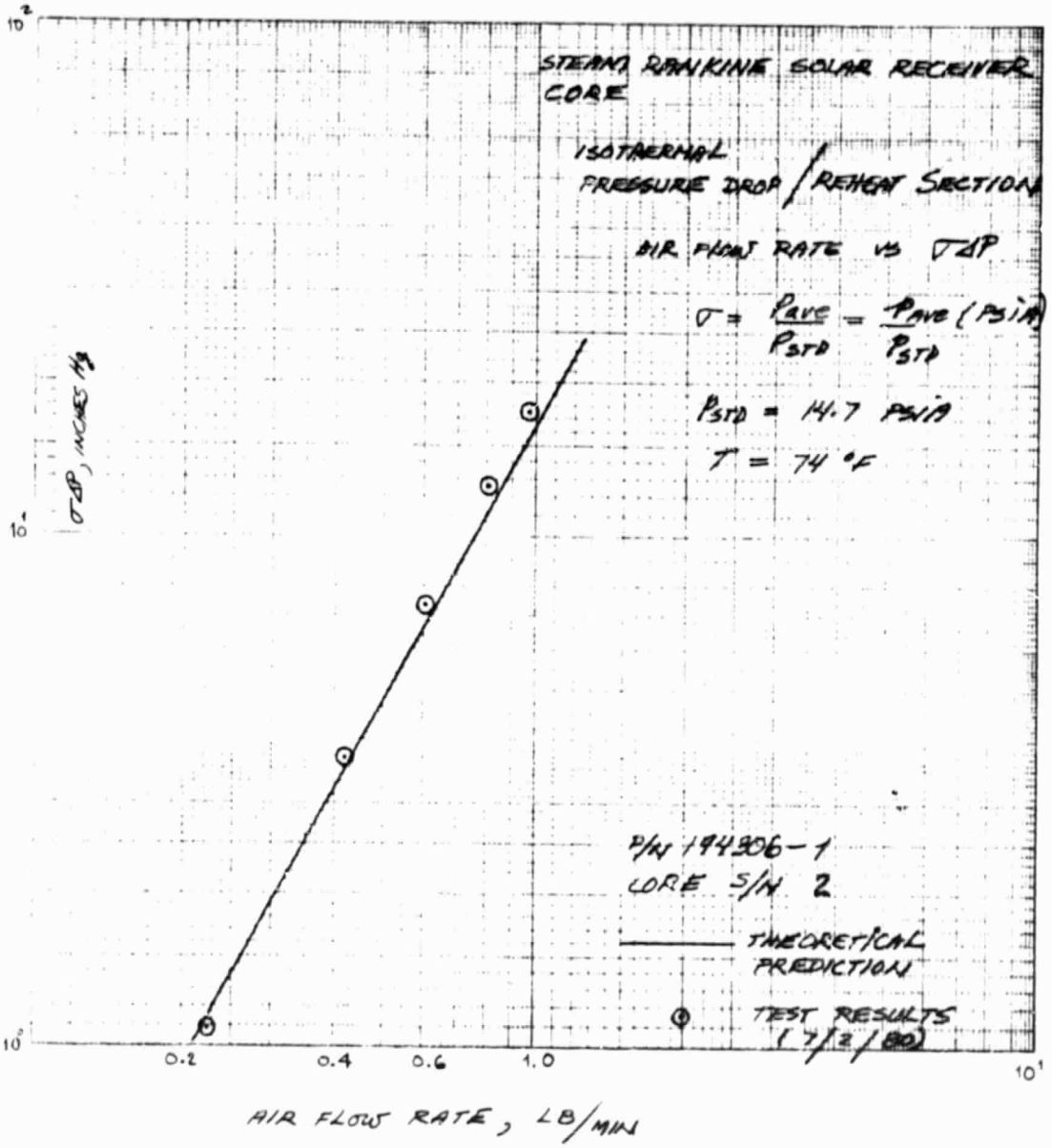

Figure 5-6. Isothermal Pressure Drop/Reheat Section, Core S/N 2

APPENDIX A

STEAM RANKINE SOLAR RECEIVER

DETAIL DESIGN DRAWINGS

DETAIL DRAWINGS

Drawing No.	Name
193129	Primary Core Assy.
193131	Reheat Core Assy.
193134	Solar Receiver Core Assy.
193188	Case Assy.
194307	SRSR Final Assy.

PART NO.	A DIA	B DIM
193129-1	17.69-17.81	15.31-15.37
193129-2	17.63-17.75	15.50-15.56

ORIGINAL PAGE IS OF POOR QUALITY

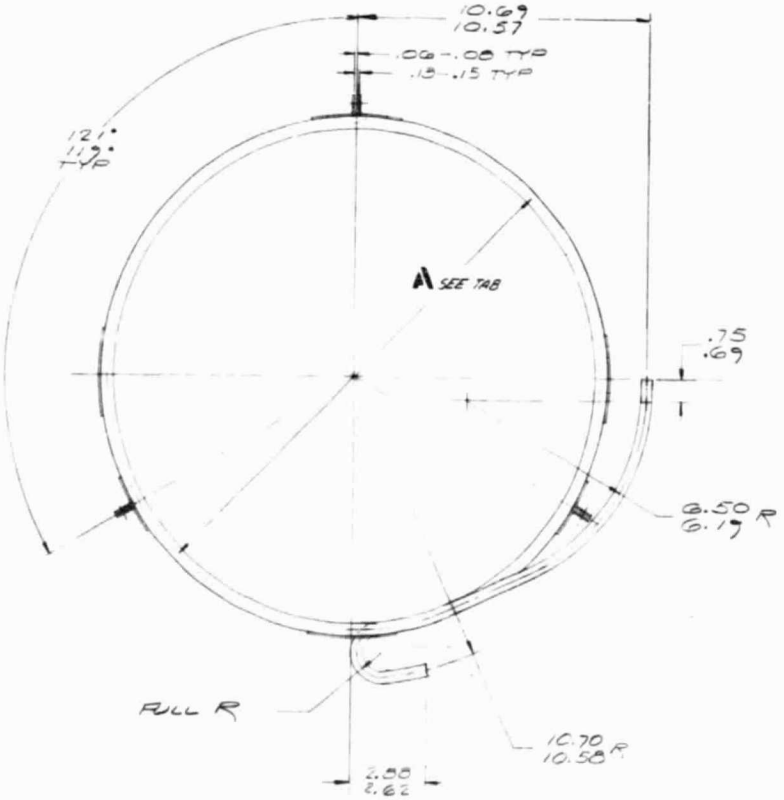

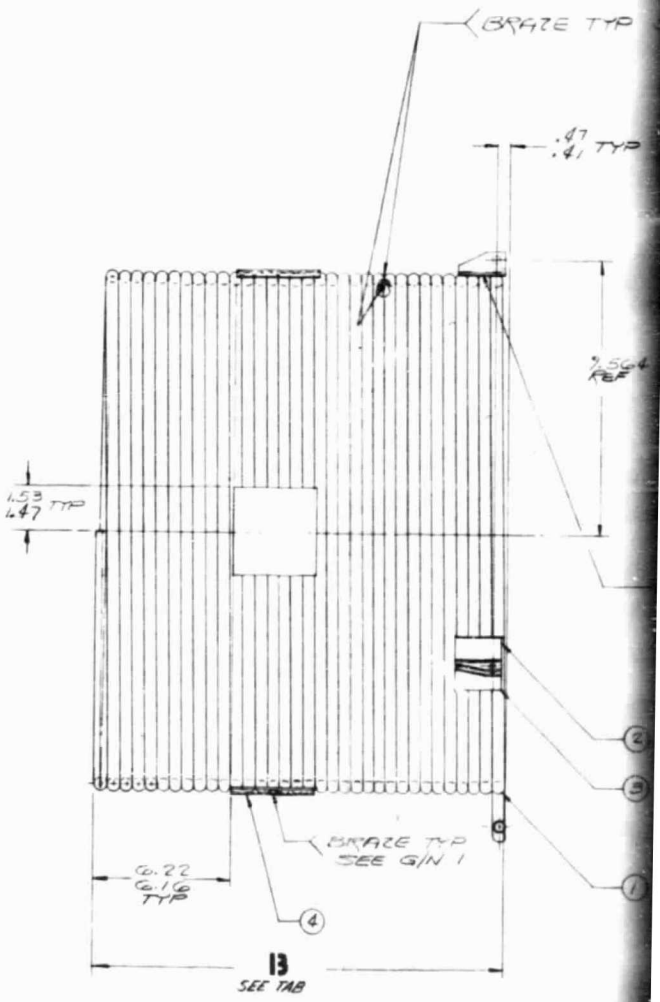

FOLDOUT FRAME

ZONE												
LTR	AA	AB	AD	AE	AF	AG	AH	AJ	AK	AL		
ZONE	AT	AS										
	AU	AR										
LTR	A	B	D	E	F	G	N	J	K	L	M	P	S	T	U	V	W

LETTER ASSIGNMENT AND LOCATION RECORD FOR DETAILS, SECTIONS, VIEWS AND TABULATIONS

NOTES: UNLESS OTHERWISE SPECIFIED

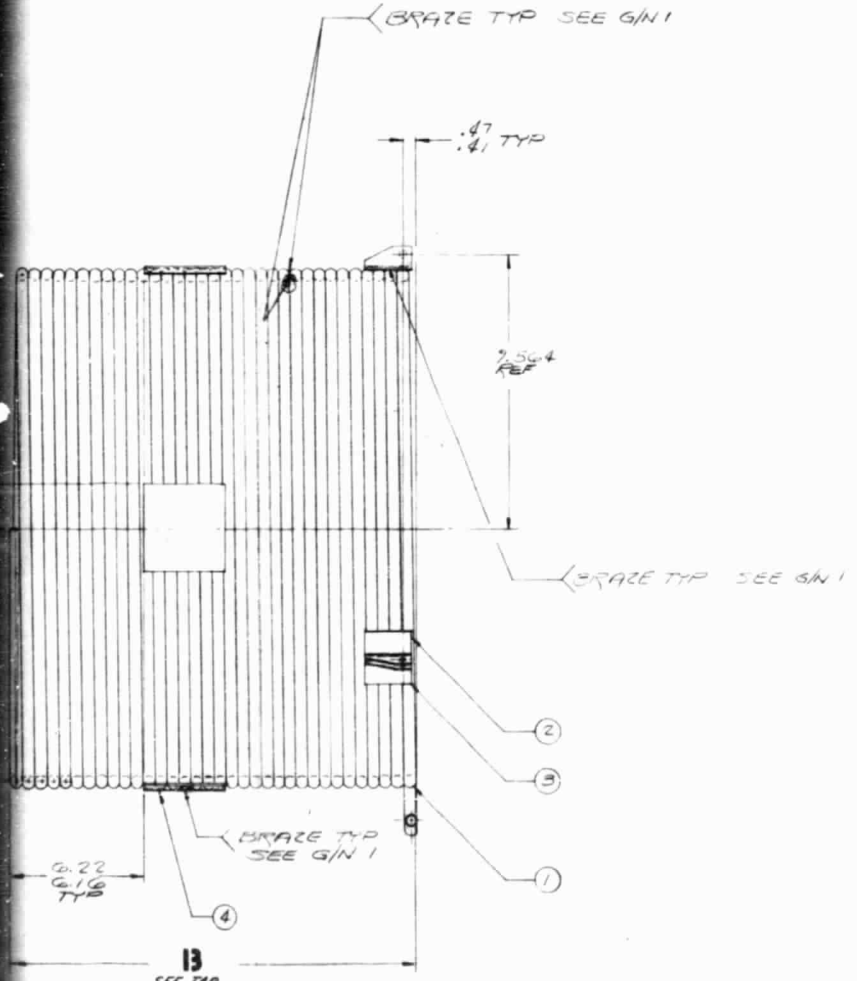

REVISIONS

ZONE	LTR	DESCRIPTION	DATE	APPROVED
	A	SEE EO		

FOLDOUT FRAME

SEE SEPARATE PARTS LIST FOR REQUIRED ITEMS AND GENERAL NOTES

NOTES: UNLESS OTHERWISE SPECIFIED

APPLICATION

AIRESEARCH MANUFACTURING COMPANY OF CALIFORNIA
A DIVISION OF THE GARRETT CORPORATION
TORRANCE, CALIFORNIA

CORE ASSEMBLY, PRIMARY

E 70210 193129

SCALE 1/2

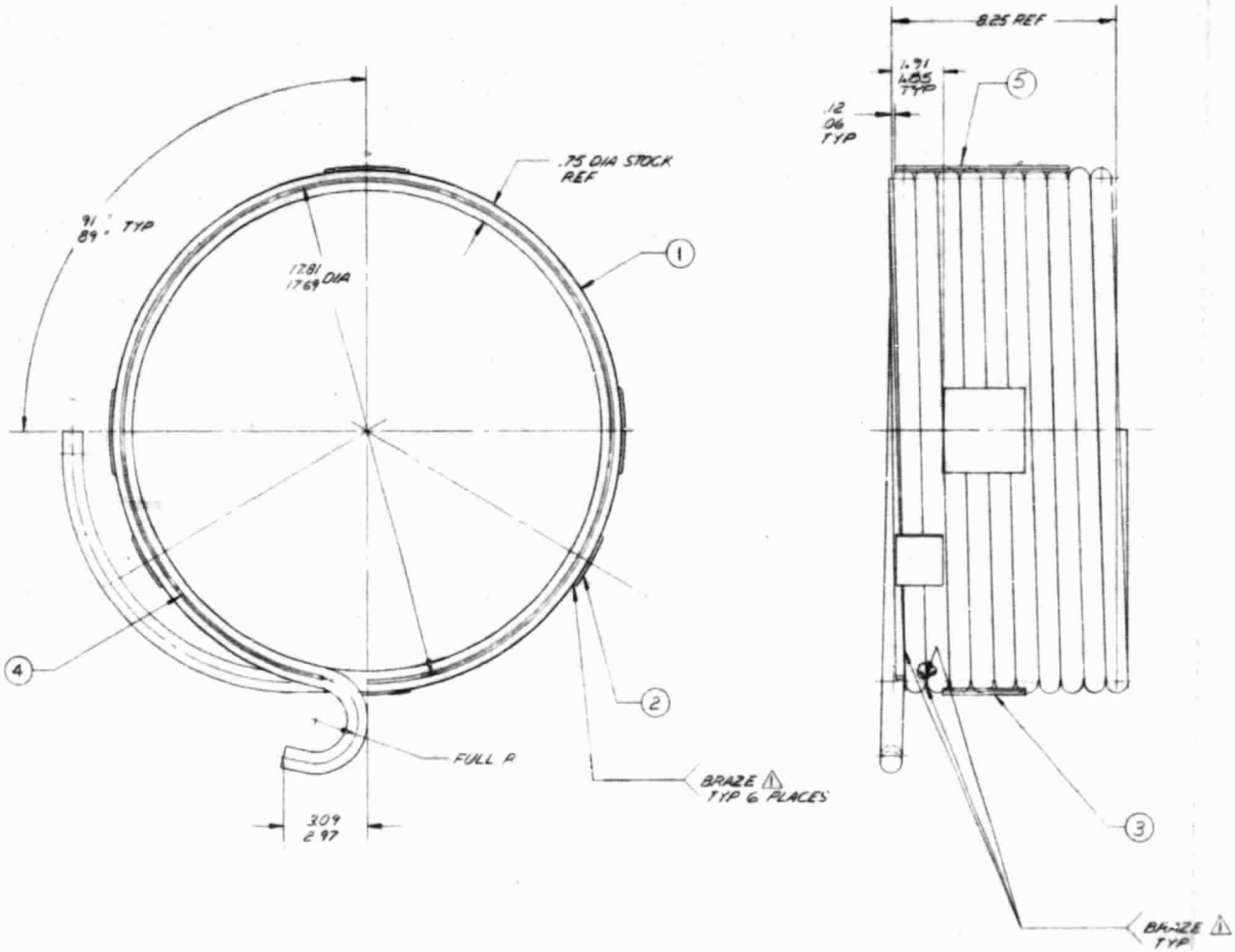

FOLDOUT FRAME

NOTES: UNLESS OTHERWISE SPECIFIED

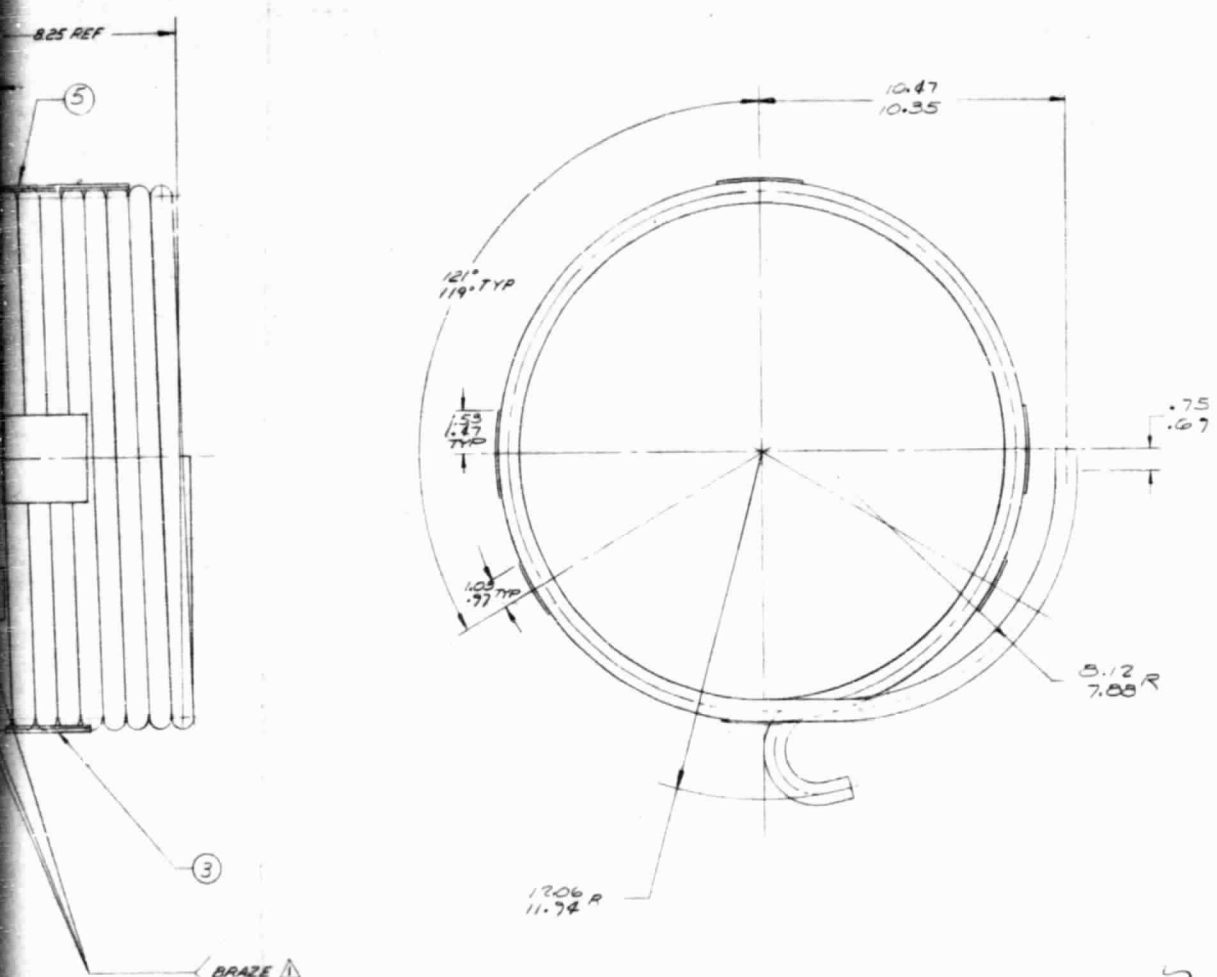

FOLDOUT FRAME 2

SEE SEPARATE PARTS LIST FOR REQUIRED ITEMS AND GENERAL NOTES.

NOTES: UNLESS OTHERWISE SPECIFIED

PART NO	
	AIRESEARCH MANUFACTURING COMPANY OF CALIFORNIA
	CORE ASSY, REHEATER
SIZE E	CODE IDENT NO 70210
	DWG NO 193131
SCALE 1/2	SHEET 1 OF 1

APPLICATION

193131

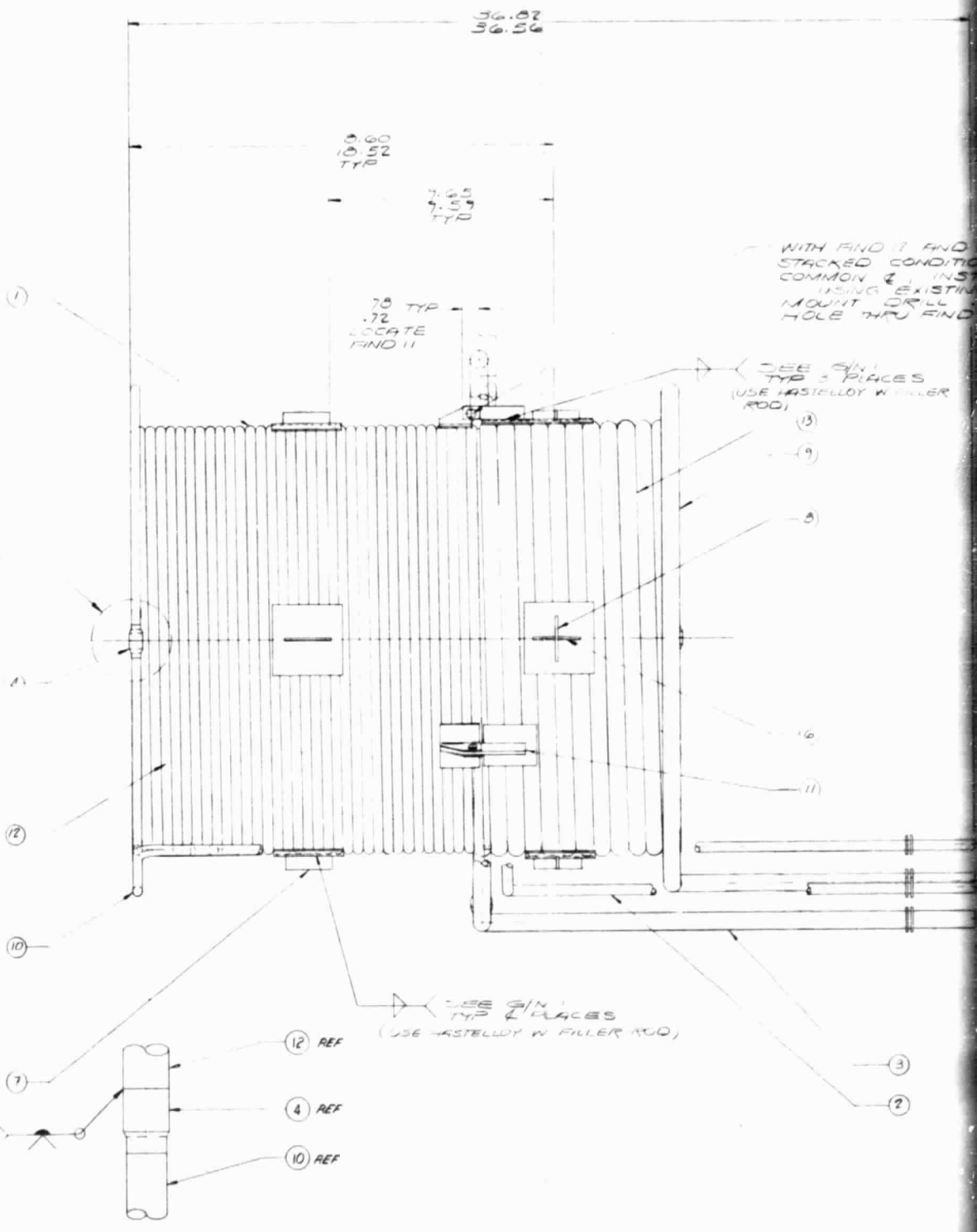

FOLDOUT FRAME

DETAIL A
FOR -5 ASSY ONLY
TYP 2 PLACES
SCALE: 2/1

193134

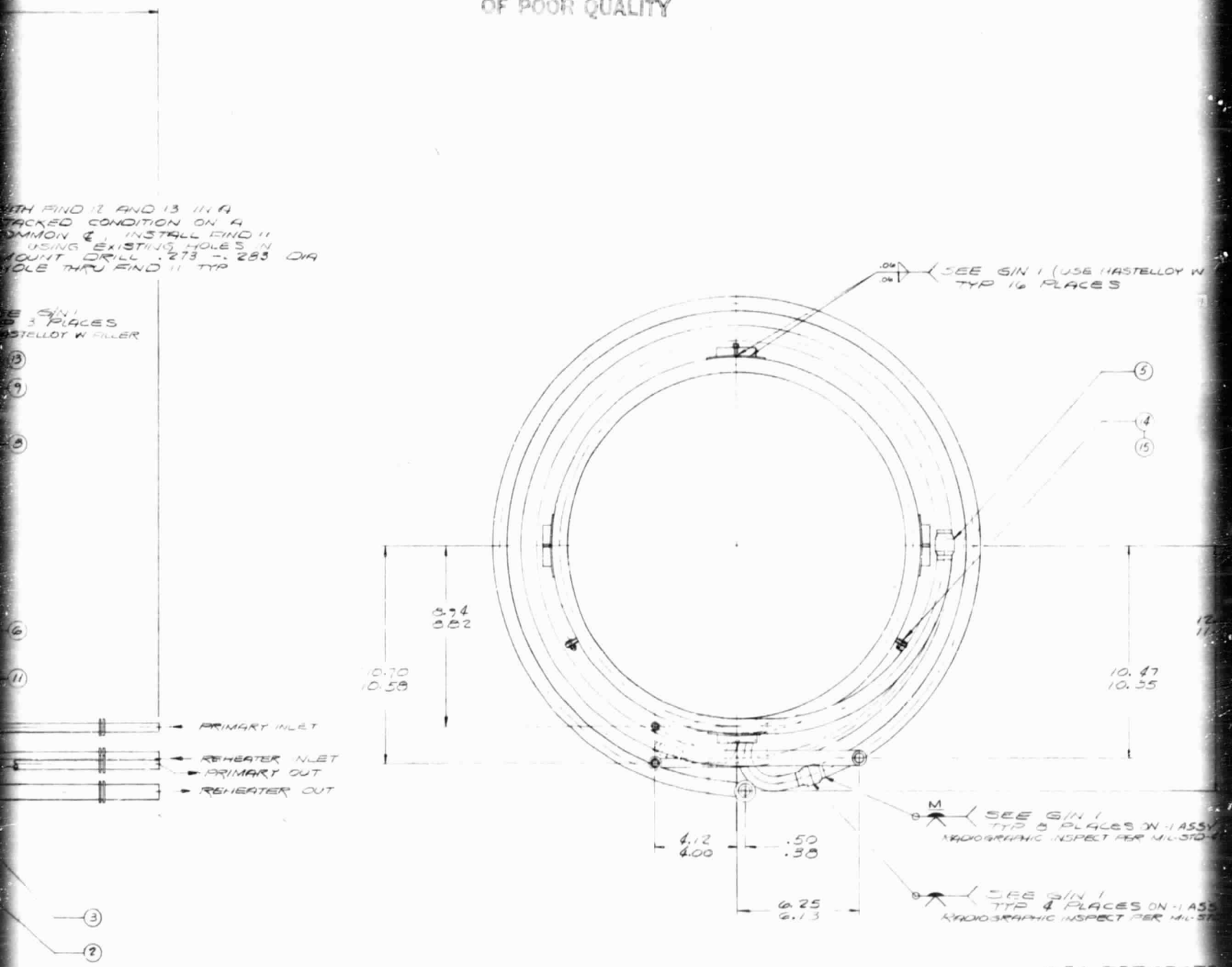

SEE SEPARATE
REQUIRED ITE

FOLDOUT FRAME 2

NOTES: UNLESS OTHERWISE SPECIFIED

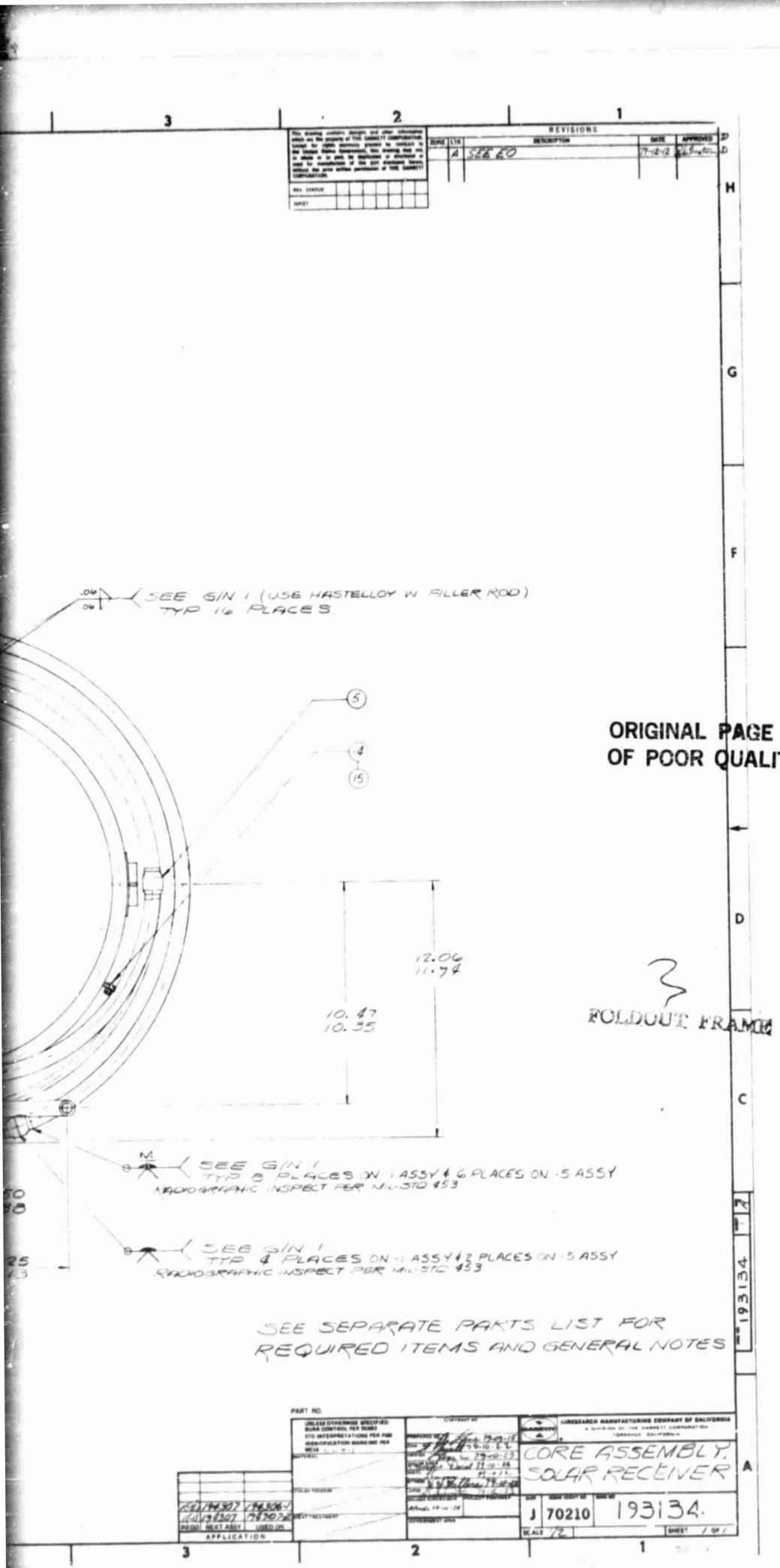

ORIGINAL PAGE IS
OF POOR QUALITY

ORIGINAL PAGE IS
OF POOR QUALITY

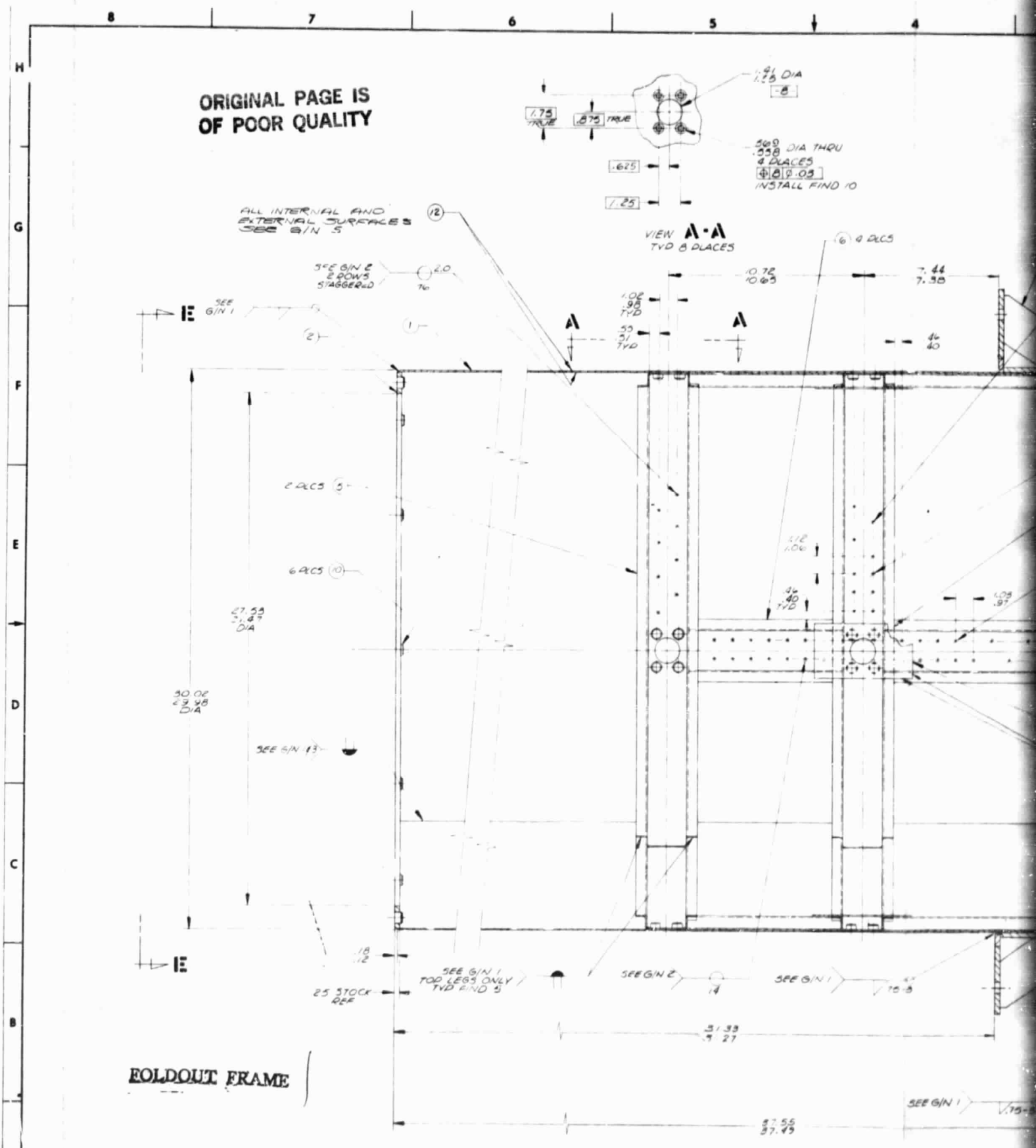

FOLDOUT FRAME

NOTES: UNLESS OTHERWISE SPECIFIED

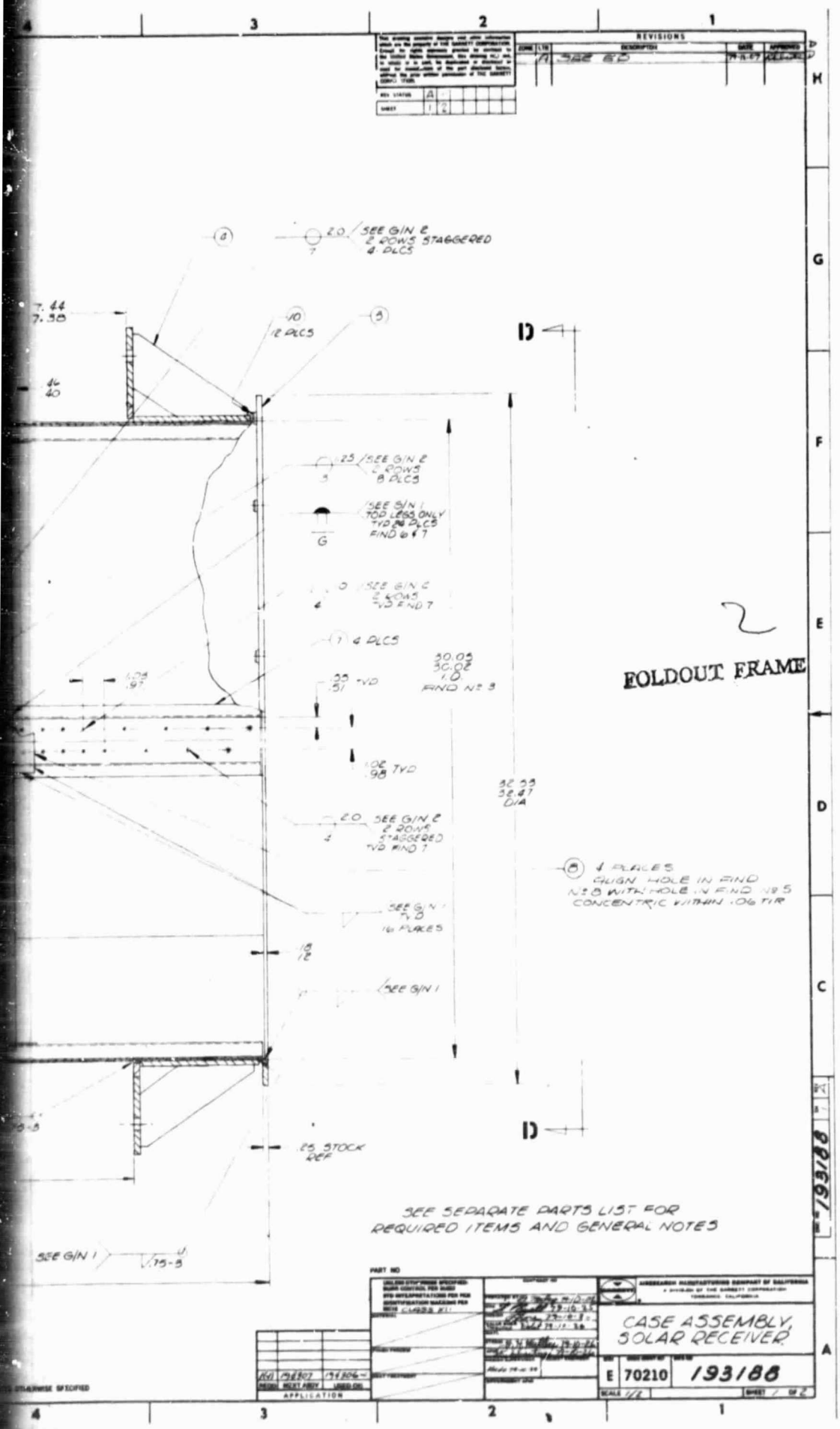
REVISIONS
SEE G/N 2
2 ROWS STAGGERED
4 PLCS
SEE G/N 2
2 ROWS
8 PLCS
SEE G/N 1
TOO LONG ONLY
TYP 8 PLCS
FIND NO 7
SEE G/N 2
2 ROWS
TYP FIND 7
4 PLCS
30.03
30.02
I.D.
FIND NO 3
TYP
TYP
32.39
32.47
O/A
SEE G/N 2
2 ROWS
STAGGERED
TYP FIND 7
4 PLACES
ALIGN HOLE IN FIND
NO 8 WITH HOLE IN FIND NO 15
CONCENTRIC WITHIN .06 TIR
SEE G/N 1
I.D
16 PLACES
SEE G/N 1
SEE G/N 1
FOLDOUT FRAME
SEE SEPARATE PARTS LIST FOR
REQUIRED ITEMS AND GENERAL NOTES
CASE ASSEMBLY,
SOLAR RECEIVER
E
70210
193188
SCALE 1/2
SHEET 1 OF 2

ORIGINAL PAGE IS
OF POOR QUALITY

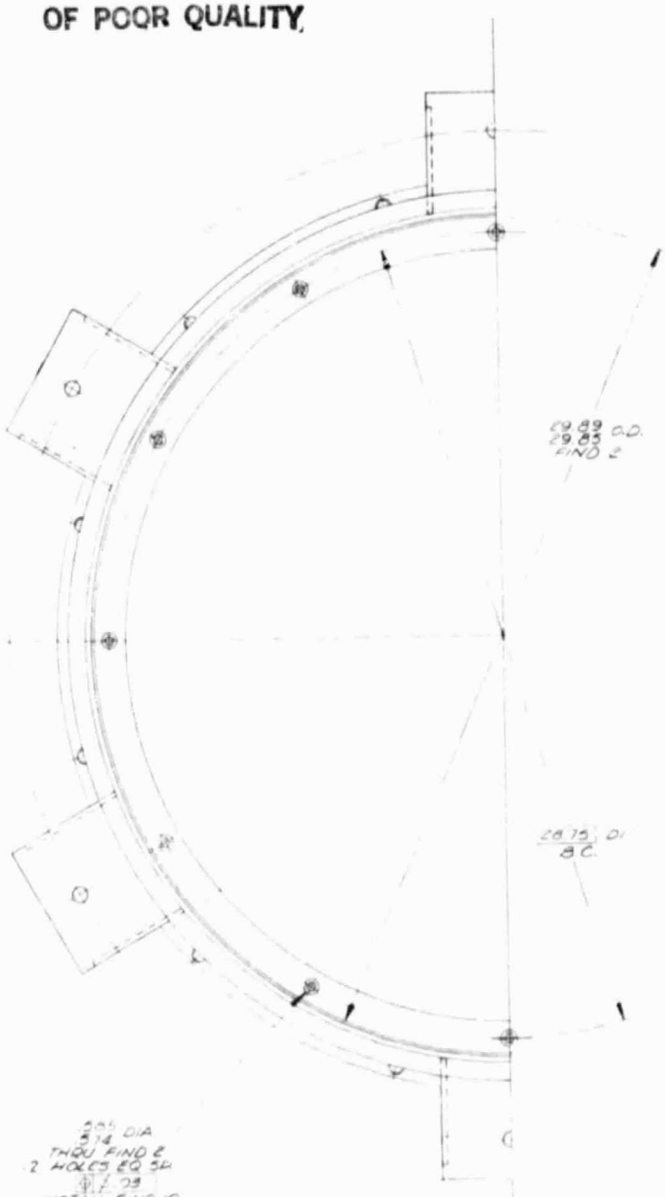

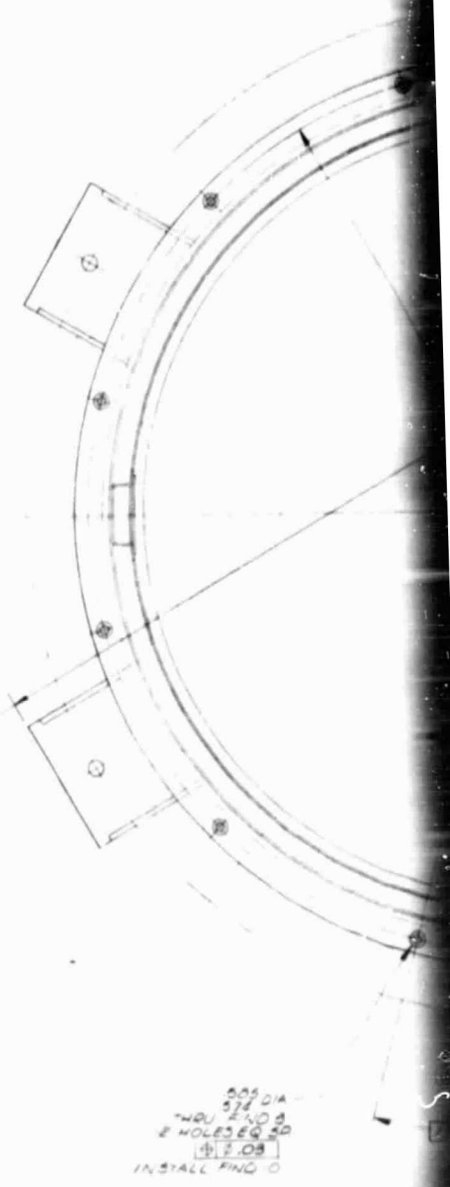

VIEW E - E

FOLDOUT FRAME

NOTES: UNLESS OTHERWISE SPECIFIED

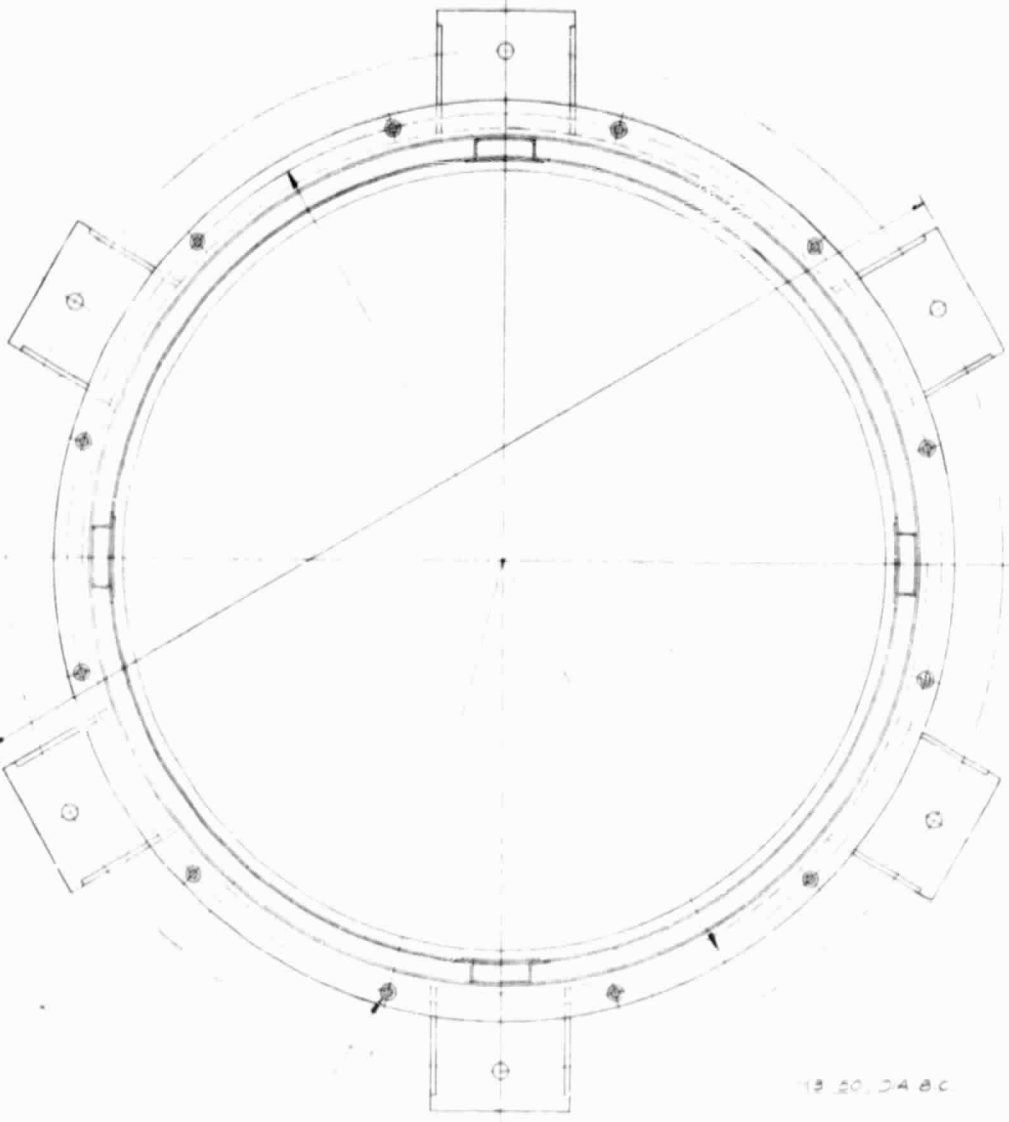

VIEW D-D

BOLDUCK FRAME

E	70210	193188

NOTES: UNLESS OTHERWISE SPECIFIED

ORIGINAL PAGE IS
OF POOR QUALITY

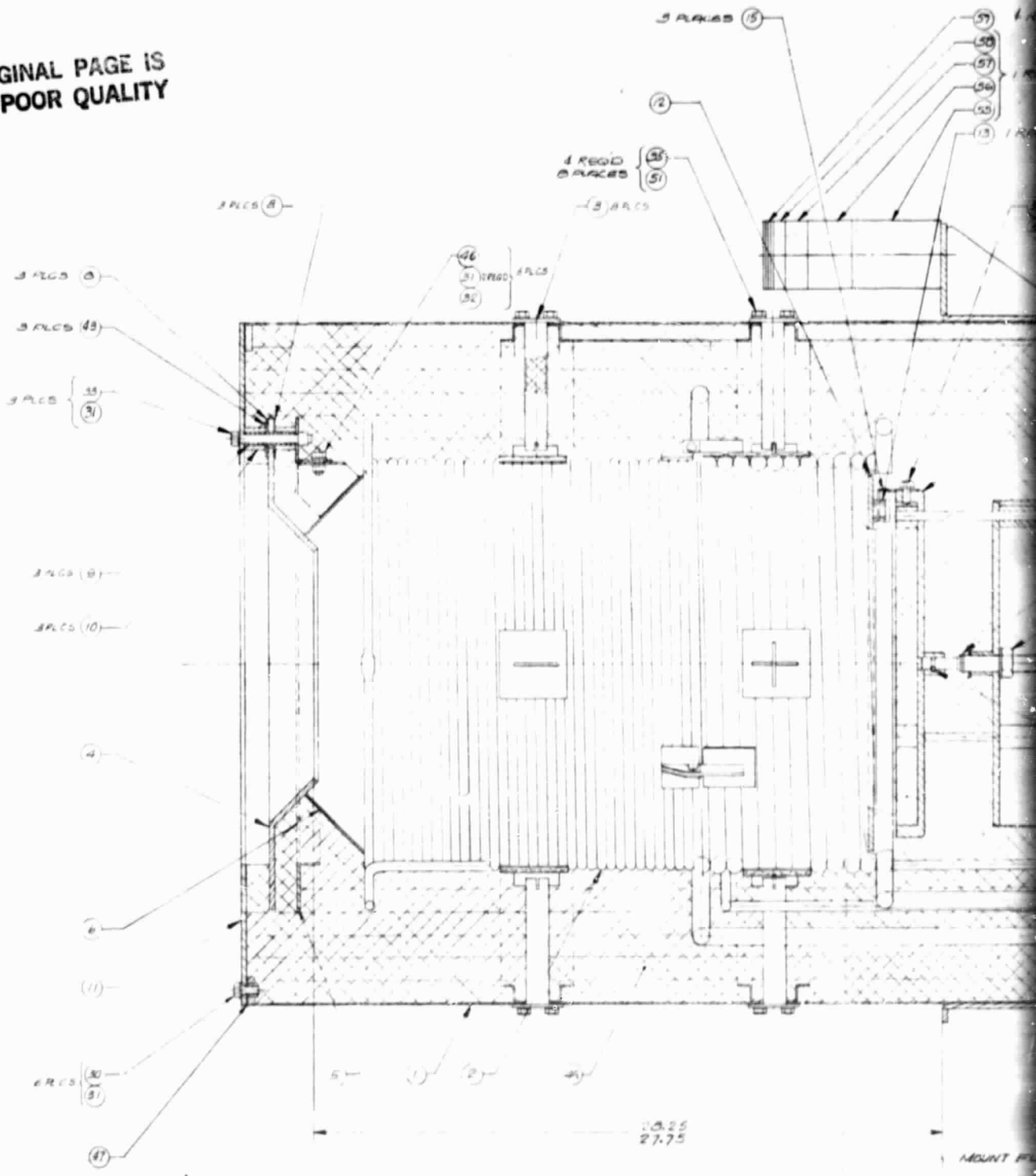

SECTION A-A

FOLDOUT FRAME

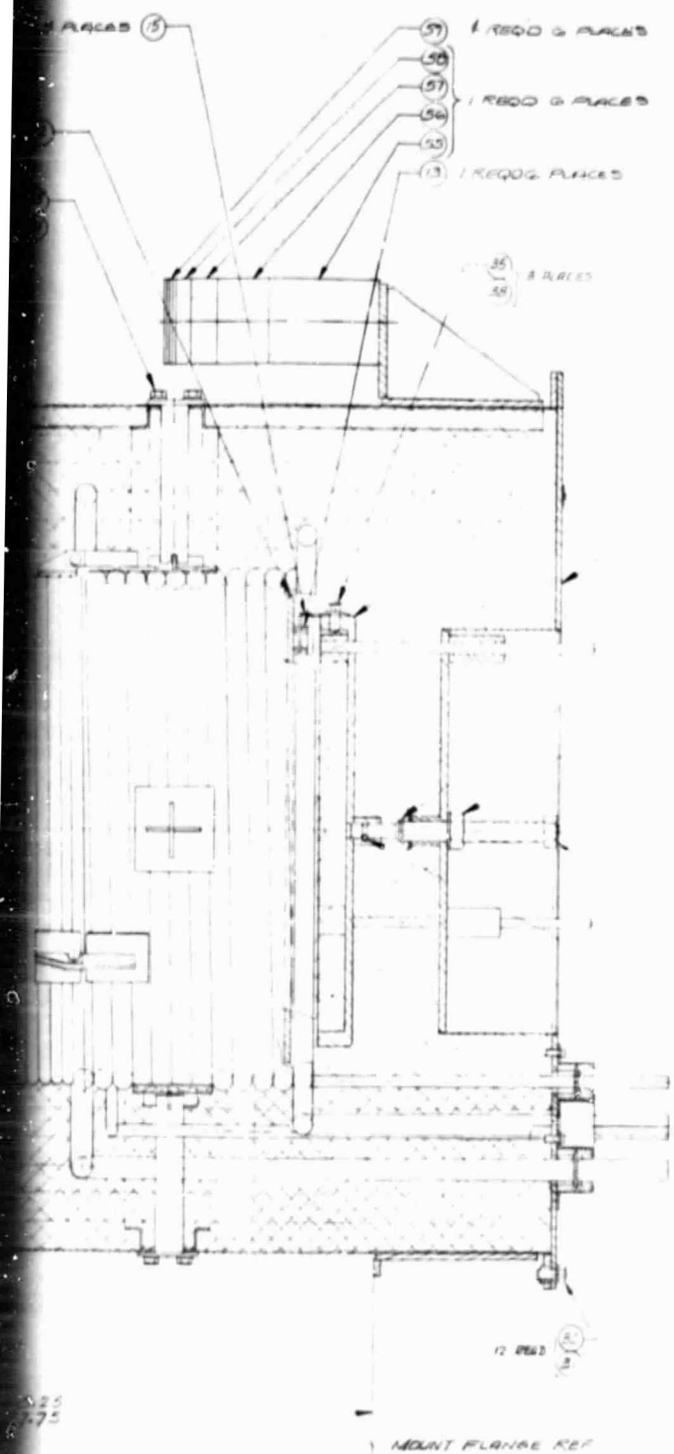

A-A

ORIGINAL PAGE IS
OF POOR QUALITY

FOLDOUT FRAME

SEE SEPARATE PART'S LIST FOR REQUIRED ITEMS AND GENERAL NOTES

SOLAR RECEIVER ASSEMBLY, STEAM, RANKINE

E 70210 194307

194307

FOLDOUT FRAME

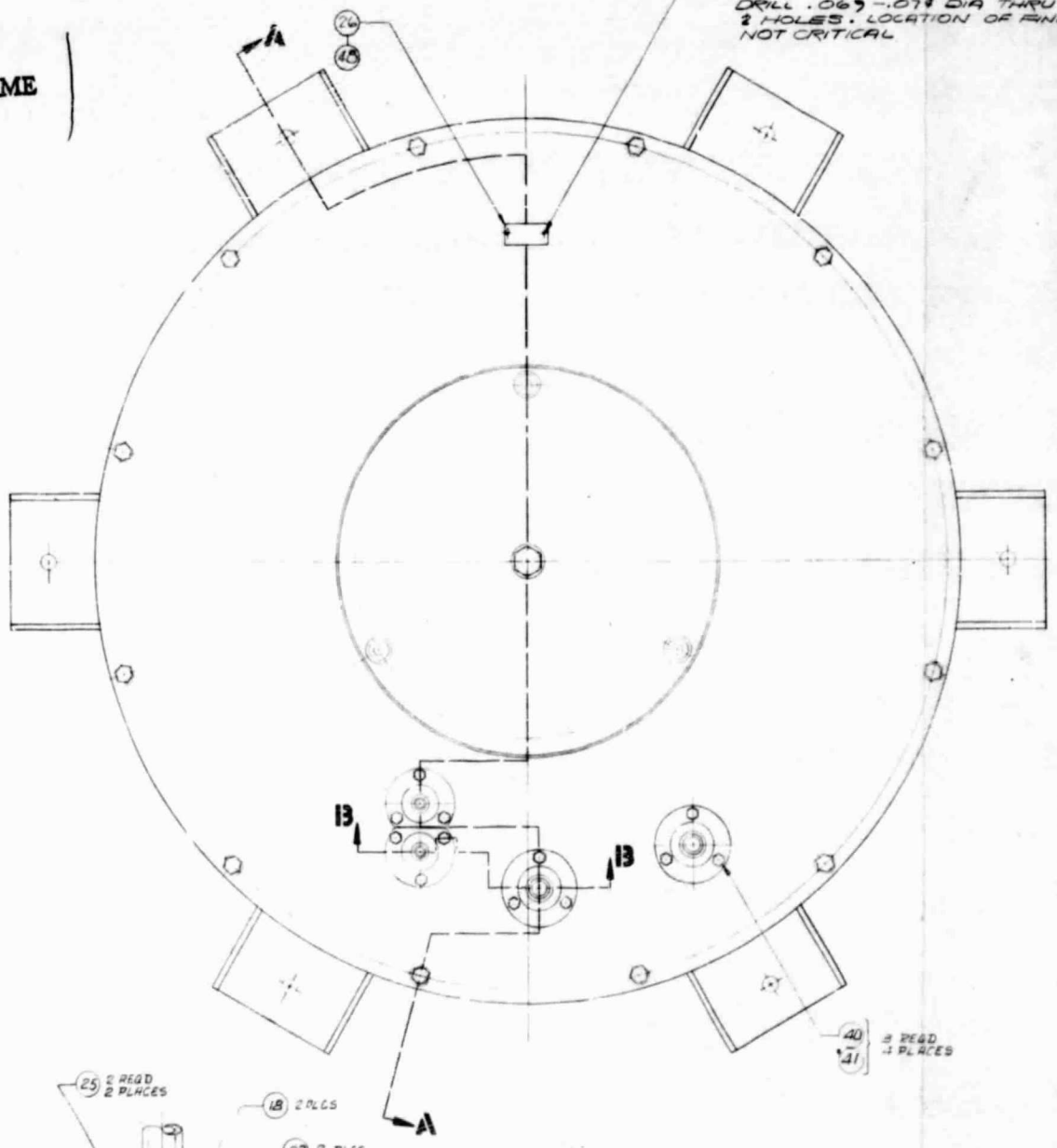

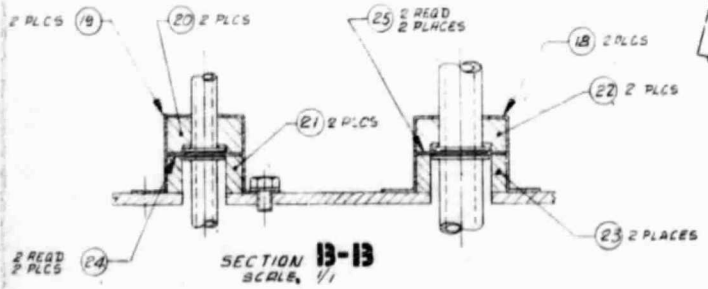

SECTION B-B
SCALE, 1/1

ORIGINAL PAGE IS
OF POOR QUALITY

NOTES: UNLESS OTHERWISE SPECIFIED

REVISIONS				
ZONE	LTR	DESCRIPTION	DATE	APPROVED
	D	SEE E.O.	10-8-20	

USING FIND Nº 26 FOR SPACING.
DRILL .067 -.071 DIA THRU FIND Nº 16.
2 HOLES. LOCATION OF FIND Nº 26
NOT CRITICAL

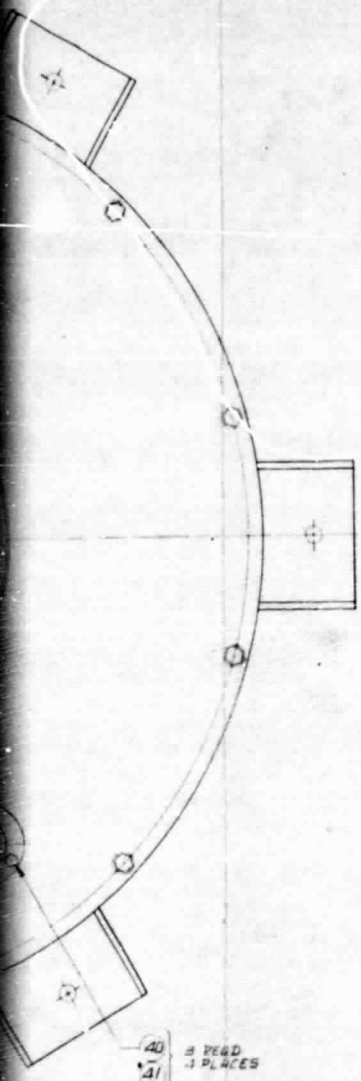

(40) (41) 2 PLCS 4 PLACES

2

FOLDOUT FRAME

NOTES: UNLESS OTHERWISE SPECIFIED

	AIRESEARCH MANUFACTURING COMPANY OF CALIFORNIA A DIVISION OF THE GARRETT CORPORATION TORRANCE, CALIFORNIA		
USE ON	SIZE	DRG NO	
	E	70210	194307
	SCALE 1/2		SHEET 2

194307